

## A CATALOG OF NORTHERN STARS WITH ANNUAL PROPER MOTIONS LARGER THAN $0''.15$ (LSPM-NORTH CATALOG)<sup>1,2</sup>

SÉBASTIEN LÉPINE<sup>3</sup> AND MICHAEL M. SHARA

Department of Astrophysics, Division of Physical Sciences, American Museum of Natural History,  
Central Park West at 79th Street, New York, NY 10024

Received 2004 May 4; accepted 2004 November 30

### ABSTRACT

The LSPM catalog is a comprehensive list of 61,977 stars north of the J2000 celestial equator that have proper motions larger than  $0''.15 \text{ yr}^{-1}$  (local-background-stars frame). The catalog has been generated primarily as a result of our systematic search for high proper motion stars in the Digitized Sky Surveys using our SUPERBLINK software. At brighter magnitudes, the catalog incorporates stars and data from the Tycho-2 Catalogue and also, to a lesser extent, from the All-Sky Compiled Catalogue of 2.5 million stars. The LSPM catalog considerably expands over the old Luyten (Luyten Half-Second [LHS] and New Luyten Two-Tenths [NLTT]) catalogs, superseding them for northern declinations. Positions are given with an accuracy of  $\lesssim 100 \text{ mas}$  at the 2000.0 epoch, and absolute proper motions are given with an accuracy of  $\approx 8 \text{ mas yr}^{-1}$ . Corrections to the local-background-stars proper motions have been calculated, and absolute proper motions in the extragalactic frame are given. Whenever available, we also give optical  $B_T$  and  $V_T$  magnitudes (from Tycho-2, ASCC-2.5), photographic  $B_J$ ,  $R_F$ , and  $I_N$  magnitudes (from USNO-B1 catalog), and infrared  $J$ ,  $H$ , and  $K_s$  magnitudes (from 2MASS). We also provide an estimated  $V$  magnitude and  $V - J$  color for nearly all catalog entries, useful for initial classification of the stars. The catalog is estimated to be over 99% complete at high Galactic latitudes ( $|b| > 15^\circ$ ) and over 90% complete at low Galactic latitudes ( $|b| < 15^\circ$ ), down to a magnitude  $V = 19.0$ , and has a limiting magnitude  $V = 21.0$ . All the northern stars listed in the LHS and NLTT catalogs have been reidentified, and their positions, proper motions, and magnitudes reevaluated. The catalog also lists a large number of completely new objects, which promise to expand very significantly the census of red dwarfs, subdwarfs, and white dwarfs in the vicinity of the Sun.

*Key words:* astrometry — solar neighborhood — stars: kinematics — stars: Population II — surveys — white dwarfs

*Online material:* machine-readable tables

### 1. INTRODUCTION

The search for and identification of stars with large proper motions has traditionally been the dominant method for finding nearby stars. Stellar distances are ultimately determined with parallax measurements, but these generally require substantial effort, and until the *Hipparcos* mission (1991), large systematic parallax surveys were impractical. One therefore had to rely on secondary diagnostics of proximity that could be more easily measured, such as large proper motions. It is a historical fact that the vast majority of the stars within 25 pc of the Sun (the local volume of space known as the “solar neighborhood”) have first been identified as high proper motion stars. These include some of our closest neighbors, such as Proxima Centauri (Innes 1915) and Barnard’s Star (Barnard 1916), which still is the star with the largest known proper motion ( $\mu \simeq 10''.3 \text{ yr}^{-1}$ ).

Massive, large-scale searches for high proper motion stars have been performed, and continually improved, throughout the 20th century, thanks to innovations in wide-field astrophotography. Early compilations of known stars with large proper motions (van Maanen 1915) were expanded by catalogs such as Max Wolf’s *Katalog von 1053 starker bewegten Fixternen* (Wolf

1919), which he complemented over the years with several new additions, naming a total of 1567 stars after himself. Frank E. Ross also contributed numerous discoveries, publishing lists of new high proper motion stars over a period of 14 years (1925–1939), discovering a total of 1080 nearby objects (Ross 1939). These early investigations were made with the use of a visual blink comparator; photographic plates obtained at different epochs were blinked in succession and examined by eye. The typical motions of the stars detected (which were at that time simply called “proper motion stars”) were  $\approx 0''.2\text{--}1''.0 \text{ yr}^{-1}$ .

Over the years, the discovery of increasingly fainter stars having large proper motions pointed to the existence of a significant population of low-luminosity stars. Some of the most extreme examples were discovered as faint, common proper motion companions of brighter objects (van Biesbroeck 1961). The very first free-floating brown dwarf was also discovered in a survey of high proper motion stars (Ruiz et al. 1997). Besides being an extremely useful tool in the identification of nearby populations of low-luminosity objects, proper-motion surveys are also very sensitive to high-velocity stars. Because high-velocity (e.g., thick disk, halo) stars are detected out to larger distances than nearby disk stars in proper-motion–selected samples, they are significantly overrepresented in catalogs of high proper motion stars. Far from being a problem, this makes proper-motion catalogs highly useful tools for the study of Galactic stellar populations (including low-luminosity halo stars). This has motivated intensive searches for faint high proper motion stars over the whole sky.

<sup>1</sup> Based on data mining of the Digitized Sky Surveys (DSSs), developed and operated by the Catalogs and Surveys Branch of the Space Telescope Science Institute (STScI), Baltimore.

<sup>2</sup> Developed with support from the National Science Foundation (NSF), as part of the NASA/NSF NStars program.

<sup>3</sup> American Museum of Natural History (AMNH) Kalbfleisch Research Fellow.

The largest deep surveys of high proper motion stars were carried out by the Lowell Observatory and by Willem J. Luyten at the University of Minnesota. Results from the Lowell Proper Motion Survey were compiled and published in two large catalogs (Giclas et al. 1971, 1978) listing a total of 11,749 stars with proper motions larger than  $0''.2 \text{ yr}^{-1}$ . Luyten's work, on the other hand, was constantly updated over the decades, culminating in the publication of two major catalogs: the *New Luyten Catalogue of Stars with Proper Motions Larger than Two Tenths of an Arc-second* (Luyten 1979b), known in short as the NLTT, listing 58,845 objects, and *A Catalogue of Stars with Proper Motions Exceeding  $0''.5$  Annually* (Luyten 1979a), known as the LHS, which is essentially a subset of the NLTT listing 4470 of the fastest moving stars.

Most of Luyten's success stems from his use of the National Geographic Palomar Sky Survey (POSS-I), completed in the 1950s. Luyten obtained second-epoch images in the late 1950s and 1960s using the same instrument and setup (at the Palomar Schmidt telescope). Luyten also developed a laser-scanning microdensitometer machine to process the northern sky images, considerably improving over previous eye-blinking methods. The depth of the Palomar plates allowed him to probe deeper than anyone before, mapping the turnover in the local luminosity function at the bottom of the main sequence (Luyten 1968); he was, however, limited by the depth of his second-epoch plates, which were about 1 mag shallower (19th magnitude limit) than the POSS-I plates (20th magnitude limit). Until today, the NLTT catalog remains the largest and most complete list of high proper motion objects, at least for declinations north of  $-32.5^\circ$  (the southern limit of POSS-I).

Because the LHS and NLTT catalogs contain large numbers of astrophysically significant objects, they have been used as a source of targets in many follow-up programs, with the faster LHS stars naturally taking precedence. Photometric studies have included the search for nearby dwarfs (Weis 1984, 1996), multi-band studies of halo stars (Ryan 1989), low-luminosity dwarfs, and subdwarfs (Bessell 1991). Spectroscopic follow-up surveys have resulted in the identification of new nearby stars (Gizis & Reid 1997), cool halo subdwarfs (Ruiz & Anguita 1993), and white dwarfs (Hintzen 1986; Bergeron et al. 1992; Vennes & Kawka 2003). Despite numerous studies and observing programs, hundreds of LHS stars and the majority of NLTT stars are still lacking formal spectral classification. The NLTT catalog in particular remains a gold mine of astrophysically interesting but uncharacterized targets. Perhaps the most intensive follow-up study to date is a recent program devoted to the identification of nearby stars missing from the census of objects within 20 pc of the Sun (Reid & Cruz 2002; Reid et al. 2002, 2003; Cruz & Reid 2002).

Modern astrometric techniques require much more accurate positions and proper motions than initially recorded by Luyten. One example is the identification of future possible microlensing events (Salim & Gould 2000). Motivated by these requirements, proper motions and positions of the LHS stars have been recently recalculated by Bakos et al. (2002), who systematically searched for all the stars in the Digitized Sky Surveys (DSSs). A revision of the NLTT positions and proper motions was also initiated by Gould & Salim (2003) and Salim & Gould (2003), using the USNO-A2 catalog (Monet et al. 1998) as a first epoch and the Two Micron All Sky Survey (2MASS) second incremental release as a second epoch. These revisions revealed that a significant fraction of LHS/NLTT entries contained large positional errors, up to several arcminutes in some cases. Indeed, a comparison of NLTT and LHS positions for stars appearing in both catalogs has revealed the existence of typographical errors

in both catalogs (Lépine et al. 2002b). The uncertainties in Luyten's positions explain in part the difficulty in carrying out follow-up observations of his objects and raises the possibility that background stars have been mistaken for NLTT stars, resulting in erroneous spectral classifications. This motivates a complete reevaluation of the positions of all NLTT objects.

The problem of the completeness of the NLTT has been much debated (see Pokorny et al. 2003 and references therein). The reason is that statistical studies of the Luyten stars (LHS stars in particular) have been used in estimates of the local density of low-mass and degenerate stars. In particular, the NLTT has been used to estimate the local density and luminosity function of white dwarfs (Liebert et al. 1988; Leggett et al. 1998) and the density and luminosity function of the local halo population (Dawson 1986; Lee 1991; Gould 2003a). The accuracy of those statistical studies, however, is entirely dependent on the completeness of the underlying sample, or at least on their *estimated* completeness. Hence the importance of being able to estimate the completeness (as a function of position, magnitude, proper motion, etc.) of the NLTT catalog.

As initially noted by Dawson (1986), the NLTT and LHS catalogs are notably incomplete in two distinct areas: (1) south of  $-32.5^\circ$  in declination and (2) in a band within  $\pm 10^\circ$  of the Galactic plane. However, outside of these specific areas, in an area referred to as the Completed Palomar Region (CPR), the catalogs do appear to be significantly complete ( $\geq 80\%$ ) at least down to 19th magnitude. This is significant because the magnitude distribution of NLTT stars reflects the turnover at the faint end of the luminosity function: the number density of NLTT stars peaks at  $R \approx 15$ , well before the limiting magnitude of the POSS-I plates on which they are based. Because they probe the luminosity function turnover and because they contain significant samples of both disk and halo stars, the LHS and NLTT catalogs are major tools in the determination of the local luminosity function of both the Galactic disk and Galactic halo. In any case, the accuracy of the luminosity function and of the stellar density is dependent on a proper evaluation of the completeness of these proper-motion-selected samples (Gould 2003a).

The completeness of a proper-motion catalog can be determined either *internally* or *externally*. One internal test was devised by Flynn et al. (2001) and uses the fact that both the magnitude and proper motion are a function of distance. For example, if one takes subsamples with a lower proper motion limits  $\mu_1$  and  $\mu_2 = 1.259\mu_1$ , sample 1 should contain objects that are on average more distant by a distance modulus of 0.5. The completeness at a magnitude  $V_1$  in sample 1 can thus be determined by comparing the relative number of stars in bins  $V_1$  and  $V_2 = V_1 - 0.5$  in sample 2. One can then work iteratively, starting from a bin  $V_2$  assumed to be complete. Applying the technique to the NLTT, Flynn et al. (2001) estimated that the completeness in the CPR (for stars with  $\mu > 0''.2 \text{ yr}^{-1}$ ) falls linearly from 100% at  $V = 13$  to 60% at  $V = 18$  and then breaks down to 0% at  $V = 20$ . The method was, however, put in doubt by Monet et al. (2000), who noted that at high Galactic latitudes the density of stars decreases with distance, and sample 2 is thus not equivalent to the more distant sample 1; the method of Flynn et al. (2001) would thus tend to underestimate the completeness. Gould (2003a) discusses this problem (see his Appendix) and concludes that there is little evidence to suggest the Flynn et al. (2001) result to be in error. The main problem is a lack of reliable external completeness estimates.

External completeness tests are based on a direct comparison of the proper-motion catalog (the NLTT) to a deeper or more sensitive proper-motion survey conducted over a selected area.

The main caveat of that method is that the results then become dependent on the completeness of the new survey itself, which has to be estimated by other means. Of course, if the new survey is conducted over a sufficiently large area, it can simply supersede the former catalog.

From a small sample of only  $100 \text{ deg}^2$  from the APM Proper Motion Project, Evans (1992) concluded that the NLTT has an incompleteness of  $\approx 16\%$ , most of it probably due to random measurement errors at the lower proper-motion limit of  $\mu = 0''.18 \text{ yr}^{-1}$ . This completeness level is larger than suggested by the internal test of Flynn et al. (2001), but the small area and limited number of objects puts this external test in doubt. A much larger survey of  $1378 \text{ deg}^2$  in the northern sky (Monet et al. 2000) was performed using pairs of plates from the Second Palomar Sky Survey (POSS-II; Reid et al. 1991). Because of the short timespan between pairs of plates, this survey was limited to the detection of stars with very large proper motions ( $0''.4 \text{ yr}^{-1}$ ). Nevertheless, 15 stars were found that had been missed by Luyten, of which six have proper motions  $\mu > 0''.5 \text{ yr}^{-1}$ , suggesting a completeness  $\geq 90\%$  for the LHS catalog. (Note that while the Monet et al. paper cites 17 “new” objects, two of them were subsequently found by Gould 2003a to be the NLTT catalog stars 58785 and 52890.) Unfortunately, their survey did not cover the  $0''.18 \text{ yr}^{-1} < \mu < 0''.4 \text{ yr}^{-1}$  range, in which most of the NLTT stars are found, leaving open the question of the NLTT completeness.

Many more attempts have been made at conducting more sensitive proper-motion surveys in the south. Because the NLTT is well known to be much less complete south of  $-32.5^\circ$ , the potential payoff is much higher. In the Calán-ESO Proper Motion Survey—famous for its discovery of Kelu-1, the first free-floating brown dwarf (Ruiz et al. 1997)—14 pairs of ESO Schmidt plates were used, covering an area of  $350 \text{ deg}^2$  (Ruiz et al. 2001). Fourteen new stars with  $\mu > 0''.5 \text{ yr}^{-1}$  were found, suggesting a completeness of only  $\approx 60\%$  for the LHS in the south. But since several of their areas are south of  $-32.5^\circ$ , this overestimates the incompleteness of the NLTT in the CPR. The larger survey conducted by Wroblewski & Torres (1989, 1991, 1994, 1996, 1997) and continued by Wroblewski & Costa (1999, 2001) now covers a total of  $3275 \text{ deg}^2$  in 131 scattered areas. This survey is performed by direct visual inspection of photographic plates, using a Zeiss-Jena plate comparator. The survey now has 2495 cataloged objects, all of which are new (i.e., not in the NLTT). Within the limits of the CPR, they typically discover  $\approx 50$  new stars with  $\mu > 0''.2 \text{ yr}^{-1}$  in every  $100 \text{ deg}^2$  area. When compared to the NLTT density of roughly 90 stars ( $100 \text{ deg}^2$ ) $^{-1}$  in the same areas, this yields an overall estimated completeness of  $\approx 65\%$  for the NLTT, but a more detailed analysis would be warranted.

Other large southern surveys are built from lists of objects generated from machine scans of photographic Schmidt plates. A survey of  $2000 \text{ deg}^2$  near the south polar Galactic cap was made with lists of objects from UK Schmidt plates, scanned with the Automatic Plate Measuring machine (Scholz et al. 2000). This survey is ongoing and may eventually cover much larger areas of the southern sky. The Liverpool-Edinburgh high proper motion survey (Pokorny et al. 2003) is based on lists of objects from ESO Schmidt and UK Schmidt plates, scanned with the SuperCOSMOS machine, and has a lower proper motion limit of  $0''.18 \text{ yr}^{-1}$ ; the survey is currently limited to a moderately large area of the southern sky, covering  $\approx 3000 \text{ deg}^2$  around the south Galactic cap. More recently, Hambly et al. (2004) have also used SuperCOSMOS data to search  $\approx 3000 \text{ deg}^2$  south of  $-57.5^\circ$  for stars with proper motion  $\mu > 0''.4 \text{ yr}^{-1}$  (although they only list

those they found having  $\mu > 1''.0 \text{ yr}^{-1}$ ). What is clear from these southern sky surveys is that the LHS/NLTT catalogs are definitely incomplete south of  $-32.5^\circ$ . The number of new high proper motion stars discovered is a sizable fraction of all the high proper motion stars identified. The consensus is that in the southern sky, the NLTT is no more than  $\approx 70\%$  complete down to  $R = 19$  and possibly much less complete in some areas.

More massive astrometric catalogs based on lists of objects from scanned Schmidt plates are in preparation, including the second Guide Star Catalog (GSC-II). By combining lists of objects from multiple epochs, these will attempt to provide proper motions for all stars detected. The already available USNO-B1.0 catalog (Monet et al. 2003) is a first attempt at such a deep, all-sky, astrometric catalog with proper motions. For the northern sky, the plate material includes the Oschin Schmidt plates from the first- and second-epoch Palomar Sky Surveys (POSS-I, POSS-II), providing a large temporal baseline and deep ( $R = 20$ ) limiting magnitude; in the southern sky scans of the ESO Schmidt and UK Schmidt were also used. Unfortunately, the huge number of objects involved (1 billion sources) and the large number of false detections (plate defects and mismatches from multiple epoch detections) makes the identification of high proper motion stars very difficult. An analysis of the USNO-B1.0 catalog by Gould (2003b) shows a huge contamination rate (200 to 1) in bogus high proper motion objects. Recent efforts (Gould & Kollmeier 2004; Munn et al. 2004) have, however, shown that it is possible to eliminate most of the false detections by cross-correlating the USNO-B1.0 catalog with other large-area surveys like the Sloan Digital Sky Survey (SDSS; Stoughton et al. 2002). Unfortunately, the completeness of the USNO-B1.0 for high proper motion stars (based on the recovery of NLTT stars) does not exceed 90% over the whole sky and drops to 70% at low Galactic latitudes.

Very high completeness levels have however been achieved by us in a novel approach to surveys of high proper motion stars (Lépine et al. 2002b, 2003). Instead of working with lists of objects identified from plate scans, we work directly with the pixel data, using an image subtraction algorithm. With the help of a specialized software (SUPERBLINK), we have performed a very successful proper-motion survey based on a massive re-analysis of all image scans of the Oschin Schmidt plates (POSS-I and POSS-II) made at the Space Telescope Science Institute (STScI) for the DSSs. The image subtraction method used by SUPERBLINK is significantly more efficient in densely populated fields, where examination with the blink comparator is difficult, and identification of point stellar sources by scanning machines considerably less efficient because of crowding. Our initial survey was a search for stars with very large proper motions  $\mu > 0''.5 \text{ yr}^{-1}$  over the whole  $20,000 \text{ deg}^2$  of northern sky. We showed our method to be extremely successful, by recovering essentially all LHS stars and by discovering of 198 new stars with  $\mu > 0''.5 \text{ yr}^{-1}$ . This yielded the definitive completeness measure of the LHS catalog in the northern sky ( $1662/1866 = 89.1\%$ ) and confirmed the results of Monet et al. (2000) about the northern sky completeness of the LHS. However, it left open the question of the completeness of the NLTT. Our new, expanded proper-motions catalog, presented in this paper, directly addresses this problem since it is an extension of our survey to smaller proper motions ( $\mu > 0''.15 \text{ yr}^{-1}$ ), with a completeness level exceeding 99% down to  $R_F = 19$ . The executive summary is *in the northern hemisphere, we find and report 40,843 stars with  $\mu > 0''.18 \text{ yr}^{-1}$ , of which 28,486 are NLTT objects; the LSPM catalog also lists an additional 21,133 stars with  $0''.15 \text{ yr}^{-1} < \mu < 0''.18 \text{ yr}^{-1}$ , only 2875 of which are in the NLTT catalog.* Our analysis

demonstrates that in the CPR, the completeness of the NLTT is 85% at  $V = 18$  and breaks down at  $V = 19$ , while at low Galactic latitudes ( $|b| < 10^\circ$ ), its completeness falls from 90% at  $V = 15$  to only 30% at  $V = 17$ . This suggests that the internal test of Flynn et al. (2001) underestimates the completeness of the NLTT in the CPR.

Note that other major proper-motion surveys, which have been extremely successful in determining highly accurate proper motions of selected stars, are not very helpful in increasing the completeness of our proper-motion catalogs. These include the astrometric survey conducted with the *Hipparcos* satellite, whose data are now compiled in the Tycho-2 catalog (Høg et al. 2000). Only stars brighter than  $V = 9$  were observed systematically, and an input catalog was used for stars down to the limiting magnitude ( $V = 13$ ). Bright NLTT stars were included in the survey, but very few new high proper motion stars were discovered above Luyten's cutoff. Also limited as tools for finding new high proper motion stars are the Lick Northern Proper Motion Program (Klemola et al. 1987) and its southern extension, the Yale/San Juan Proper Motion Survey (van Altena & López 1991). Both programs aim at very precise astrometric measurements of *selected* stars and largely rely on an input catalog, although a subset of stars were picked at random. Another highly accurate astrometric survey is the US Naval Observatory CCD Astrograph program (Zacharias et al. 2000), from which an all-sky astrometric catalog (UCAC) is being assembled (Zacharias et al. 2004). Although extremely promising as an expansion to the Tycho-2 catalog, the UCAC will have a limiting magnitude of  $R = 16$ , and it is unclear how sensitive the survey will be for stars with very large proper motions. At this time, it appears that our image subtraction method holds the best promise for generating an all-sky replacement to the LHS/NLTT catalogs.

As part of the NASA/NSF NStars initiative, we have been expanding our DSS-based survey, aiming at the systematic detection and verification of all stars in the northern sky with proper motions larger than  $0.05'' \text{ yr}^{-1}$ . Our goals are to achieve optimal detection rates, with completeness exceeding 99% down to  $R = 19.0$  over most of the sky, with minimal contamination from false detections. This paper presents our first major data release: a catalog of all known stars in the northern sky with proper motions larger than  $0''.15 \text{ yr}^{-1}$ . This catalog, which we refer to as the LSPM catalog, includes improved astrometry and photometry for more than 31,000 high proper motion stars previously listed in the LHS and NLTT catalogs. The LSPM catalog also incorporates bright high proper motion stars from the Tycho-2 catalog. Finally, the LSPM catalog contains over 28,000 newly discovered high proper motion stars.

The LSPM catalog represents a major improvement over the NLTT catalog. Not only is it much more complete, but the positions and proper motions are also much more accurate. In effect, the LSPM supersedes the NLTT for the sky north of the celestial equator and should now be used in its place for all applications. This paper provides information that is essential in understanding how the LSPM catalog was built and what are its strengths and limitations. A description of the SUPERBLINK code, used to find LSPM candidates in the DSS, follows in § 2. The detailed procedure for the inclusion of a star in the LSPM catalog is detailed in § 3. The sources used for the photometry are presented in § 4, whereas the catalog astrometric accuracy is discussed in § 5. The format of the catalog is explained in § 6. The completeness of the LSPM is discussed in § 7. A preliminary analysis of the stellar contents of the catalog is given in § 8. Plans for future expansion and improvement of the catalog are summarized in the conclusion (§ 9).

## 2. A NEW SURVEY FOR HIGH PROPER MOTION STARS

### 2.1. The SUPERBLINK Software

SUPERBLINK is an automated blink comparator developed by S. L. and first described in Lépine et al. (2002b). Given two different images of the same patch of sky on input (up to  $2k \times 2k$  pixels in size), SUPERBLINK automatically identifies any object that has moved between the two epochs, such as a star with a large proper motion. On output, the software generates a list of possible moving objects in the field, with their positions, proper motions, image magnitude, and a probability index that estimates the likelihood of the object being real. The software also generates identification charts ( $151 \times 151$  pixels in size) centered on each object. These charts are dual-epoch and can be blinked on the computer screen for easy examination of the moving object. The two core elements of SUPERBLINK are an image superposition and subtraction algorithm (SUPER) and a shift-and-match search algorithm (BLINK).

The current version of the code has been optimized for use with DSS images (first-epoch DSS and second-epoch XDSS) to look for stars with large proper motions. Pairs of images are provided to the code on input, each pair consisting of one  $17' \times 17'$  field extracted from the DSS at a specified position and a second  $17' \times 17'$  extracted from the XDSS and centered on the same position. In the northern sky, the DSS image invariably consists of a POSS-I scan, with a typical resolution of  $1''.7 \text{ pixel}^{-1}$ , whereas the XDSS image is a POSS-II scan with a resolution of  $1''.01 \text{ pixel}^{-1}$ . The POSS-II image is generally of higher quality than the POSS-I image: the background noise is lower, the image reaches about 1 mag deeper, and the astronomical resolution (seeing) is better.

The SUPER procedure performs image transformations to make the two images in the pair look as similar as possible. The procedure uses the first image (DSS) as a template and attempts to modify/degrade the second image (XDSS) in such a way that it can be subtracted from the first with the smallest residuals possible. The SUPER procedure follows a series of steps described below.

*Rescaling.*—The two images, on input, can have different resolutions; the SUPER procedure resets the two images to the same angular scale. Typically, the higher resolution second-epoch image (XDSS) is remapped onto a grid that matches the resolution of the lower resolution first-epoch (DSS).

*Rectification.*—Images are rectified so that their background levels (sky) are uniform and set to a value of 1. The code uses a procedure that marks each pixel as either “sky” or “object” (based on the statistics of intensity values). A two-dimensional linear fit is then performed on the “sky” pixels. The image is then divided by this fit, setting background levels to unity. Although the background level is never strictly linear on a photographic plate (edge effects are important), it is a good approximation on the scale of the images provided on input ( $17' \times 17'$ ), which are much smaller than the typical size of the POSS plates ( $384' \times 384'$ ).

*Normalization.*—The total flux from all “object” pixels is determined for each image. The second image is then normalized so that the total flux (above background) from “object” pixels is equal to that in the first image. Note that this normalization might be inaccurate if there are bright objects showing up in only one of the two images. This does happen, particularly if the two images are not exactly aligned initially. It may then happen that, e.g., a bright star near the edge of one image does not show up in the other and vice versa. The renormalization procedure (see below) will generally correct for any normalization error.

*Shift and rotate.*—The second image is shifted vertically and horizontally ( $\Delta X$ ,  $\Delta Y$ ) and rotated ( $\Delta\theta$ ), before being subtracted from the first image. The procedure is repeated recursively, first using small incremental values of  $\Delta X$ ,  $\Delta Y$ , and  $\Delta\theta$  until a good match is found, i.e., until the residuals are significantly smaller than the total flux in each image. More precise values for the shift and rotation are then determined using a multidimensional downhill simplex minimization routine, which identifies a strong minimum in the residuals in ( $\Delta X$ ,  $\Delta Y$ ,  $\Delta\theta$ ) space. Note that this procedure accurately superposes the two images using the assumption that most stars in the field are “fixed.” Any systematic motion in the background “fixed” stars will be eliminated. This means that all proper motions calculated by SUPERBLINK will be proper motions *relative to the background of “fixed” stars and not absolute proper motions.*

*Renormalization.*—The second image is normalized again, as described above, but this time using only “object” pixels that are common to both images in the pair. These can now be easily determined since we know from the preceding shift-and-rotate procedure which part of the field is common to both images.

*Convolution.*—The second image is then degraded so that its point-spread function (PSF) matches that of the first one. A convolution profile of variable width is applied to the second image, which is then subtracted from the first image. The width of the profile is increased until a minimum value in the residuals is found. The shape of the convolution profile has been determined by trial and error. Several different shapes have been considered; a simple profile generated by a sum of two Gaussians of different widths was found to yield the best results. This same general profile was applied to all our fields. After this final procedure, the first and second images generally look extremely similar. In the best of cases, it is very difficult to tell the two images apart just by looking at them. The only obvious differences are variations in the noise patterns, or the presence of a variable star, an asteroid track, or a high proper motion star.

The BLINK procedure starts with one pair of images that have first been superposed with SUPER and proceeds to identify any object that has moved between the first and second epoch. Stars with very large proper motions essentially appear as pairs of objects, one at each epoch, that do not cancel out after image subtraction; these are fairly easy to find. On the other hand, stars whose total motion between the two epochs are less than their apparent sizes on the POSS plates show a more complex pattern in the residuals, having been partially canceled out. On scans of POSS-I plates, typical sizes (FWHM) of stars range from  $\approx 3$  pixels ( $5''.1$ ) for unsaturated stars ( $R_F > 15$ ) to  $\approx 15$  pixels ( $25''.5$ ) for the brightest, saturated objects detectable by SUPERBLINK ( $R_F \approx 10$ ). The minimum motion of stars in our catalog is about  $6''$  between the POSS-I and POSS-II plates ( $0''.15 \text{ yr}^{-1}$  in 40 yr). This means that while the fainter stars are always well separated after plate subtraction, the images of many of the brighter proper-motion stars will overlap and will partially cancel out after subtraction. The following procedures in BLINK allow for a correct treatment of all moving objects, whether or not they partially cancel out on plate subtraction.

*Subtraction and cataloging of residuals.*—The two images processed by SUPER are subtracted from each other. Any object that has moved significantly between the two epochs induces a large, local maximum/minimum on the residual image. All the minima/maxima are mapped, cataloged, and matched to their source on the first or second image.

*Removal of the candidate moving objects from the first-epoch image.*—Each object on the first-epoch image that is associated with a large residual is removed from that image, with all pixels

set to the sky level. A new residual image is then calculated by subtracting the second image from the first one (which now lacks the profile of the candidate moving star). Because the moving object has now been removed from the first image, its second-epoch profile now shows up in its entirety in the residuals. This allows for an easy identification of the slow-moving objects, which would otherwise be canceling themselves out partially on the residual image.

*Search and match the moving star on the second epoch.* The profile of the object that was removed from the first image is then recursively shifted in  $X$  and  $Y$  and added to the residual image. If the star is indeed a moving object, there will be a near exact replica of it on the residual image. Because the second epoch has been subtracted from the first, the replica will be a negative source of similar flux. Hence, the object will cancel out its second-epoch replica when it is shifted by the  $\Delta X$  and  $\Delta Y$  that correspond to its motion on the plate between the first- and second-epoch images.

*Calculate likelihood.*—For each candidate moving object selected on the first-epoch image, the code identifies the best possible match for that star on the second-epoch image, within a radius of 1.5. The software distinguishes between actual moving objects and accidental matches of unrelated features based on the quality of the match. A probability index is calculated for each candidate moving object that is a function of (1) the difference in the object magnitude between the first and second epoch and (2) the difference in the magnitude density of the object between the first and second epoch. A detection thus has a high likelihood if the object has the same magnitude on both images, provided that the type of object (compact/extended) is also the same. Criterion (2) essentially prevents stars from being matched with galaxies and vice versa.

*Repeat for candidate moving objects from the second-epoch image.*—The procedure is repeated, but this time only the second-epoch counterparts are considered. The object is subtracted from the second-epoch image, residuals are recalculated, and the object is shifted until it cancels out its first-epoch profile, now showing in its entirety in the residuals. Note that this means that most high proper motion stars are identified *twice* by the code, once from their first-epoch location and once from their second-epoch location. This redundancy is necessary for the identification of stars whose profile is superposed on the profiles of other stars at either epoch (especially in fields with significant crowding). In effect, this increases the chance of detection for blended stars; the star will be detected even if it blended with another source in either of the two epochs. This is especially useful for faint stars moving in the vicinity of brighter objects or in crowded fields.

Once the image has been completely analyzed and searched, the code generates a list of all candidate moving objects along with their positions, relative proper motions (in pixels per year), integrated plate magnitudes, and likelihood index. The code uses the plate solutions and epochs (found in the image headers) to determine the local scale and orientation of the plates and calculate the magnitude (in arcseconds per year) and direction of the proper-motion vector on the sky. The software also extracts  $151 \times 151$  pixel<sup>2</sup> finder charts from the superposed images. These charts are extremely useful, as they are used to subsequently verify each and every detection by eye, on the computer screen.

## 2.2. Application to the Digitized Sky Surveys

The first epoch of the DSS in the northern sky consists of scans of photographic plates from POSS-I, obtained circa 1950. The scans were performed with the GAMMA machine by the

Catalogs and Surveys Branch at the Space Telescope Science Institute (STScI). Only the red plates (xx103aE emulsion + plexi) have been scanned. The second epoch of the DSS (XDSS) consists, for the northern sky, of scans of POSS-II (Reid et al. 1991). Images from the POSS-II include scans of plates from all three photographic bands of the survey: the blue (IIIaJ emulsion with GG385 filter), red (IIIaF emulsion with RG610 filter), and near-infrared (IVN emulsion with RG9 filter). The data from both the DSS and XDSS are publicly available from a variety of online databases.<sup>4</sup>

We divided the northern sky into 615,800 areas distributed on a grid with a separation of 12' in declination and a mean separation of 10' in right ascension. At every grid point, we extracted from the DSS (our first epoch) and XDSS (our second epoch—red band only) pairs of images each 17' × 17' on a side. We deliberately extracted images that are much larger than the grid point separation, thus allowing for a significant overlap between neighboring image pairs.

We allowed for a large overlap between neighboring subfields in part because of the required rotation of one of the images in the superposition process. Square subfields extracted from the DSS are generally not oriented with the  $Y$ -axis pointing toward the north celestial pole; rather they follow the local  $XY$  coordinates of the scanned POSS plates. As a result, pairs of images extracted from the DSS and XDSS are generally not aligned, and the XDSS image has to be rotated (by up to 30° at high latitudes) by the SUPER procedure. Areas near the corners of the square subfields are thus cut out. We therefore allow for a 1' wide band running along the edge of each subfield so that no gaps in sky coverage occur.

A large overlap is also required for completeness because a high proper motion star, to be detected by SUPERBLINK, must be present in a given subfield at each of the two epochs. A star that has moved from one subfield to another would not be detected as a moving object but rather as two distinct “variable” stars. A star with a proper motion  $\mu \leq 2''.0 \text{ yr}^{-1}$  can move up to 1.5 between the two epochs of the POSS-I and POSS-II. This is why we also allocated an additional band 1.5 wide running along the edge of each field, to help in the detection of stars with very large proper motions.

In summary, the different angular scales, scanning resolution, nonalignment of subfields, different pixellation grids and offsets between scans, and different image quality and limiting magnitude are all accounted for and corrected by SUPERBLINK.

All of our DSS scans were extracted from *The Digitized Sky Surveys* series of CD-ROMs, published by STScI. All the XDSS scans were downloaded off the Internet directly from the STScI archive (where they are stored on a CD-ROM jukebox), with kind permission of the STScI Catalogs and Surveys Branch. All subfields were processed as they were downloaded. Complete uploading/downloading and analysis of all 615,800 subfields was performed over a period of 11 months, from 2001 May through 2002 March. Computations were performed on a dual Pentium-III processor machine running Linux. Scripts were used to automate the procedure, and the downloading and processing of the whole northern sky with SUPERBLINK was completed with minimal user interaction. Most of our human effort went into the quality control phase, described in § 2.3.

### 2.3. Visual Confirmation of Candidates

False detections are inevitable when one is looking for high proper motion stars on photographic plates. The POSS plates

are filled with plate defects of different sorts, such as grains and bubbles in the emulsion, dust specks, and scratches. The plates also contain transient images left by solar system bodies (asteroid tracks) and the occasional meteor trail, narrow artificial satellite track (POSS-II only), or wide airplane track. A combination of plate defects and/or space junk may conspire to create the illusion, on a DSS/XDSS pair, of an object moving at a rate within our detection limits ( $0''.15 \text{ yr}^{-1} < \mu < 2''.00 \text{ yr}^{-1}$ ). Of course, SUPERBLINK automatically eliminates most such bogus detections with the requirement that candidate high proper motion stars must have comparable fluxes and flux densities on both plates. However, it is not uncommon to see plate defects of the same magnitude within arcseconds, or arcminutes, of each other on two different epochs, mimicking the behavior of a high proper motion star. This is especially true for faint features near the detection limit of the plate, which tend to be very numerous.

Another major source of false detections is the long diffraction spikes associated with the brighter stars. Because fields from the DSS and XDSS often do not have the same orientation on the sky, the position angles of the diffraction spikes change from the first to the second epoch. Once the two images are superposed and subtracted out in SUPERBLINK, diffraction spikes systematically show up as intense residual features. When the superposed images are blinked on the computer screen, the spikes display a remarkable rotating motion between the two epochs. This motion is of course recorded by SUPERBLINK, which systematically lists moving spikes as possible proper-motion objects. One solution that was considered at first was to reject any detection of a moving object within a certain distance of a bright star. However, after the detection of several faint high proper motion stars in the vicinity of bright diffraction spikes, we decided to investigate them all, to maximize the detection rate of genuine high proper motion stars.

The most direct and reliable way to eliminate false detections is by visually inspecting each and every candidate high proper motion star, using a blink comparator. A trained eye can easily distinguish real stars from plate defects, for objects down to a magnitude of  $r \approx 19$ . The XDSS also contains images in the  $B_J$  and  $I_N$  band, which can be used as a third epoch for confirmation of ambiguous objects.

Blinking each and every object identified by SUPERBLINK is a daunting task. However, the task is actually made easy (if only time consuming) thanks to the convenience of the finding charts generated by SUPERBLINK. The SUPERBLINK charts are more than just pairs of DSS/XDSS scans. While the first epoch of the chart is essentially the DSS image centered on the candidate moving object, the second epoch of the chart (as explained in § 2.1 above) is an XDSS image that has been processed and modified by SUPERBLINK to match the appearance and quality of the DSS image. Using simple software (designed by S. L.), it is possible to blink sequentially large numbers of finder charts, accepting and rejecting stars with a single keystroke, and automatically updating the list of confirmed high proper motion stars. With a little training, it is possible to quickly sift through hundreds of candidates, at a rate of about 1 star  $\text{s}^{-1}$ . False detections typically outnumber real objects by a factor of 3 to 4. The visual confirmation of  $\approx 60,000$  high proper motion stars carried out for this catalog thus represents a total of about 75 hr of intensive human inspection.

An interesting benefit of the 60,000 individual visual inspections was the identification of close proper motion pairs. The SUPERBLINK software does not discriminate between point sources and extended objects, and in the course of the survey, several extended objects were found to be moving. Many of these turned out to be double stars with small separations ( $\approx 1''\text{--}5''$ ).

<sup>4</sup> Including <http://archive.stsci.edu/>.

Close pairs, on the POSS plates, produce images that are sometimes elliptical, if the two stars are of equal magnitude, and sometimes “pear-shaped,” if the stars have different magnitudes. While these were all identified as single moving objects by SUPERBLINK, they were flagged as probable multiple systems during visual inspection. All those that could be confirmed were then listed as distinct objects in the catalog (see § 3.2 below).

### 3. BUILDING THE LSPM CATALOG

#### 3.1. Stars Identified with SUPERBLINK in the Digitized Sky Surveys

Using SUPERBLINK, we have successfully analyzed DSS/XDSS fields covering 99.23% of the northern sky ( $20,460 \text{ deg}^2$ ). Areas that were not analyzed include a small patch of sky north of  $87^\circ$  in declination ( $\approx 30 \text{ deg}^2$ ), which we avoided because of problems associated with the very large rotation angles required in the superposition of the first- and second-epoch images. SUPERBLINK also failed to analyze some 4766 scattered subfields, covering a total area of  $295 \text{ deg}^2$ ; these were rejected after SUPERBLINK was unable to superpose the two images because of the presence of a very bright, saturated object in the field. Rejected fields include all those containing a star brighter than 5th magnitude, fields containing cores of bright globular clusters, parts of M31, and of a few other extended and saturated objects.

Stars identified by SUPERBLINK with proper motions in the  $0''.15 \text{ yr}^{-1} < \mu < 2''.0 \text{ yr}^{-1}$  range and confirmed by visual inspection are found to disproportionately consist of slower moving objects. As the proper motion of a star is inversely proportional to the distance, a uniform density distribution of stars in the volume around the Sun is expected to result in a cumulative distribution inversely proportional to the cube of the proper motion. The objects identified with SUPERBLINK very closely follow such a  $N \sim \mu^{-3}$  relationship, as illustrated in Figure 1. The sharp drop in objects above  $\mu = 2''.0 \text{ yr}^{-1}$  and below  $\mu = 0''.15 \text{ yr}^{-1}$  simply results from the detection limits imposed on SUPERBLINK. While the upper limit was firmly set into the software, the lower limit has been set only for the purpose of the present catalog. We allowed SUPERBLINK to identify stars with proper motions as small as  $\mu = 0''.04 \text{ yr}^{-1}$  (totaling nearly one million objects), but only those with  $\mu < 0''.15 \text{ yr}^{-1}$ , considered the most valuable, were examined visually and retained for the present analysis. The much more numerous slower moving objects are only now being examined, and their publication is planned for a future release.

In the area analyzed by SUPERBLINK, the software identified a total of 56,238 objects with proper motions exceeding  $0''.15 \text{ yr}^{-1}$ . Among these, a total of 1159 objects were subsequently found to be double stars (see § 3.2 below) and are listed as two distinct objects in the LSPM catalog. This makes a total of 57,397 individual high proper motion objects identified with SUPERBLINK. The distribution on the sky is displayed in Figure 2, along with their distribution as a function of optical  $V$  magnitude (see § 4.4 for a discussion on how  $V$  magnitudes are derived for SUPERBLINK detections).

At magnitudes fainter than  $V=19$ , we observe a sharp drop in the number of high proper motion stars detected with SUPERBLINK. This reflects the limited capabilities of SUPERBLINK to detect stars near the magnitude limit of the POSS-I plates. While it is true that the POSS-II plates are marginally more sensitive, SUPERBLINK demands a detection at both epochs in order to identify the object as moving, and thus the detection threshold of SUPERBLINK is determined by the sensitivity of the POSS-I plates.

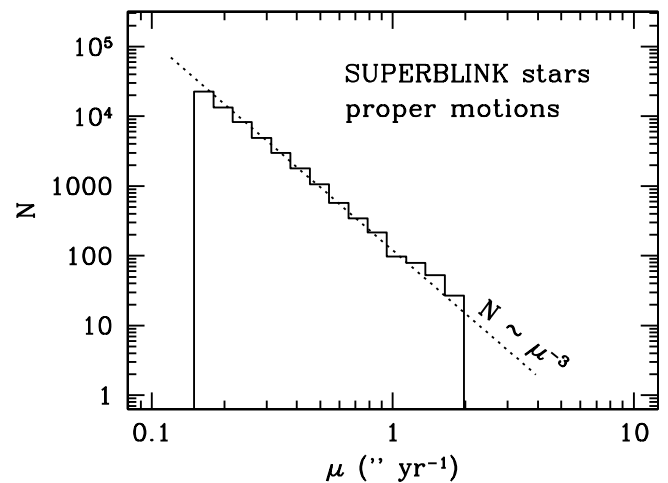


FIG. 1.—Distribution as a function of the proper motion of stars found with SUPERBLINK. The number density very closely follows a  $N \sim \mu^{-3}$  law (dashed line, this is not a fit).

At the bright end of the distribution ( $V < 12.0$ ), we observe a steady decline in the number of stars detected, falling to zero for  $V < 8$ . While one naturally expects to find fewer high proper motion stars with very bright magnitudes, many more high proper motion stars are known with ( $V < 12.0$ ) than have been detected by SUPERBLINK. The lack of stars detected at bright magnitudes reflects the inability of SUPERBLINK to deal with stars that have a strong saturated core on the photographic POSS-I and POSS-II plates. Tests made with fields containing known, bright high proper motion stars showed that SUPERBLINK generally does well with stars fainter than  $V = 10.0$ , correctly identifying them. However, tests revealed that SUPERBLINK has much trouble identifying brighter stars. What generally happens is that the BLINK procedure typically fails to determine the centroid of bright saturated stars and is thus unable to calculate a proper motion; such objects are simply rejected by the code. In the most extreme cases, i.e., for stars brighter than  $V = 4$ , a complete failure occurs in the SUPER procedure: the code is unable to superpose the two  $17' \times 17'$  subfields that display extended, saturated patches from the bright star. These fields are basically not processed by the code. Unfortunately, this also guarantees that any fainter high proper motion star that would normally be detected by SUPERBLINK but happens to be in a subfield occupied by a very bright star will also be missed by the code.

We identified all possible counterparts of the SUPERBLINK objects in the *Hipparcos* and *Tycho-2* catalogs (see § 3.3 below) and adopted for those stars the more precise proper motion value from the *Tycho-2* catalog. As a result, 91 SUPERBLINK objects that were initially above our proper-motion threshold were found to have *Tycho-2* proper motions below  $\mu = 0''.15 \text{ yr}^{-1}$ . These rejected objects are not considered in the current analysis and are not counted among the 57,397 stars officially identified with SUPERBLINK. The 57,397 SUPERBLINK stars form the core of our new LSPM catalog and include thousands of newly identified high proper motion stars.

#### 3.2. Resolved Common Proper Motion Doubles

Common proper motion doubles with separations in the range  $\approx 1'' - 10''$  are not uncommon in the field. These objects usually show up on the POSS plates as elongated, or oddly shaped, objects and can be mistaken for distant galaxies or short asteroid tracks. Our SUPERBLINK software identifies all moving objects,

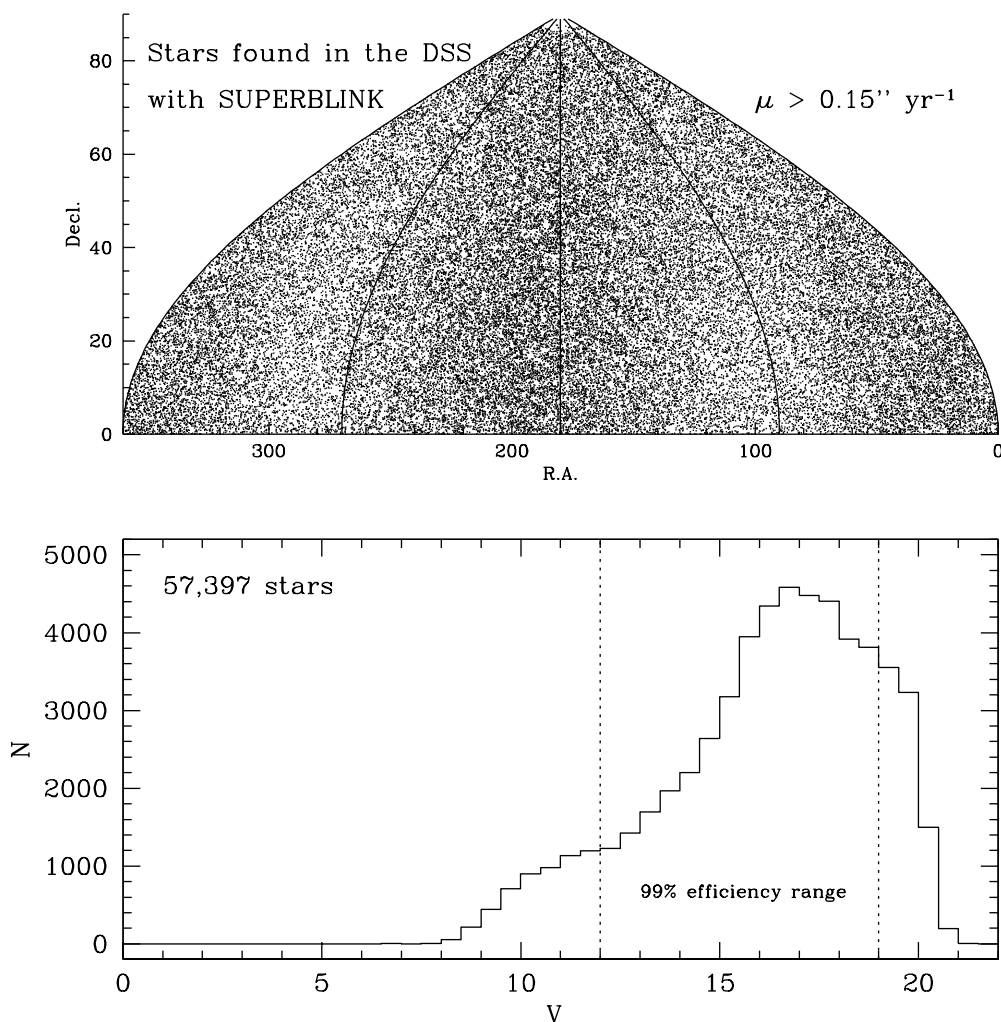


FIG. 2.—*Top*: distribution on the north celestial hemisphere of the 57,763 high proper motion stars identified in the DSSs with the SUPERBLINK software. *Bottom*: distribution as a function of optical  $V$  magnitude. The detection efficiency of SUPERBLINK exceeds 99% in the magnitude range  $12.0 < V < 19.0$ . The efficiency drops for brighter ( $V < 12$ ) stars as the stellar images become saturated on the POSS plates and at fainter magnitudes ( $V > 19$ ) as one reaches the POSS plate limit. The turnover in the distribution beyond  $V = 16$  is real and is not a result of a declining detection rate. It occurs because proper-motion-selected samples survey a limited volume, combined with the fact that field stars also have a turnover in their luminosity function.

regardless of their shape, and so it picks out barely resolved common proper motion doubles just as well as single stars. On visual inspection, any moving object with an odd shape is flagged for further analysis.

Objects flagged as possible common proper motion doubles are searched for in the 2MASS All Sky Point Source Catalog to see whether they are featured as pairs of stars. The resolution of the 2MASS infrared CCD images is significantly better than the POSS plates, and pairs of objects with separations smaller than  $1''$  are often resolved. We found that the vast majority of the stars that were initially flagged by us as possible doubles indeed did show up as pairs of resolved stars in the 2MASS catalog.

All the objects found by SUPERBLINK were eventually searched in the 2MASS catalog, in order to determine their infrared ( $J$ ,  $H$ , and  $K_s$ ) magnitudes (see § 4.2 below). In this process, several more objects identified by SUPERBLINK and not initially flagged by us as candidate doubles were also found to be resolved into pairs in 2MASS.

Using all available images from the DSS (POSS-I, POSS-II in three colors) plus the 2MASS Quicklook Images obtained from the NASA/IPAC Infrared Data Archive,<sup>5</sup> we examined all

the pairs to determine whether they were actual common proper motion doubles or chance alignments. We found about equal numbers of each. In areas with significant crowding (low Galactic latitude fields) there were an abundance of cases in which the high proper motion star happened to be in the vicinity of a background source; these were easily filtered out by noticing that the background source had not moved between the POSS-I/POSS-II and 2MASS epochs. In most other cases, it was clear from the POSS scans and 2MASS images that we were dealing with a moving pair. There were only a few ambiguous cases, for which we conservatively assumed the star to be single.

In the end, we resolved 1159 SUPERBLINK objects into common proper motion pairs; each component is included in the LSPM catalog as a separate entry. However, since it was generally not possible to obtain proper motions for each component individually (SUPERBLINK only gave a proper motion for the pair), the two stars are listed as having exactly the same proper motion. This, of course, is only approximate, and one should not conclude that the two stars do not show any significant relative proper motion.

A number of common proper motion doubles were already listed as such in the NLTT catalog. In those instances, we have tried to assign the correct NLTT numbers for each star of the

<sup>5</sup> See <http://irsa.ipac.caltech.edu/applications/2MASS/QL/interactive.html>.

pair. To check our assignments, we have first used the coordinates listed in the NLTT to determine which star of the pair was to the north or east of the other. In many cases, the two stars were listed in the NLTT as having exactly the same position. In those cases, we looked for notes to the NLTT catalog, which usually specified the position angle of the secondary.

A separate paper (Lépine et al. 2005, in preparation) will provide a detailed analysis of all the common proper motion doubles identified in our survey.

### 3.3. Additional Stars from the Tycho-2 and ASCC-2.5 Catalogs

Our SUPERBLINK survey of the POSS plates has a bright magnitude limit that limited our identification of very bright ( $V < 12$ ) high proper motion stars. In order to build a catalog that is the most complete possible, we need to complement the SUPERBLINK stars with lists of known, bright high proper motion stars.

The two sources we used to complement our catalog are the Tycho-2 Catalogue of the 2.5 Million Brightest Stars (Tycho-2) and the All-sky Compiled Catalogue of 2.5 million stars (ASCC-2.5). The Tycho-2 catalog (Høg et al. 2000) is the product of a reanalysis of data from the ESA *Hipparcos* satellite and combines space-determined positions and proper motions for 2.5 million of the brightest stars in the sky (the catalog is complete down to about  $V_T = 12$ ) with ground-based astrometry from a variety of sources. The ASCC-2.5 (Kharchenko 2001) is a catalog largely built from the Tycho-2 catalog and the *Hipparcos* and Tycho Catalogues (ESA 1997) and providing essentially similar information on positions and proper motions. However, the ASCC-2.5 includes complete data on a number of stars whose proper motions and/or photometric data were missing in the Tycho-2 (including stars from the Tycho-2 supplement-1, which contains all *Hipparcos* stars not listed in the Tycho-2 catalog). The ASCC-2.5 also includes astrometric information (including proper motions) on an additional number of fainter stars, obtained from various ground-based astrometric surveys. The ASCC-2.5 extends the Tycho-2 catalog down to slightly fainter magnitudes.

The Tycho-2 catalog was used as our primary source of bright, high proper motion stars, while the ASCC-2.5 was used as a complement to the Tycho-2. We extracted from Tycho-2 all stars listed with proper motions exceeding  $\mu = 0''.15 \text{ yr}^{-1}$ . We found 8,225 objects in the northern sky spanning a range in magnitude  $2.1 < V < 13.6$  (see § 4.4 for our derivation of  $V$  magnitudes from the Tycho-2  $V_T$  and  $B_T$  magnitudes), with 93% of the stars brighter than  $V = 12.0$  (Fig. 3). Scanning the ASCC-2.5 catalog for additional objects, we identified 5239 stars listed with a proper motion  $\mu > 0''.15 \text{ yr}^{-1}$  that were not listed in the Tycho-2 or whose proper-motion data were unavailable in Tycho-2. The additional ASCC-2.5 stars spanned a range in magnitude  $0.0 < V < 15.5$  but with 95% of the objects fainter than  $V = 10.0$ . The vast majority of the  $V < 10$  stars in the ASCC-2.5 catalog are listed in the Tycho-2.

A comparison of the list of bright Tycho-2/ASCC-2.5 high proper motion stars with the list of SUPERBLINK detections indicated that 4252 of the Tycho-2 stars and 3603 of the ASCC-2.5 stars were already in the list of  $\mu > 0''.15 \text{ yr}^{-1}$  stars detected by SUPERBLINK. Among the stars that were not found in the SUPERBLINK list, there were significant numbers of objects with a Tycho-2/ASCC-2.5 proper motion close to the  $0''.15 \text{ yr}^{-1}$  limit of our initial list of SUPERBLINK detections. We thus surmised that some might have been detected by SUPERBLINK but ranked in a lower proper-motion range. This is especially true of brighter ( $V < 10$ ) stars that are strongly satu-

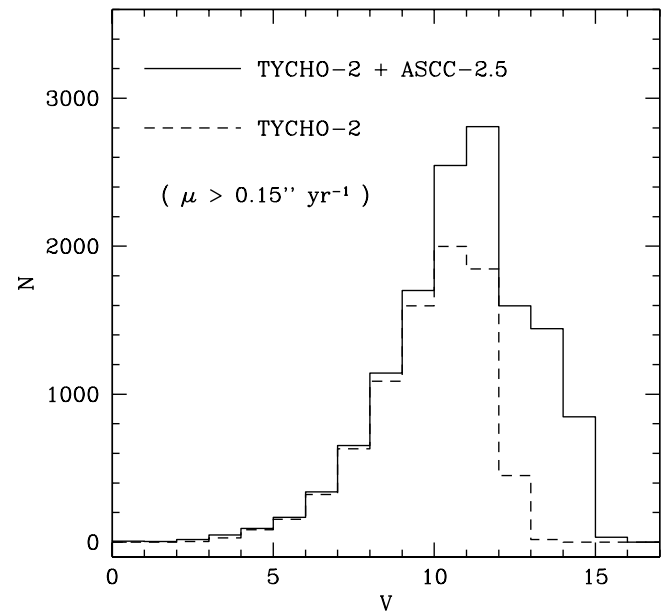


FIG. 3.—Distribution as a function of magnitude for stars listed in the Tycho-2 and ASCC-2.5 catalogs with proper motions larger than  $0''.15 \text{ yr}^{-1}$ . The dashed lines show stars listed only in Tycho-2, while the full line shows the full set of Tycho-2 stars complemented by additional objects from the ASCC-2.5 catalog. The complete set is most probably complete down to  $V = 10$  but has a sharp drop in completeness fainter than  $V = 12$ , at which point, fortunately, the detection efficiency of SUPERBLINK reaches high levels (see Fig. 2).

rated on the POSS plates and thus have larger SUPERBLINK proper-motion errors. We searched for possible matches in a preliminary list of stars found by SUPERBLINK with calculated proper motion  $0''.10 \text{ yr}^{-1} < \mu < 0''.15 \text{ yr}^{-1}$ . We found matches to an additional 846 Tycho-2 and 21 ASCC-2.5 stars. Because our Tycho-2 sample contains brighter stars on average than our ASCC-2.5 sample, it comes as no surprise that most of the additional matches were from Tycho-2 objects (whose proper motion errors in SUPERBLINK are larger).

This left us with 3127 stars from Tycho-2 and 1615 stars from ASCC-2.5 that had not been detected by SUPERBLINK. On visual inspection of DSS/XDSS images centered on those objects, we discovered that *a significant fraction of them do not show any detectable proper motion*. This suggests that some of the Tycho-2/ASCC-2.5 stars had their proper motions overestimated, which would explain why they were not identified by SUPERBLINK.

In order to verify the proper motions quoted in the Tycho-2 and ASCC-2.5 catalogs, we identified counterparts for all these objects in the 2MASS All-Sky Catalog. We then recalculated their proper motions using the 2MASS positions (epochs 1997–2001) and the *Hipparcos*-based positions from the Tycho-2 and ASCC-2.5 catalogs (epoch 1991.25). The 2MASS positions for these bright stars are accurate to about 120 mas, which means that it should be possible to derive proper motions to an accuracy of  $12 \text{ mas yr}^{-1}$  (for a 10 yr baseline) to  $20 \text{ mas yr}^{-1}$  (for a 6 yr baseline). This assumes, of course, that the Tycho-2 and ASCC-2.5 positions are significantly more accurate than the 2MASS positions (as they should be).

Results showed that a few hundred of the Tycho-2 stars and over a thousand of the ASCC-2.5 stars had been missed by SUPERBLINK for a good reason: their actual proper motion is definitely below our adopted threshold of  $0''.15 \text{ yr}^{-1}$ . Figure 4 compares the proper motions quoted in the Tycho-2/ASCC-2.5 catalog with the proper motions determined from the differences

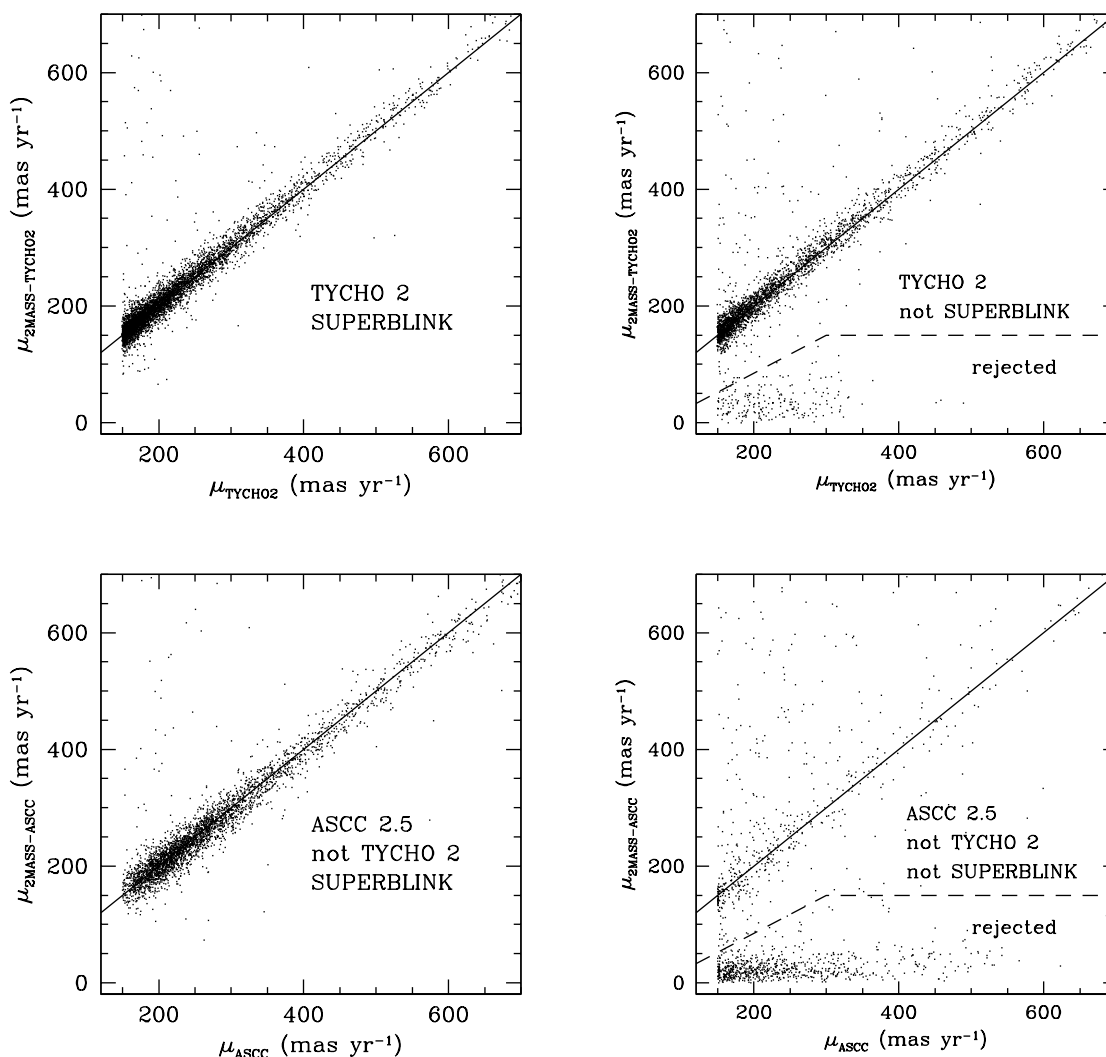


FIG. 4.—Comparison between the proper motions quoted in the Tycho-2/ASCC-2.5 catalogs (*abscissa*) and the proper motions calculated from the difference between the 2MASS position (epoch 1997-2001) and the Tycho-2/ASCC-2.5 position (epoch 1991.25). *Top left*: 5098 high proper motion stars from Tycho-2 that have been recovered by SUPERBLINK. *Bottom left*: 3624 stars from the ASCC-2.5 (but not listed in Tycho-2) that have been recovered by SUPERBLINK. *Top right*: 3127 stars from the Tycho-2 catalog that have not been recovered by SUPERBLINK (mostly because they are too bright for SUPERBLINK to handle). *Bottom right*: 1615 stars from the ASCC-2.5 catalog (but not in Tycho-2) that were not recovered by SUPERBLINK. A significant fraction of the Tycho-2/ASCC-2.5 stars that were not recovered by SUPERBLINK are found to have 2MASS-derived proper motions inconsistent with their quoted values (*areas below dashed lines*). These have not been included in the LSPM catalog.

in the 2MASS and Tycho-2/ASCC-2.5 positions. We plot the results separately for four groups of objects: (1) stars from the Tycho-2 catalog that were also recovered by SUPERBLINK (*top left*), (2) stars not listed in the Tycho-2 catalog but listed in the ASCC-2.5, and that were identified by SUPERBLINK (*bottom left*), (3) stars listed in Tycho-2 that were not recovered by SUPERBLINK (*top right*), and (4) stars in the ASCC-2.5 but not in Tycho-2 and that were not identified by SUPERBLINK (*bottom left*). First of all, the top left and lower left plots show that there is a good correlation between the 2MASS-derived proper motions and those quoted in Tycho-2 and ASCC-2.5, at least for stars that had their proper motions confirmed by SUPERBLINK. We find a dispersion of  $15 \text{ mas yr}^{-1}$  in the difference between the Tycho-2– and 2MASS-derived proper motions and  $18 \text{ mas yr}^{-1}$  in the difference between the ASCC-2.5– and 2MASS-derived proper motions, in good agreement with the predicted values (see above). There are very few outliers in the distribution, with perhaps a few dozen stars (out of several thousand) whose 2MASS-derived proper motion appears to be clearly overestimated, which can be accounted for by an

occasional, large error in the 2MASS or Tycho-2/ASCC-2.5 position.

The upper right and lower right plots, on the other hand, tell quite a different story. A significant number of stars are found to have 2MASS-derived proper motions around and below  $50 \text{ mas yr}^{-1}$ . Given the positional errors on the 2MASS positions, these values are consistent with the stars having no detectable proper motion. We have visually inspected DSS/XDSS pairs of images for over a hundred stars rejected in the procedure and confirmed that indeed none of these stars showed any significant proper motion. The dashed lines in Figure 4 shows where we have set the limits under which a star is considered to have no measurable proper motion, in which case the quoted Tycho-2/ASCC-2.5 proper motion is assumed to be in error. A total of 230 Tycho-2 and 917 ASCC-2.5 presumed high proper motion stars were thus determined to be actual low proper motion objects.

Erroneous proper-motion entries in the Tycho-2 catalog are certainly cause for concern. We note that most of them are associated with stars near the faint end of the Tycho-2 catalog (Fig. 5);

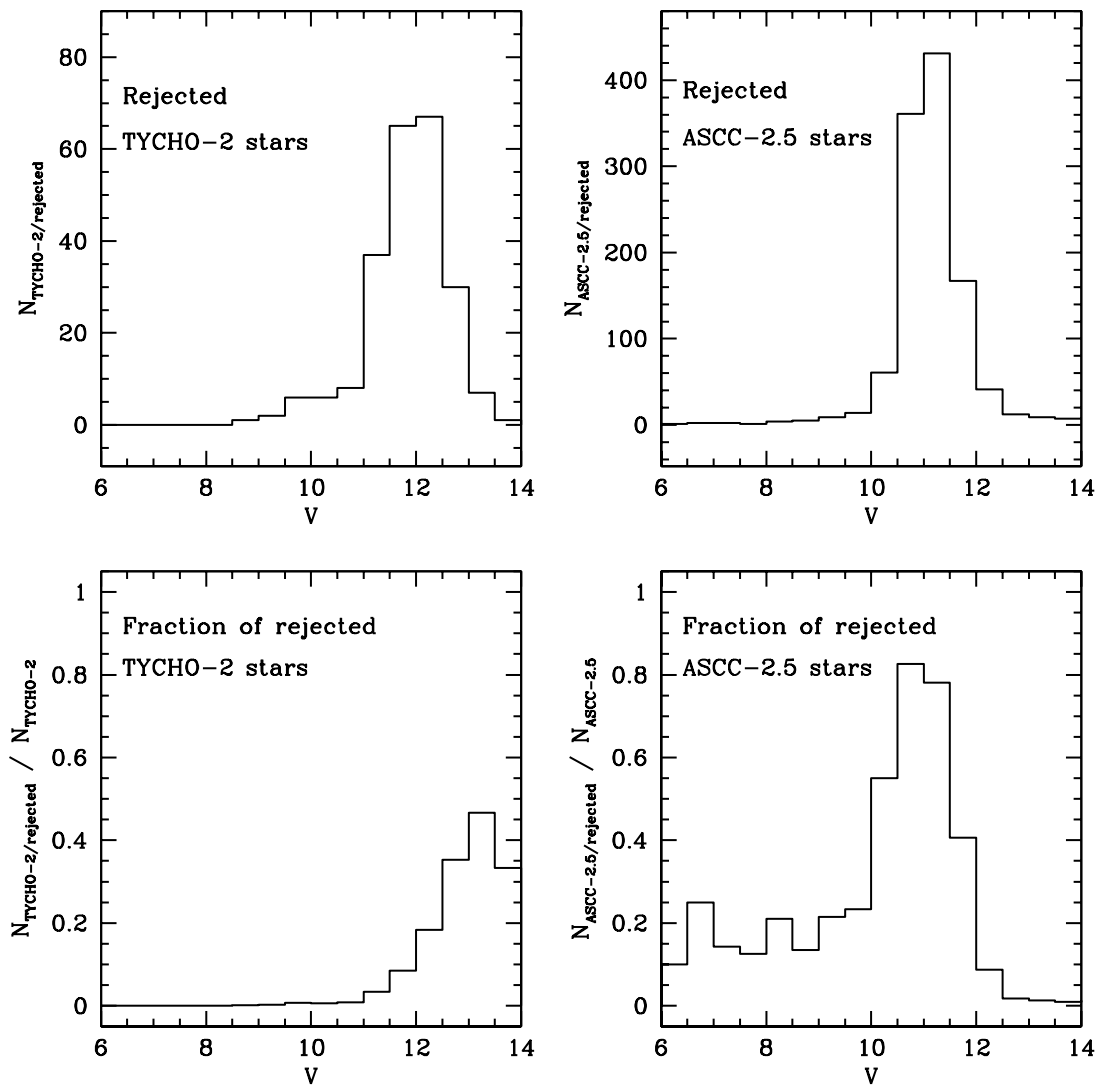


FIG. 5.—*Top left*: distribution as a function of  $V$  magnitude of Tycho-2 stars that have not been included in the LSPM catalog (see Fig. 4). *Top right*: same, but for additional stars from the ASCC-2.5 catalog, i.e., stars in the ASCC-2.5 catalog listed with  $\mu > 0''.15 \text{ yr}^{-1}$  and that have no Tycho-2 counterparts. The fractional contribution of these misidentified high- $\mu$  stars to the full Tycho-2/ASCC-2.5 samples is shown in the bottom plots. Up to  $\approx 40\%$  of the  $V > 12.5$  Tycho-2 stars listed with  $\mu > 0''.15$  do not actually have large proper motions. While a very significant fraction ( $\approx 65\%$ ) of the  $10 < V < 12$  ASCC-2.5 (non-Tycho-2) stars are bogus, almost all of the  $V > 12$  object are correctly identified. (Note that most of the latter have also been identified with SUPERBLINK.)

most erroneous entries have  $V \approx 12$ . We plot in Figure 5 the fraction of Tycho-2 stars with quoted proper motion  $\mu > 150 \text{ mas yr}^{-1}$  that actually made it into the LSPM catalog. One can see that fully 20% of  $V > 12$  stars were found to be low proper motion objects.

Furthermore, we could not find any 2MASS counterpart for 230 of the ASCC-2.5 stars. Visual inspection of DSS/XDSS images showed no trace of these stars at the position quoted in the ASCC-2.5, and no high proper motion star was found within  $2'$  of the quoted position. We thus assume these entries to be bogus, although we cannot rule out the possibility of a very large error (several arcminutes) in the quoted ASCC-2.5 position.

In addition, there were 66 Tycho-2 stars and 239 ASCC-2.5 stars that are listed as close visual companions of brighter Tycho-2 objects. These are not resolved on the 2MASS images and thus have no 2MASS catalog counterparts. They are, of course, not resolved on the DSS/XDSS images either, and we thus cannot obtain an independent confirmation of their existence. (We also found no mention of them in the Luyten catalogs.) We refrain from

including them in the LSPM catalog at this point, while we are still investigating their status. We do point out that at least all the primary components are in the LSPM, which should make these secondaries (and probably many more unsuspected ones) easy to recover eventually.

In the end, we were left with 2831 stars from Tycho-2 and 229 stars from ASCC-2.5 that are bona fide high proper motion stars. Each of these stars has been included in the LSPM catalog. The vast majority of those additions are stars brighter than  $V = 10$ . Their distribution on the celestial sphere is shown in Figure 6. We find that 271 of the additional Tycho-2/ASCC-2.5 stars are located in areas that were not processed by SUPERBLINK. These areas include the north polar cap and all areas containing very bright stars that could not be overlapped properly with the SUPER procedure. The distribution of those stars as a function of  $V$  magnitude is plotted separately in Figure 6. It is obvious that many of the rejected areas are coincident with very bright stars, as the rejected fields contain a disproportionate number of  $V < 5$  objects. We finally find 2775 stars with proper motion  $\mu > 0''.15 \text{ yr}^{-1}$  in fields that were analyzed by

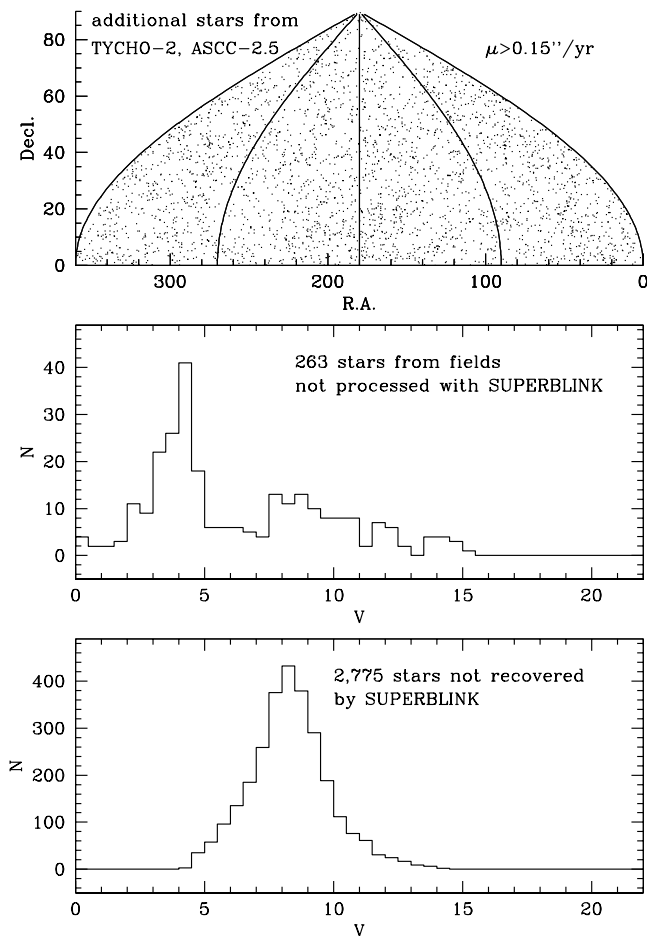


FIG. 6.—High proper motion stars listed in the Tycho-2/ASCC-2.5 catalogs that were not recovered by SUPERBLINK. *Top*: distribution on the northern celestial hemisphere. *Center*: distribution as a function of magnitude of the 278 stars that were in areas of the northern sky not processed with SUPERBLINK ( $325 \text{ deg}^2$ ). *Bottom*: distribution as a function of magnitude of the 3787 stars missed by SUPERBLINK because they were too bright and their images saturated on the DSS scans. These additional bright high proper motion stars have all been incorporated into the LSPM catalog.

SUPERBLINK but that were missed by the code. Their distribution peaks at a magnitude  $V \simeq 8.5$  and spans a range in magnitude in which the efficiency of the SUPERBLINK software is limited because of saturation on the POSS plates.

### 3.4. Additional Stars from the LHS and NLTT Catalogs

A comparison with the LHS and NLTT catalogs reveals a small number of stars that are absent from our list of SUPERBLINK detection and that are too faint to be in the Tycho-2 and ASCC-2.5 catalogs. All the objects were investigated individually in order to determine whether they are real and whether they should be added to the LSPM catalog.

First of all, the LHS includes a list of 13 faint stars with proper motions exceeding  $\mu = 2.0'' \text{ yr}^{-1}$ ; much too fast to have been detected with SUPERBLINK. Generally, LHS stars with very large proper motions also happen to be relatively bright and are thus also present in the Tycho-2 catalog. However, those 13 LHS stars are fainter than  $V = 14$ , which explains why they are not in the Tycho-2/ASCC-2.5 catalogs either. In any case, they were easily reidentified by direct inspection of DSS scans and have been added to the LSPM catalog.

Second, and most importantly, a significant number of NLTT stars that are not in the LSPM were actually recovered

by SUPERBLINK but found to have proper motions below the  $0.15'' \text{ yr}^{-1}$  cutoff of the current version of the LSPM catalog. There are also 214 bright NLTT stars that are listed in Tycho-2 as  $\mu < 0.15'' \text{ yr}^{-1}$  stars. From a search of a preliminary list of  $0.10'' \text{ yr}^{-1} < \mu < 0.15'' \text{ yr}^{-1}$  high proper motion stars identified with SUPERBLINK, we also recovered an additional 1204 stars from the NLTT catalog. A small fraction of these stars were already listed in the NLTT catalog as having low proper motions, but most were listed with having proper motions  $0.18'' \text{ yr}^{-1} < \mu < 0.25'' \text{ yr}^{-1}$ .

Third, we found 161 additional NLTT stars that are actually listed in the NLTT as close companions ( $< 10''$ ) of brighter NLTT objects. These companions are not resolved on the POSS scans, and neither are they resolved on the 2MASS images, which explains why they did not show up in our initial search. However, Luyten provided separations and position angles for most common proper motion doubles in the NLTT in a comment line, which is available in the electronic version of the catalog. Using this information, we rederived the locations of those companions (using the revised positions of the primaries) and included the companions as separate LSPM entries. Exceptionally for those secondaries, the quoted optical  $b$  and  $r$  magnitudes (in our LSPM catalog) are directly recopied from the NLTT catalog.

While investigating potential NLTT secondaries that might have been missed in our initial search, we also found 39 duplicate entries. These stars are apparently objects whose positions and/or proper motions have been remeasured at some point, but for which the initial, erroneous entry had been kept in the NLTT catalog by mistake. They can be easily identified in that while the two stars were supposed to be two objects of equal magnitude and colors within  $20''\text{--}60''$  of each other, only one object of the pair was found on the DSS scans. The fact that the two entries are listed in the NLTT catalog with *exactly* the same magnitude and color betrays the fact that they are indeed one and the same.

A more time-consuming job was to investigate the existence of the remaining 900 or so NLTT stars that remained unaccounted for. Our methodology was simple: we retrieved pairs of  $17' \times 17'$  DSS/XDSS scans centered on the quoted positions of the NLTT stars. The pairs were aligned (shift-rotated) using SUPERBLINK subroutines and examined by eye by blinking them on the computer screen. We searched for the presence of a moving object within a  $5' \times 5'$  area centered on the presumed location of the NLTT star. In 395 fields, no moving object could be found whatsoever. In those instances, we must assume that the NLTT entry is bogus. In seven more cases, we did recover a moving object, but its proper motion was very clearly smaller than our  $0.15'' \text{ yr}^{-1}$  limit. All of these NLTT stars, none of which were included in the LSPM catalog, are listed in a separate table in the Appendix.

Finally, we positively identified a total of 492 NLTT stars from the DSS/XDSS scans, with proper motions in the  $0.15'' \text{ yr}^{-1} < \mu < 0.4'' \text{ yr}^{-1}$  range (Fig. 7). Of those genuine high proper motion stars, a total of 174 were found to be located in areas that were initially mishandled and rejected by SUPERBLINK and that were thus not part of the survey. In particular, there were 40 stars located north of  $\delta = 86.5^\circ$ , the area near the north celestial pole that was not properly processed.

The distribution of stars in areas not analyzed by SUPERBLINK very closely follows the distribution of high proper motion stars detected by SUPERBLINK in the rest of the sky, if Tycho-2/ASCC-2.5 stars are excluded. In Figure 7, we superpose (*dotted line*) the distribution of SUPERBLINK objects that do not have a Tycho-2 or ASCC-2.5 counterpart over the

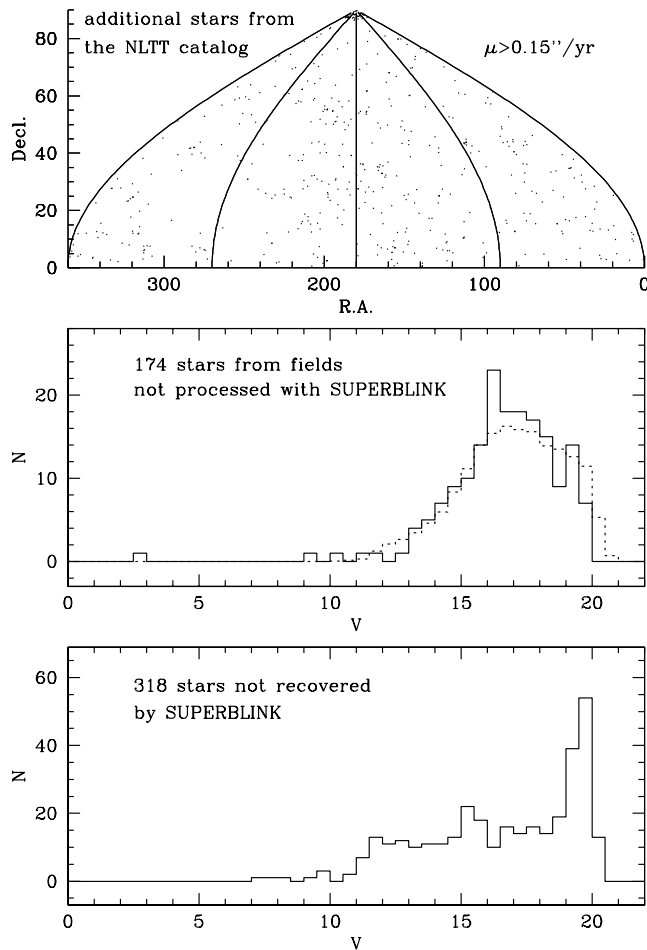


FIG. 7.—High proper motion stars listed in the LHS and NLTT catalogs of high proper motion stars but that were not recovered by SUPERBLINK and are not listed in the Tycho-2 catalog either. *Top*: distribution on the northern celestial hemisphere (Aitkins projection). *Center*: distribution as a function of magnitude of the 174 stars that were in areas of the northern sky not processed with SUPERBLINK ( $325 \text{ deg}^2$ ). The normalized distribution of SUPERBLINK stars found in the rest of the sky and that are not in the Tycho-2/ASCC-2.5 catalog is shown for comparison (dotted line). *Bottom*: distribution as a function of magnitude of the 318 stars missed by SUPERBLINK. These stars have all been added to our catalog.

distribution of additional NLTT stars found in the areas not analyzed by SUPERBLINK. The two curves are in very close agreement, with a peak around  $V = 17$ . (The main difference is that the SUPERBLINK distribution extends to slightly fainter magnitudes, which is consistent with a higher completeness of SUPERBLINK over the NLTT beyond  $V = 19$ .) This is exactly what is expected for stars that are missing because they are outside the SUPERBLINK survey areas: they should follow the same general magnitude distribution as the stars extracted inside the SUPERBLINK survey areas.

The remaining 318 NLTT stars are in areas that were processed by SUPERBLINK but that were nevertheless missed by the code. Several of these elusive objects were within  $1'$  of very bright stars at one of the POSS-I or POSS-II epochs, were close to plate edges, or were coincident with local plate defects, making their identification difficult. The distribution of these stars with  $V$  magnitude is skewed toward very faint objects (see Fig. 7, *bottom*), with a peak at magnitude  $V = 19.5$ . This marks the range at which SUPERBLINK is beginning to suffer from incompleteness, as it reaches the magnitude limit of the POSS-I plates.

### 3.5. Other Additional Objects

Two more stars that were included in our catalog are objects with very large proper motions that were discovered in the past two years. Both are too faint to have been in the Tycho-2 or ASCC-2.5 catalogs, and because they are very recent additions, they are, of course, not in the Luyten catalogs either.

The first star is LSR 1826+3014, discovered by Lépine et al. (2002). The star has a proper motion  $\mu = 2''.38 \text{ yr}^{-1}$  and a magnitude  $V = 19.4$ . In our catalog, it bears the name LSPM J1826+3014. The star was actually discovered in the course of our own survey but is regarded as a serendipitous discovery: it was not initially identified as a high proper motion star by SUPERBLINK but rather as a pair of variable stars within  $2'$  of each other, which we examined further out of curiosity. This makes one seriously consider the possibility that there still exist faint stars with very large proper motions waiting to be discovered.

The second star is the extremely high proper motion object SO 025300.5+165258 discovered by Teegarden et al. (2003). The star has a proper motion  $\mu = 5''.05 \text{ yr}^{-1}$  and a magnitude  $V = 15.4$  and is identified as LSPM J0253+1652 in our catalog. It is believed to be a very nearby star. Its extremely large proper motion is beyond the detection limit ( $2''.0 \text{ yr}^{-1}$ ) of SUPERBLINK. What is interesting is that the survey by Teegarden et al. (2003) that led to its discovery was initially aimed at the identification of solar system objects and uses a temporal baseline of months to a few years. It thus appears that a pair of all-sky surveys with a short separation in time (e.g., 1–2 yr) might well lead the way to locating any possible remaining faint stars with proper motions in excess of  $2''.0 \text{ yr}^{-1}$ .

We note that most of the L dwarfs and T dwarfs discovered in recent years (Kirkpatrick et al. 1999, 2000; Hawley et al. 2002; Cutri et al. 2003) very probably have proper motions within the range of our catalog; however, no effort was made to include any high proper motion brown dwarf at this point. Proper motions have so far been determined only for a small number of L and T dwarfs (Dahn et al. 2002), and additional work would be required to obtain accurate proper motions for most of them. For now, we have limited ourselves to the very few L dwarfs that do show up on the POSS-I and POSS-II plates and that were recovered by SUPERBLINK, although we do plan to add high proper motion brown dwarfs to the LSPM catalog in the near future.

Adding up all the stars found by SUPERBLINK, those retrieved from the Tycho-2 and ASCC-2.5 catalog, the LHS/NLTT stars missed by our code, and the two additional objects discussed in this section, we come to a total and final tally of 61,618 stars in the LSPM catalog.

### 3.6. Counterparts in the UCAC2 Astrometric Catalog

The Second US Naval Observatory CCD Astrograph Catalog (UCAC2) is the second release in an all-sky astrometric survey of stars in the magnitude range  $7.5 < R_F < 16.0$  (Zacharias et al. 2004). The current version lists 48,330,571 stars in the declination range  $-90 < \text{decl.} < +50$ , and gives positions with an accuracy of 20–70 mas (depending on magnitude). It also provides proper motions for all cataloged stars with an accuracy  $\sim 5 \text{ mas yr}^{-1}$ .

We found UCAC2 counterparts for 9151 of the LSPM stars. All the counterparts are south of  $\text{decl.} = +53^\circ 23'$ , reflecting the current, limited sky coverage of the UCAC2 (Fig. 8). Fewer stars are found below a declination of  $10^\circ$ , where the UCAC2 apparently has a brighter magnitude limit ( $V < 12$ ). Overall, the UCAC2 lists stars down to a magnitude  $V \simeq 16.0$  but appears to be significantly incomplete for high proper motion stars at all magnitudes and positions.

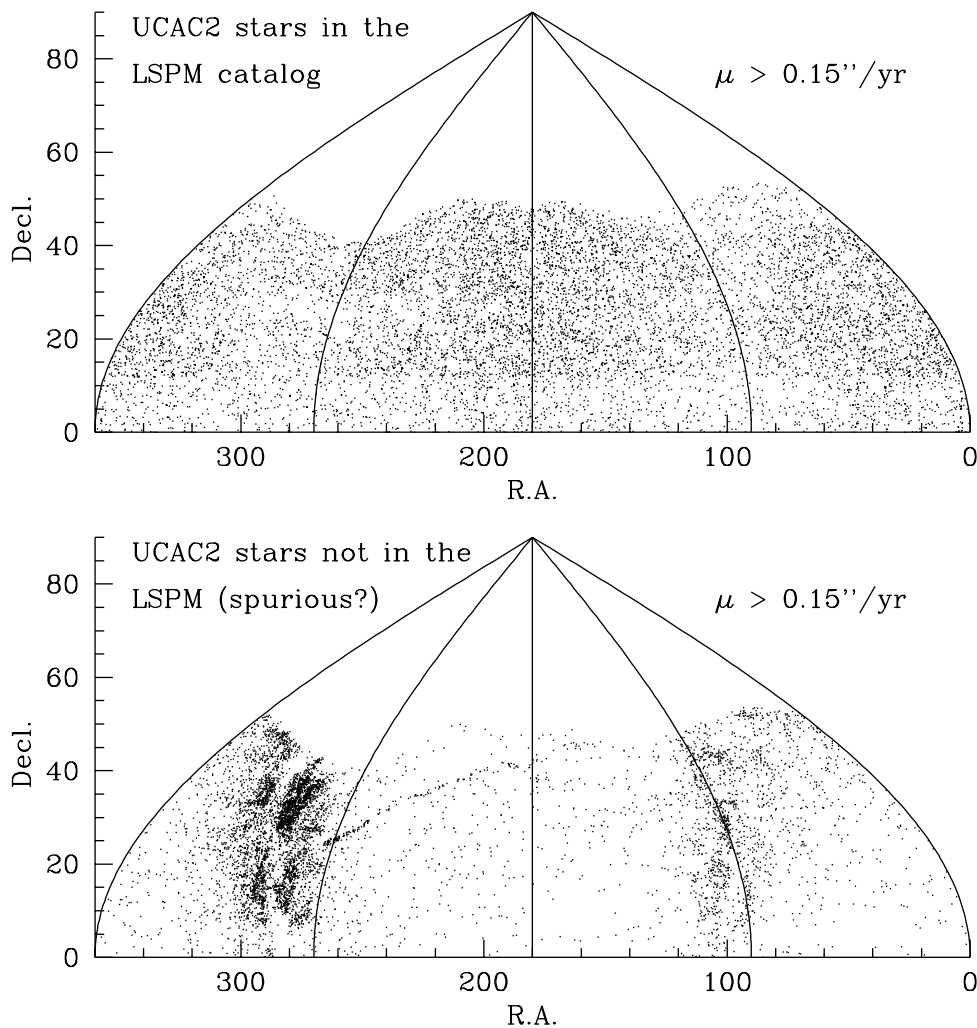


FIG. 8.—High proper motion stars in the UCAC2 astrometric catalog. *Top*: positions of 9151 stars with  $\mu > 0.15 \text{ yr}^{-1}$  that are also listed in our LSPM catalog. *Bottom*: positions of 7370 stars listed in the UCAC2 as having proper motions  $\mu > 0.15 \text{ yr}^{-1}$  but that are not in the LSPM; these appear to be spurious entries.

Although we were initially hoping to use the UCAC2 as an additional source of bright stars with large proper motions for the LSPM catalog, we found this to be impractical at this point. The main reason is that it appears that the UCAC2 is plagued with a large number of spurious high proper motion entries. We retrieved all the stars in the UCAC2 that are in the northern sky and listed as having a proper motion exceeding  $0.15 \text{ yr}^{-1}$ . Apart from the 9168 objects also listed in our LSPM catalog, we found an additional 7370 entries (see Fig. 8) with a very nonuniform distribution. The vast majority of the additional entries are located at low Galactic latitudes, and they have cataloged proper motions in the range  $0.15 \text{ yr}^{-1} < \mu < 0.25 \text{ yr}^{-1}$ . Our examination of several DSS/XDSS scans centered on the presumed location of those stars failed to reveal any of them as high proper motion objects.

Good UCAC2 counterparts do, however, prove useful as a means to estimate the astrometric accuracy of the LSPM from an independent source. A comparison of the UCAC2 and LSPM positions and proper motions for the stars common to both catalogs is presented in §§ 4.3 and 4.4 below.

#### 4. PHOTOMETRY

##### 4.1. Optical Magnitudes from Tycho-2 and ASCC-2.5: $B$ and $V$

Optical  $B_T$  and  $V_T$  magnitudes are obtained from Tycho-2 catalog counterparts (see § 3.3 above). Photometric errors are

0.013 mag for  $V_T < 9$  and 0.1 mag for  $9 < V_T < 12$ . A simple conversion transforms these into Johnson  $B$  and  $V$  magnitudes:

$$B = B_T - 0.24(B_T - V_T), \quad (1)$$

$$V = V_T - 0.09(B_T - V_T), \quad (2)$$

following the prescription in the introduction to the *Hipparcos* and Tycho catalogs.

The ASCC-2.5 catalog provides both  $B$  and  $V$  magnitudes (converted from  $V_T$  and  $B_T$ ) and can also be used as a relatively reliable source of optical magnitudes for bright stars. In particular, we are using it to obtain magnitudes of bright stars that are not listed in the Tycho-2 catalog. For stars fainter than about  $V = 12.0$ , ASCC-2.5 magnitudes are derived from a variety of sources and may not be as accurate as the Tycho-2 magnitudes, but since they were obtained from photoelectric or CCD measurements, they should be relatively reliable.

We have gathered  $B$  and  $V$  magnitudes from Tycho-2/ASCC-2.5 for a total of 11,719 LSPM stars. The fraction of stars with Tycho-2/ASCC-2.5 optical photometry is plotted in Figure 9 as a function of  $V$ . It shows that the LSPM contains reliable optical photometry for essentially all stars brighter than  $V = 12.0$ . This is fortunate, because these are stars for which photographic magnitudes are subject to large errors, because of saturation on the

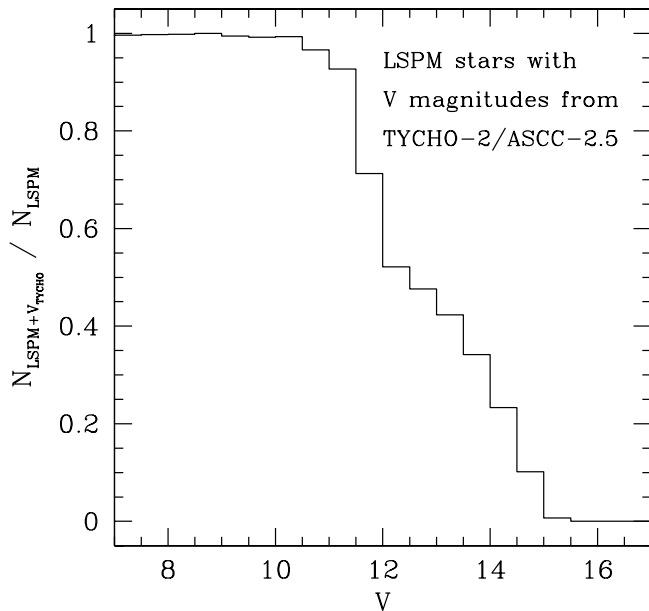


FIG. 9.—Fraction of LSPM catalog stars with  $B$  and  $V$  magnitudes obtained from the Tycho-2 and ASCC-2.5, plotted as a function of the visual magnitude. This indicates that we have reliable optical photometry for essentially all stars brighter than  $V = 12.0$ . For fainter objects, we have to rely on photographic magnitudes to estimate  $V$ .

POSS plates. For fainter stars, and especially those with  $V > 14.0$ , we do need to rely mainly on photographic magnitudes to cover the optical regime: the only existing all-sky catalogs of faint optical stars are based on photographic plate material.

#### 4.2. USNO-B1.0 Photographic Magnitudes: $B_J$ , $R_F$ , $I_N$

The USNO-B1.0 Catalog (Monet et al. 2003) is an all-sky catalog made from scans of several photographic sky surveys, including the POSS-I and POSS-II. Astronomical objects have been identified using the PMM scanning machine. The catalog gives positions, proper motions, photographic magnitudes in five passbands, and star/galaxy estimators for 1,042,618,261 objects. While the USNO-B1.0 provides proper motions for all objects detected in the POSS plates, it is not a reliable source for stars with large proper motions. The main difficulty with the USNO-B1.0 is the exceedingly large number of spurious entries (Gould 2003b); at high Galactic latitudes, up to 99% of objects listed with  $\mu > 0''.18 \text{ yr}^{-1}$  are not real. The catalog also suffers from serious incompleteness for high proper motion stars at low Galactic latitude (up to 30%), as estimated from its recovery of NLTT stars.

The USNO-B1.0 is, however, an extremely valuable complement to the LSPM catalog because it provides reasonably accurate photographic  $B_J$ ,  $R_F$ , and  $I_N$  magnitudes (respectively IIIa-J, IIIa-F, and IV-N) derived from the POSS-II scans. Because the USNO-B1.0 is based on some of the same plate material as the DSS, it also provides a very useful check for our SUPERBLINK detections.

We have succeeded in finding USNO-B1.0 counterparts for 60,396 of our LSPM stars. Searching the USNO-B1.0 for high proper motion objects, however, turned out to be a difficult and time-consuming problem. Cross-correlation of the two catalogs yielded only  $\approx 75\%$  of unambiguous matches. The large number of ambiguous cases fell into three broad classes: (1) stars with erroneous USNO-B1.0 proper motions; (2) moving stars not identified as such in the USNO-B1.0 and listed as separate stars, one for each epoch in which the stars was detected; and (3) confusion with background stars at the detection epoch.

One common problem was USNO-B1.0 entries with large errors in their quoted proper motions ( $\mu_{\text{USNO-B1.0}}$ ). Since their quoted J2000 right ascension and declination are calculated by extrapolating the position from the mean epoch of observation with their estimated proper motions, some stars have quoted positions incorrect by up to several arcseconds. In most cases, we were able to recover the star by extrapolating back to the mean epoch of observations and recalculating the J2000 right ascension and declination positions using the proper motion determined by SUPERBLINK.

Another major source of complication was high proper motion stars listed as two or more distinct entries in the USNO-B1.0. Each entry typically corresponds to a detection of the star in a distinct photographic survey. This problem particularly affected stars with larger proper motions. A typical example is a moving star listed as three separate entries, one with the position of the star at the epoch of the POSS-I survey, one with the position of the star at the epoch of the POSS-II red and blue surveys, and one with the position of the star at the epoch of the POSS-II near-infrared survey. The confusion was such that most of these cases had to be dealt with individually.

Additional complications occurred because of confusion with background sources. This problem was common especially in low Galactic latitude fields, where crowding is significant. All these cases had to be examined one by one. Overall, we had to visually inspect  $\approx 12,000$  LSPM objects in order to determine their correct USNO-B1.0 counterpart. Again we made use of our interactive software, this time overlaying the USNO-B1.0 catalog over our SUPERBLINK finder charts. Whenever an LSPM star appeared as two or more separate USNO-B1.0 entries, a choice had to be made as to which one should be used as the “official” counterpart, in order to keep the LSPM catalog simple. In general, we picked the entry having the most complete photometric data or, in some cases, the one least likely to be contaminated by blending with background sources.

Not all USNO-B1.0 entries have magnitude information in all three bands. Whenever possible, we tried to combine magnitude data if a USNO-B1.0 star appeared as more than one entry. For example, if one high proper motion star was listed as two distinct USNO-B1 entries, one giving only  $B_J$  and  $R_F$  magnitudes, the other giving only an  $I_N$  magnitude, we would combine the information to obtain complete  $B_J R_F I_N$  photometry. For practical purposes, however, we list the counterpart ID only for one of the two entries. As a result, LSPM magnitudes are often more complete than magnitudes extracted from the USNO-B1 catalog for the listed counterpart.

Finally, we note that no USNO-B1 counterparts could be found for a total of 1580 LSPM stars. The majority of these are in close proper motion double systems or in very crowded fields and are simply not resolved in the USNO-B1.0, although most of them are resolved in 2MASS. We note that 267 of the LSPM stars have neither a 2MASS nor a USNO-B1 identifier; a majority of these are faint proper-motion companions that are not resolved in the USNO-B1 and are too faint to have been detected by 2MASS. However, 229 of them are NLTT stars, and the others all clearly show up on DSS/XDSS scans and/or 2MASS images.

#### 4.3. 2MASS Infrared Magnitudes: $J$ , $H$ , and $K_s$

The 2MASS All-Sky Point Source Catalog is an all-sky catalog of sources detected in 2MASS (Cutri et al. 2003). The catalog covers the whole sky and is complete down to  $J \simeq 16.5$ . Infrared  $J$ ,  $H$ , and  $K_s$  magnitudes are provided and are accurate to 0.02 mag down to 15th magnitude. Positions are given for the epoch of observation (1997–2001) and are accurate to

70–80 mas for the fainter sources ( $J > 9$ ) and 120 mas for the brighter ones.

The vast majority of the LSPM catalog stars are found to have counterparts in the 2MASS All-Sky Point Source Catalog: we have reliable matches for 59,684 of our high proper motion stars. Finding 2MASS counterparts was straightforward for  $\approx 90\%$  of the LSPM objects and was obtained by a simple cross-correlation of the SUPERBLINK and Tycho-2/ASCC-2.5 high proper motion star positions with the 2MASS source positions. To make the search more effective, all positions were locally extrapolated to the epoch of the 2MASS observations. Most 2MASS counterparts were found within  $1''$  of their predicted position. There were multiple possible matches for  $\approx 3,000$  of the LSPM objects, most of them in very crowded, low Galactic latitude fields. We used again a software package developed by S. L., which overlays 2MASS catalog entries on the  $3.25 \times 3.25$  charts generated by SUPERBLINK. All matches were then made interactively, by direct visual inspection. All common proper motion doubles (see § 3.2 above) were also examined, and their 2MASS identification were verified with the same software. No 2MASS counterparts were found for 2292 LSPM stars; in the majority of cases, these are simply too faint in the infrared to have been detected in the 2MASS survey.

Because of its relatively high astrometric accuracy, we have adopted the 2MASS catalog as the *primary source of positional information* for stars that are not listed in the Tycho-2 catalog (see § 5.3 below). We believe the 2MASS is the best possible choice to pinpoint the positions of those stars because (1) it contains the majority of the LSPM objects, (2) its positions are given in the International Celestial Reference System (ICRS) and are reasonably accurate, and (3) the 2MASS observation epochs are very close to 2000.0. The advantage of having all the 2MASS positions to within a few years of the 2000.0 epoch is that it minimizes positional errors introduced by the errors in the proper motions, when one extrapolates the position of a high proper motion star to the 2000.0 epoch.

#### 4.4. Estimated $V$ Magnitudes and $V-J$ Colors

We have attempted to place all our stars on a simple, uniform magnitude/color system that includes both an optical and an infrared magnitude. We do have uniform, reliable measurements of infrared magnitudes (from 2MASS) for the vast majority of LSPM stars. However, some of our objects do not have 2MASS counterparts. Furthermore, we are in a situation in which our optical magnitudes are in two different systems. On the one hand, we have  $V$  and  $B$  magnitudes accurate to 0.1 mag but only for a small fraction of our stars (those with Tycho-2 counterparts). On the other hand, we have much less reliable photographic magnitudes ( $B_J$ ,  $R_F$ , and  $I_N$ ), accurate to  $\approx 0.3-0.5$  mag (Monet et al. 2003) but most likely affected by systematic errors (Sesar et al. 2004). Additional complications include the fact that one or more of the photographic magnitudes are sometimes missing. It is claimed by Salim & Gould (2003) that photographic  $R$  magnitudes from the USNO-A2.0 are accurate to 0.25 mag, which is significantly better than USNO-B1.0. On the other hand, the USNO-B1.0 catalog is more complete than the USNO-A2.0, particularly for faint ( $V > 19$ ) stars and also at low Galactic latitudes. Nevertheless, we are currently trying to find USNO-A2.0 counterparts of LSPM stars, and USNO-A2.0 magnitudes will be included in future versions of the catalog.

In any case, it is desirable to provide an immediate means to classify the stars in our catalog according to color and magnitude (even roughly). The general idea is thus to get estimates of the optical  $V$  magnitude and of the optical-to-infrared  $V-J$

color for all the stars in the catalog. We already have reliable  $V$  magnitudes for LSPM stars with Tycho-2 (see eq. [2]) or ASCC-2.5 counterparts, and  $J$  magnitudes for all stars with a 2MASS counterpart. What we need is a transformation system to obtain estimates of  $V$  and  $V-J$  using the photographic magnitudes from the USNO-B1.0 catalog. Although one might be tempted to use the excellent 2MASS infrared magnitudes to obtain estimates of optical  $V$ , this cannot be done reliably. The reason is that M dwarfs, which constitute the vast majority of the LSPM stars with no Tycho-2 counterparts, are largely degenerate in their infrared colors: all M dwarfs (except the very coolest) have  $J - K_s \approx 0.7 \pm 0.2$  for  $3 < V - J < 6$ .

The  $V$  band is located halfway between the photographic  $B_J$  and  $R_F$  bands. We estimate  $V$  using

$$V = B_J - 0.46(B_J - R_F), \quad (3)$$

a relationship that is verified for all Tycho-2 stars with USNO-B1.0 counterparts. For stars with  $B_J$  but no  $R_F$  magnitudes, we find it is possible to estimate  $V$  from the following set of transformations:

$$V = B_J - 0.23(B_J - J) - 0.10 \quad \text{if } B_J - J < 4,$$

$$V = B_J - 0.05(B_J - J) - 0.72 \quad \text{if } B_J - J > 4. \quad (4)$$

Likewise, for stars with  $R_F$  but no  $B_J$ , we can estimate  $V$  using

$$V = R_F + 0.6(R_F - J) - 0.10 \quad \text{if } R_F - J < 2,$$

$$V = R_F + 1.10 \quad \text{if } R_F - J > 2. \quad (5)$$

The  $V$  magnitudes estimated from the relationships given above are generally accurate to about  $\pm 0.5$  mag. Following these simple transformations, we calculate  $V$  magnitude estimates for 61,550 LSPM stars. Of the 427 LSPM stars for which we cannot provide a  $V$  magnitude estimates, 355 are close common proper motion doubles that are resolved in 2MASS but not on the POSS plates (see § 3.2). At this point, we refrain from trying to obtain a  $V$  magnitude using only  $J$ ,  $H$ , and  $K_s$ . The remaining 72 stars with no  $V$  estimates are stars that are not in the 2MASS or USNO-B1.0 catalogs and for which we only have  $R_F$  magnitudes estimates from SUPERBLINK.

Prospective catalog users should be warned that these  $V$  magnitude estimates are generally not very accurate and may be subject to systematic errors and other effects. The LSPM catalog  $V$  magnitudes should only be trusted for stars brighter than  $V = 12.0$ , whose  $V$  are from the Tycho-2 catalog. At fainter magnitudes, there may be errors of 0.5 mag or larger.

Since the majority of LSPM objects do have 2MASS counterparts, calculations of  $V-J$  colors are straightforward. For stars that do not have 2MASS counterparts, we use the photographic  $I_N$  magnitudes and use the following transformation:

$$V - J = 1.3(V - I_N) + 0.3. \quad (6)$$

From the 2MASS counterparts and the transformation above, we obtain  $V-J$  colors for all except 814 entries in the LSPM catalog. These include the 427 stars for which we have no  $V$  magnitude estimates (see above) and 387 stars that are not in the 2MASS catalog and for which we do have  $I_N$  magnitudes. Note that the  $V-J$  colors are only as accurate as the  $V$  magnitudes are. Since stars fainter than  $V = 12.0$  have errors of up to 0.5 mag or even larger, the  $V-J$  color estimates should be used with extreme caution.

We emphasize again that the primary goal of the LSPM catalog is *to provide the most complete list possible of high proper motion stars* and that it is not intended to be a photometric catalog. The photometry that we do provide for LSPM stars should be regarded as very preliminary and is given only as a help in identifying interesting classes of objects for follow-up observations. Future efforts will be devoted to obtaining more accurate optical magnitude estimates for all LSPM stars.

## 5. ASTROMETRY

### 5.1. Conversion to Absolute Proper Motions

The SUPERBLINK software was largely designed to achieve the highest possible recovery rate for high proper motion stars on photographic plates. As such, it was optimized for raw detection and not for accurate astrometric measurements of detected objects. The main caveat is that *proper motions are calculated relative to local background sources*. This means, typically, all objects within  $\approx 4'$  of the moving target. Because of this, the proper motions calculated by SUPERBLINK are *local, relative proper motions*. These are usually offset by up to several milliarcseconds per year relative to *absolute proper motions*, which are proper motions measured in a fixed reference frame (defined, e.g., by the positions of distant quasars, such as for the ICRS reference frame). It must be realized that most “background” sources used by SUPERBLINK as a local reference system are Galactic objects, and they all have significant proper motions at the milliarcsecond level. The local frames used by SUPERBLINK are thus moving frames, and this potentially introduces both random and systematic offsets in the SUPERBLINK proper motions. The random offsets arise because of the limited number of stars that locally define the frame. If these stars are all moving in random directions, then their mean proper motion will generally not add up to zero; it will, however, converge to zero if the number of reference stars is large enough. These random errors affect most the fields at high Galactic latitudes, where the object density is low and the local SUPERBLINK reference frames are defined by very few stars (sometimes  $\lesssim 100$ ). In any case, field background stars generally have random proper motions smaller than  $10 \text{ mas yr}^{-1}$ , which means that local random offsets will be less than  $1 \text{ mas yr}^{-1}$  in frames defined by at least 100 stars. Systematic offsets, however, are more of a problem. If all local stars participate in some local bulk motion, then the local frame used by SUPERBLINK will definitely be moving at the bulk motion rate, no matter how many stars define the frame.

Fortunately, we do have a means to estimate some of the systemic motions of the background stars and correct for them in order to obtain absolute proper motions. To that purpose, we can use all Tycho-2 stars that have also been measured with SUPERBLINK and compare their absolute and relative proper motions. The random errors on the SUPERBLINK proper motion are on the order of, or larger than, the local systemic motions, but we can average out the residuals over appropriate-sized areas and calculate *zonal corrections*.

It is true that the averaging procedure may even out some of the local fluctuations. However, background Galactic stars are expected to display mainly *global* patterns of systemic motions. The main sources are the rotation of the Galaxy, the systemic motion of the local standard of rest (LSR) relative to other Galactic stellar populations (old disk, halo), and the motion of the Sun within the LSR. The resulting systemic absolute proper motions of the background stars are dependent on their position on the sky but on a global scale. For instance, the systemic drift of old disk and halo stars is largest in a direction perpendicular

to the Galactic rotation (toward the Galactic pole) and slowly decreases as one looks more toward the direction of rotation.

The current version of the LSPM catalog only lists a few thousand stars (with  $\mu > 0''.15 \text{ yr}^{-1}$ ) for which we have both Tycho-2 and SUPERBLINK proper motions, leaving very few objects to calculate zonal corrections on a scale of less than a few tens of degrees. This tends to make the map too coarse and local values too inaccurate. However, the *complete* SUPERBLINK database actually includes detections from the DSS of stars with proper motions down to  $0''.04 \text{ yr}^{-1}$ . While most of those lower proper-motion detections are still being processed and analyzed, we have recently compiled a preliminary list of objects, which include over 30,000 Tycho-2 stars with proper motions  $0''.05 \text{ yr}^{-1} < \mu < 0''.15 \text{ yr}^{-1}$ , all of which have a relative proper-motion value measured by SUPERBLINK.

Zonal corrections have thus been calculated using a list of 33,312 stars with magnitudes  $10 < V < 13$  and proper motions  $0''.05 \text{ yr}^{-1} < \mu < 0''.50 \text{ yr}^{-1}$ . For each position of the celestial sphere, the zonal correction is calculated from the mean of the offsets between the relative (SUPERBLINK) and absolute (Tycho-2) proper motions of all stars *within a radius of  $7^\circ$* . Every position on the sky uses  $\approx 290$  stars on average. All offsets are calculated in the local plane of the specified location. Outliers with offsets more than  $3 \sigma$  away from the mean are removed from the final calculation.

Depending on the position on the sky, the mean offsets vary from  $-9.1$  to  $+12.2 \text{ mas yr}^{-1}$  in  $\mu\text{RA}$  and from  $-0.3$  to  $+13.9 \text{ mas yr}^{-1}$  in  $\mu\text{DE}$ , where  $\mu\text{RA}$  is the proper motion in the direction of right ascension and  $\mu\text{DE}$  is the proper motion in the direction of declination. A map of the zonal corrections for the northern sky is shown in Figure 10, where it is plotted in Galactic coordinates. The local distribution of offsets between the relative and absolute proper motions is also shown for three positions on the sky. The number of stars  $N$  used in calculating the local offset is noted.

From these zonal corrections, absolute proper motions are calculated from the relative SUPERBLINK proper motions. We thus obtain absolute proper motions for all LSPM stars. In the LSPM catalog, we list both the relative proper motion determined with SUPERBLINK and the absolute proper motion obtained after applying the zonal corrections.

In effect, Figure 10 plots the local mean value of the absolute proper motion of background stars. (Note that the zonal correction vectors plotted in Figure 10 all point in the direction opposite to the mean absolute proper motion.) Our plot should be compared to Figure 13 in Munn et al. (2004), which plots local mean values of the absolute proper motion of background stars, calculated by combining astrometry from the USNO-B1.0 and SDSS Data Release I. Exactly the same pattern is displayed in both figures. Our Figure 10, however, covers a much larger area on the sky ( $20,000 \text{ deg}^2$ , compared to the  $3,000 \text{ deg}^2$  of the Munn et al. survey) and conveys a more global picture of the kinematics of the background Galactic stars.

The patterns observed in Figure 10 are most probably a combination of three effects. The dominant pattern appears to be the drift of the LSR relative to the stars in the old disk and halo. The mean motion of the standard of rest relative to the centroid of the velocity distribution of all local Galactic stars is pointing in the direction of Galactic rotation ( $l = 90^\circ$ ,  $b = 0^\circ$ ), and there should thus be a general drift of the background stars in a direction opposite to the Galactic rotation ( $l = 270^\circ$ ,  $b = 0^\circ$ ). This is largely what is observed in Figure 10, although the relative proper motions diverge from a point that does not exactly coincide with ( $l = 90^\circ$ ,  $b = 0^\circ$ ). However, other systematic motions should be producing drifting motions in the background stars.

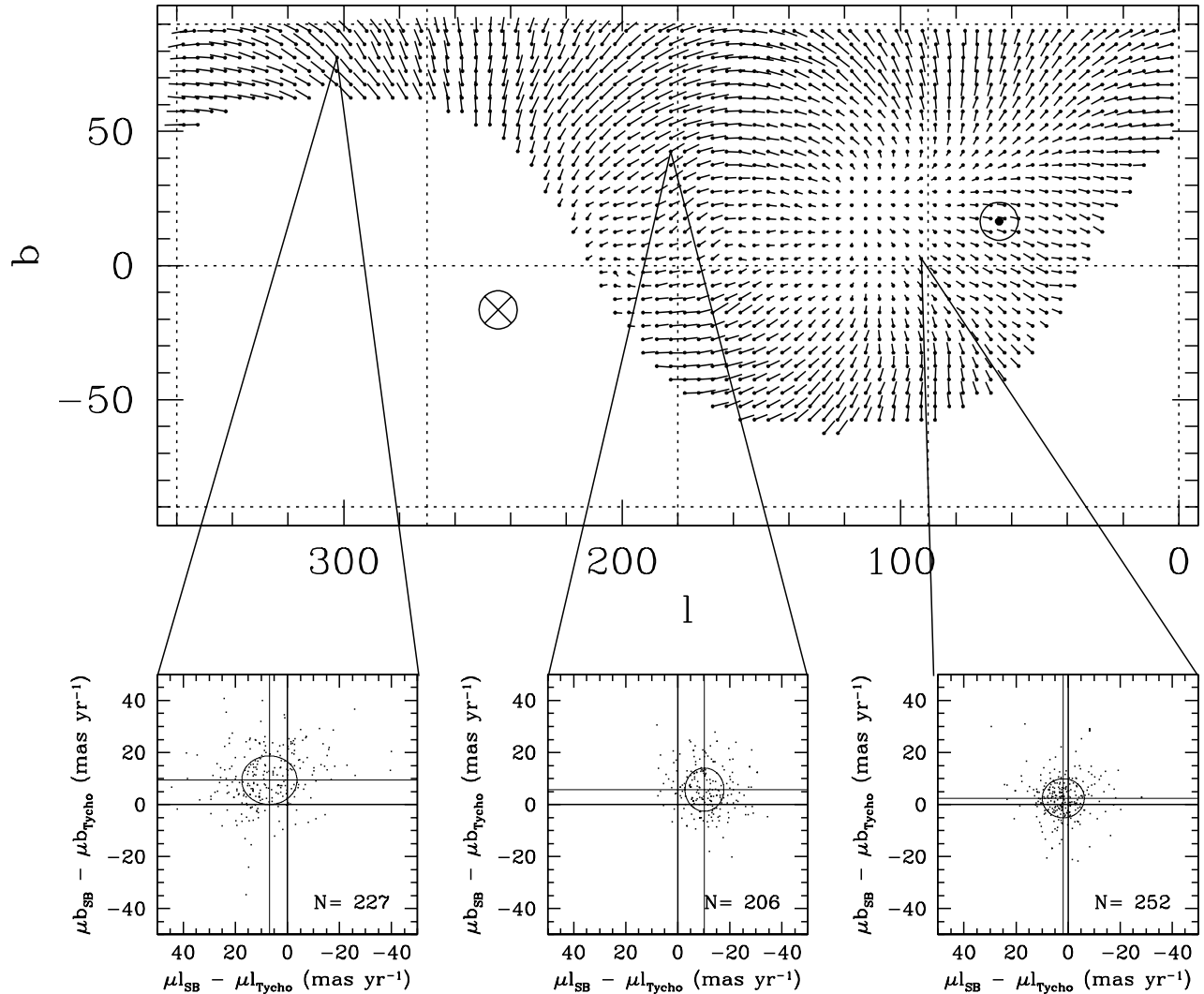


FIG. 10.—Local offsets between SUPERBLINK relative proper motions and Tycho-2 absolute proper motions. The offsets are calculated using 33,312 Tycho-2 stars with proper motions  $0''.05 \text{ yr}^{-1} < \mu < 0''.50 \text{ yr}^{-1}$  whose relative proper motions have been independently calculated with SUPERBLINK. The three bottom panels shows local differences between the relative and absolute proper motions for stars located within  $7^\circ$  of the specified location. Proper-motion differences are calculated in the local plane of the sky. The crosshairs mark the mean value of the offset, while the ellipse shows the mean standard deviation ( $1 \sigma$ ). The top panel plots proper motion difference vectors as a function of position on the sky, in galactic coordinates. The apex (*encircled dot*) and antapex (*encircled cross*) of the Sun's motion are noted. These offsets effectively map out the local mean proper motion of background field stars in the Tycho-2 (ICRS) reference system. Offsets are largest at high Galactic latitude, where there is a significant drifting motion of old disk and halo stars relative to the LSR.

One is the motion of the Sun itself relative to the stars in the LSR. It should be producing a general drifting motion pointing away from the apex of the Sun's motion. For comparison, we plot in Figure 10 the positions of the Solar apex/antapex, as determined by Fehrenbach et al. (2001). From Figure 10, it is unclear how much weight this effect has. Another effect is the rotation of the Galaxy as a whole, which should result in a rotating motion around the north and south Galactic poles.

A detailed model that would account for all those possible effects would be required for a more complete interpretation of Figure 10. We note that the information summarized in our Figure 10 can all be recovered (possibly with even greater detail) from a simple subtraction of the relative and absolute proper motions, which are listed in separate columns in the LSPM catalog.

### 5.2. Accuracy of LSPM Proper Motions

A check on the accuracy of our proper motions is obtained from LSPM stars that have counterparts in the UCAC2 catalog.

We separate these objects into two groups: stars that have their proper motions directly transcribed from the Tycho-2 and stars that have their proper motions determined by SUPERBLINK.

The first group includes 4181 Tycho-2 stars (all listed in the LSPM catalog) that also have UCAC2 counterparts. As expected, proper motions from the Tycho-2 catalog are in very close agreement with the UCAC2 proper motions. The dispersion in the difference is  $2.8 \text{ mas yr}^{-1}$  in right ascension and  $2.6 \text{ mas yr}^{-1}$  in declination. This is comparable to the quoted rms errors on the UCAC2 proper motions.

The second group comprises 4380 stars from the LSPM in the magnitude range  $12 < V < 16$  that have UCAC2, but no Tycho-2, counterparts. Overall, the difference between SUPERBLINK and UCAC2 proper motions has a dispersion of  $(7.5, 6.7) \text{ mas yr}^{-1}$  in right ascension and declination, respectively, after removal of  $3 \sigma$  outliers (Fig. 11). There is also a small offset of  $(0.9, -0.9) \text{ mas yr}^{-1}$ , which might indicate a problem in the zonal corrections procedure. Our zonal corrections are based on motions from relatively bright (Tycho-2) stars, while the local frames used by

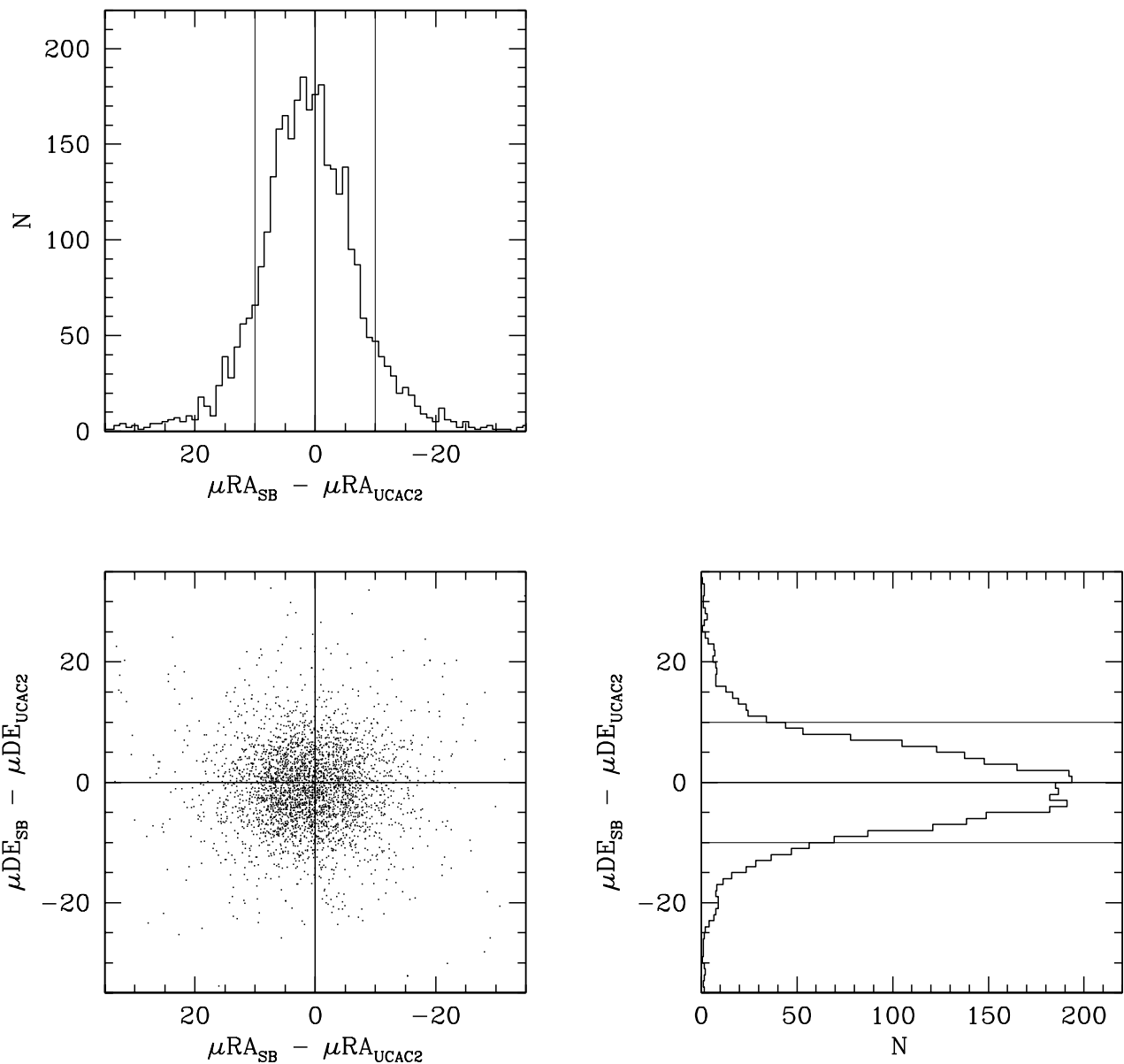


FIG. 11.—Difference between the SUPERBLINK and UCAC2 absolute proper motions. The zonal correction has been applied to the SUPERBLINK proper motions. Only stars that have no Tycho-2 counterparts are shown. There is a dispersion of  $7.9 \text{ mas yr}^{-1}$  in  $\mu\text{RA}$  and  $7.1 \text{ mas yr}^{-1}$  in  $\mu\text{DE}$ . This provides an estimate of the rms errors in the SUPERBLINK proper motions.

SUPERBLINK are largely defined with respect to the more numerous fainter stars. Perhaps the zonal corrections are dependent on both position of the sky *and* magnitude. If bright stars are on average closer to us than fainter background stars, then there could very well be a difference in their systemic proper motions. In any case, since the nominal errors on the UCAC2 proper motions are very small ( $1\text{--}3 \text{ mas yr}^{-1}$ ), the measured  $\approx 7 \text{ mas yr}^{-1}$  dispersion is a good estimate of the SUPERBLINK astrometric errors on the proper motions.

The  $3\sigma$  outliers comprise 6% of the stars in the sample and 2.5% of the objects are beyond the  $6\sigma$  limit. This means there is an extended tail to the distribution. Indeed, 90 stars have a difference in proper motion  $>100 \text{ mas yr}^{-1}$ . Whether the large difference arises from a faulty LSPM or UCAC2 proper motion remains to be determined, although we do suspect that in a significant number of cases it is the UCAC2 proper motion that is in error.

The SUPERBLINK proper motion error appears to be independent of magnitude for stars fainter than  $V = 11$  (Fig. 12).

The proper motions of fainter stars are perhaps marginally better, and we measure a dispersion of  $(7.3, 6.3) \text{ mas yr}^{-1}$  at  $V > 15$ . Astrometric errors increase significantly for brighter ( $V < 11$ ) stars, as expected from the fact that these are saturated on the DSS scans. This, however, is of little consequence for the proper motions quoted in the LSPM catalog since we use the more accurate Tycho-2 astrometry for the vast majority of the LSPM stars with  $V < 11$ . The accuracy of the SUPERBLINK astrometry is also largely independent of the proper motion (Fig. 13).

The proper-motion errors from SUPERBLINK are relatively larger than those quoted for the revised NLTT catalog (rNLTT) of Salim & Gould (2003), which are claimed to be  $\approx 5.5 \text{ mas yr}^{-1}$  in both right ascension and declination. It is possible that SUPERBLINK errors are slightly larger because SUPERBLINK uses photographic plate material for both its first and second epoch, whereas Salim & Gould (2003) used data from photographic plates only for their first epoch (USNO-A catalog, based on POSS-I), while they used the 2MASS Second Incremental

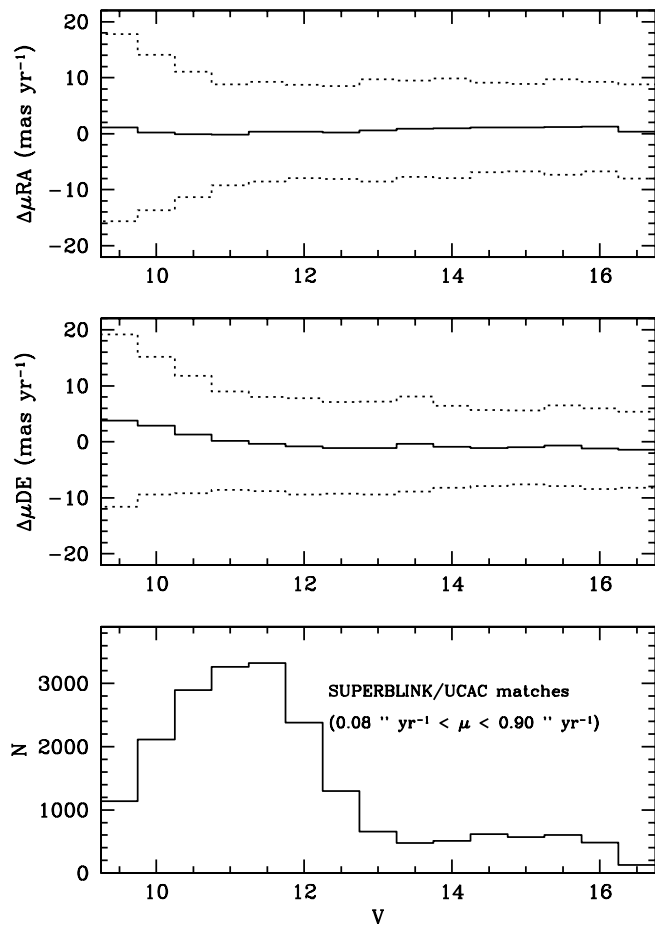


FIG. 12.—Dispersion in the difference between SUPERBLINK and UCAC2 proper motions, as a function of magnitude. The continuous line shows the mean of the difference, and the dotted lines show the  $1\sigma$  dispersion. All stars with SUPERBLINK and UCAC2 proper motions have been included here, including those that also have Tycho-2 counterparts (to increase the sample of objects at bright magnitudes). For stars brighter than  $V = 11.0$  the accuracy of the SUPERBLINK proper motions degrades as the stars gets brighter, but the mean errors are uniform in the  $11.0 < V < 17.0$  range.

Release as their second epoch. It is also possible that the larger errors in the SUPERBLINK proper motions arise from small-scale fluctuations in the systemic motions of the background stars, which could only be corrected by a higher resolution map of zonal corrections. A more likely possibility is that the SUPERBLINK proper motions are affected by systematic errors introduced by astrometric magnitude equations (see § 5.6 below).

Readers interested in having more accurate proper motions may want to check if their star is in the rNLTT catalog (Salim & Gould 2003). The recovery of rNLTT proper motions is straightforward, since both the rNLTT and LSPM catalogs provide NLTT identification numbers. One limitation is that the rNLTT only has data for 15,899 of the northern NLTT stars, or roughly a quarter of the LSPM stars.

Clearly, there is still room for improvement, and future efforts will be devoted to obtain more accurate proper-motion measurements, which will be included in future versions of the LSPM catalog. The possibility of obtaining much more accurate proper-motion measurements using data from CCD-based surveys, such as the SDSS, was demonstrated recently (Gould & Kollmeier 2004; Munn et al. 2004). Careful astrometric calibration using local quasars can yield proper motions with an accuracy  $< 4$  mas  $\text{yr}^{-1}$ .

The goal of the current version of the LSPM is to provide the most complete list of objects possible, with reasonable astro-

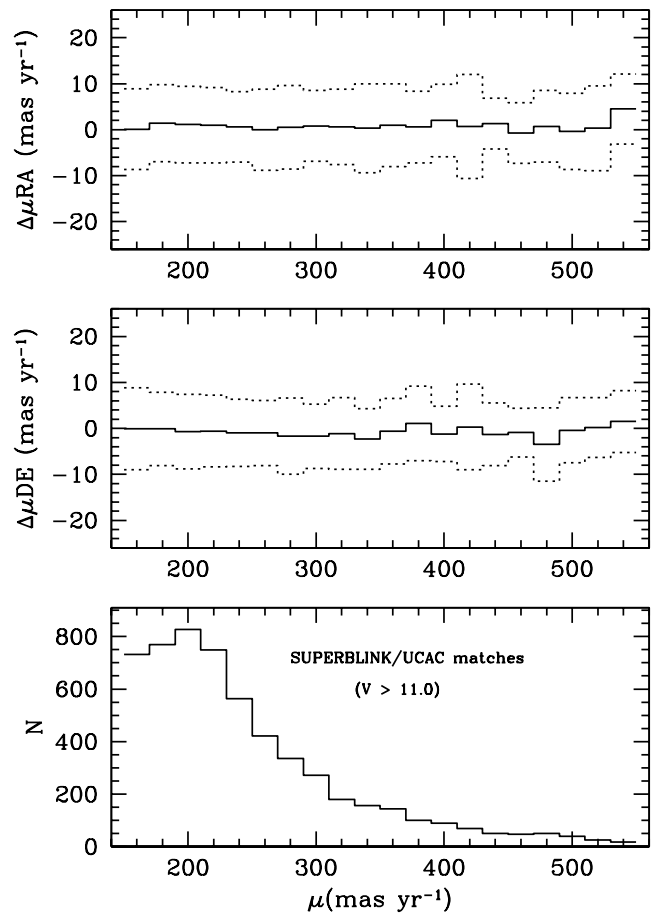


FIG. 13.—Mean and dispersion in the difference between SUPERBLINK and UCAC2 proper motions, as a function of proper motion. The continuous line shows the mean of the difference, and the dotted lines show the  $1\sigma$  dispersion. The accuracy of the SUPERBLINK proper motions is largely independent of the magnitude of the proper motions, as demonstrated here. The fluctuations above  $350$  mas  $\text{yr}^{-1}$  are due to small number statistics.

metric accuracy. Although significant improvements of the proper-motion errors are possible, at least for a fraction of the LSPM stars, this will require substantial efforts, which are beyond the scope of this paper. In any case, our positions and proper motions are accurate enough to provide a solid starting point for future improvements.

### 5.3. Accuracy of LSPM 2000.0 Positions

The brighter LSPM stars have their 2000.0 positions extrapolated from the 1991.25 positions and proper motions of their Tycho-2 counterparts. Fainter stars with no Tycho-2 counterparts have their 2000.0 positions extrapolated from the positions of their 2MASS counterparts and their SUPERBLINK-derived absolute proper motions.

We estimate the positional accuracy of the fainter ( $V > 12$ ) LSPM objects by comparing the SUPERBLINK-derived positions with those of the UCAC2 catalog (see § 3.6 above) for those stars that have UCAC2 counterparts (Fig. 14). The difference in position has a calculated dispersion (91, 88) mas in (R.A., decl.). Note that UCAC2 has a reported astrometric precision of 20–70 mas in that range of magnitudes. There is also an offset (−7.6, 6.8) mas, which is small compared to the magnitude of the dispersion, but is statistically significant. In principle, the offset could be due to small systematic errors in the SUPERBLINK proper motions, which are used to extrapolate

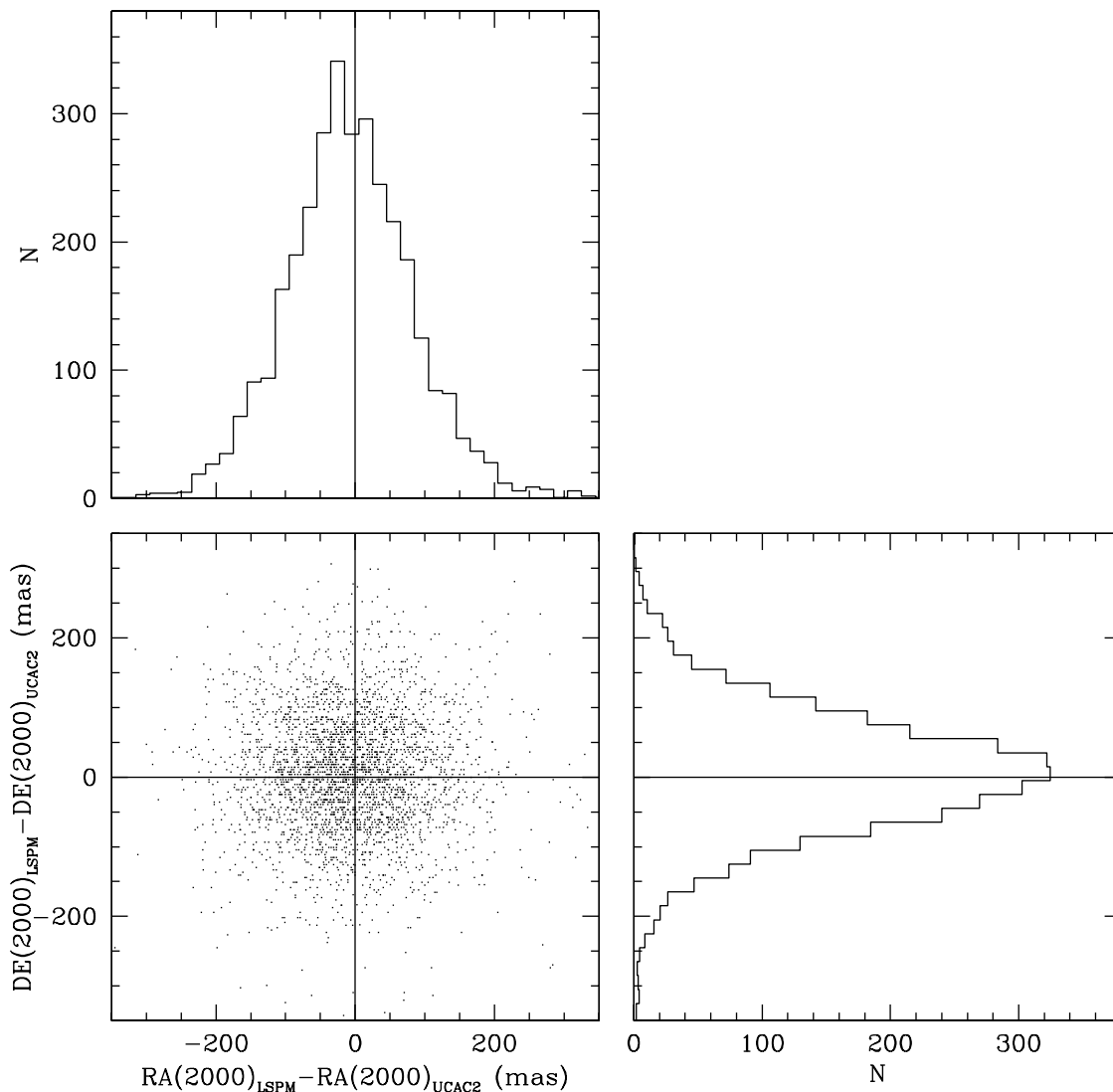


FIG. 14.—Difference between the 2MASS-derived 2000.0 positions of 9105 LSPM stars with the positions of their UCAC2 catalog counterparts. The distribution has a dispersion in (R.A., decl.) of (91, 88) mas. This provides an estimate of the accuracy of the 2000.0 epoch positions of LSPM stars with no Tycho-2 counterparts.

the 2MASS positions to the 2000.0 epoch. However, the  $(0.9, -0.9)$  mas yr<sup>-1</sup> systematic offset between the SUPERBLINK and UCAC2 proper motions is not consistent with the  $(-7.6, 6.8)$  mas positional offset. In any case, we find that our positional errors are marginally larger than those reported for the entire 2MASS catalog, which have a dispersion  $\approx 80$  mas relative to the UCAC2 catalog.

Most of the brighter LSPM stars ( $V < 12$ ) have their 2000.0 positions extrapolated from the Tycho-2/ASCC-2.5 positions (epoch 1991.25), using the Tycho-2/ASCC-2.5 proper motions. A comparison of the 2000.0 positions with those given in the UCAC2 catalog shows a dispersion of (81, 71) mas in (R.A., decl.). One must note that the positional errors in the 2MASS catalog are significantly larger for bright stars ( $>120$  mas for  $K_s < 8$ ). The Tycho-2 positions therefore remain the best choice at this time.

#### 5.4. Comparison with the NLTT Catalog

The LSPM catalog provides new estimates of the positions and proper motions of all northern stars in the NLTT catalog. As demonstrated by Salim & Gould (2003), the NLTT positions are accurate to no better than a few arcseconds, with some stars

having positional errors of up to a few arcminutes. The LSPM positions, which are accurate to within 1'' (see above) are a significant improvement. Improved positions for  $\approx 31,000$  NLTT stars are also available from the rNLTT (Salim & Gould 2003) but only for a little more than half the NLTT stars in the northern sky, while our LSPM is *complete* for northern NLTT stars.

The difference between the NLTT and LSPM proper motions shows a dispersion (20.3, 18.7) mas yr<sup>-1</sup> in ( $\mu$ RA,  $\mu$ DE) (after removal of 3  $\sigma$  outliers), with an offset (1.1, 4.4) mas yr<sup>-1</sup> (Fig. 15). This estimate of the NLTT errors is comparable to the value of  $\sigma \approx 20$  mas yr<sup>-1</sup> estimated in Salim & Gould (2003), which was based on a comparison between NLTT and rNLTT proper motions. The (2.3, 6.6) mas yr<sup>-1</sup> offset is also the result of NLTT proper motions being relative. Indeed, if we compare NLTT proper motions to the *relative proper motions* measured with SUPERBLINK, the offset is reduced to (0.2, -1.6) mas yr<sup>-1</sup>.

The accuracy of NLTT proper motions is naturally expected to be larger, since the second epoch of Luyten's survey was only  $\approx 15$  yr after the POSS-I epoch, whereas the second epoch of the DSS (POSS-II) is 40 yr after that of the POSS-I. The fact that the NLTT proper-motion errors are approximately 3 times as large as the SUPERBLINK errors is consistent with the

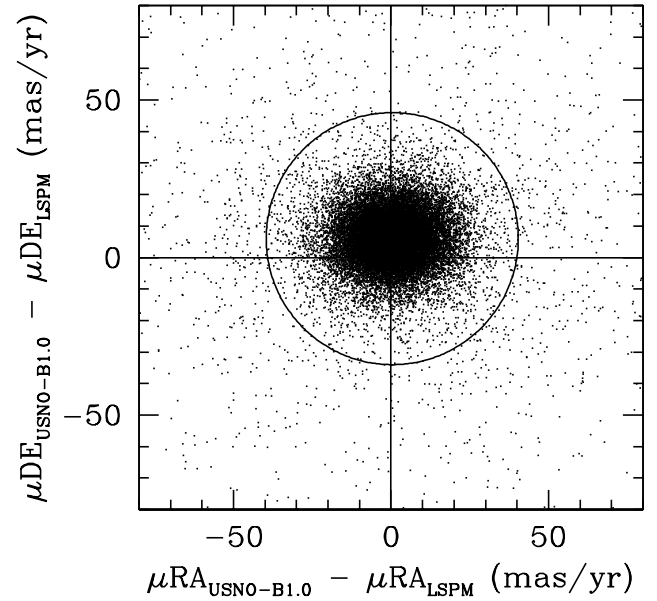
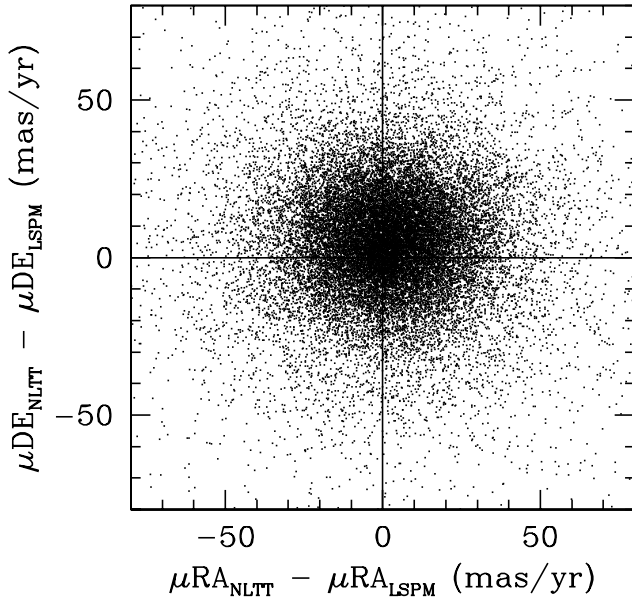
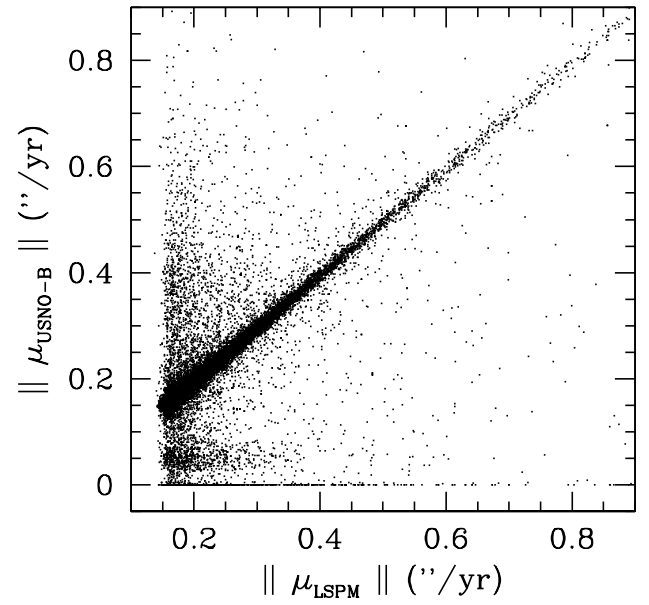
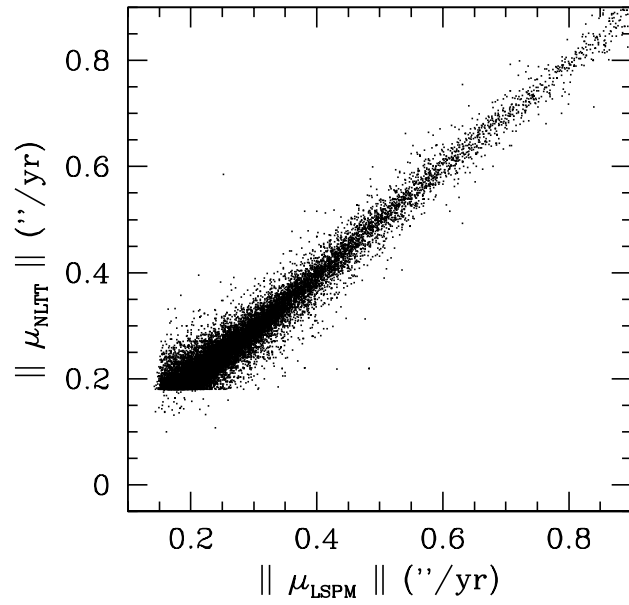


FIG. 15.—Comparison between NLTT and LSPM proper motions, for all stars in common between the two catalogs. Note that errors on  $\mu_{\text{LSPM}}$  are  $\leq 8'' \text{ yr}^{-1}$  (see Fig. 11); the measurement errors on  $\mu_{\text{NLTT}}$  are clearly larger. This accounts for the fact that  $\approx 3000$  NLTT stars have LSPM proper motions below the fiducial limit of the NLTT catalog ( $\mu = 0''.18 \text{ yr}^{-1}$ ).

difference in the temporal baseline. In any case, the LSPM proper motions are a significant improvement over NLTT proper motions. Not only is the accuracy better by a factor of 3, but the LSPM proper motions are absolute, instead of being relative to the local background stars.

##### 5.5. Comparison with the USNO-B1 Catalog

Figure 16 compares LSPM proper motions with the proper motions quoted in the USNO-B1.0. More than 75% of the stars fall within  $30 \text{ mas yr}^{-1}$  of the  $\mu_{\text{USNO-B1.0}} = \mu_{\text{LSPM}}$  line. The remaining objects are scattered around, with no obvious correlation with  $\mu_{\text{LSPM}}$ . In particular, there are 975 stars that have a USNO-B1.0 counterpart with a proper motion of exactly zero.

FIG. 16.—Comparison between LSPM and USNO-B1.0 proper motions, for LSPM stars that have USNO-B1.0 counterparts. About 75% of the stars have USNO-B1.0 proper motions within  $0''.02 \text{ yr}^{-1}$  of LSPM proper motions. Several thousand stars have  $\mu_{\text{USNO-B1.0}}$  containing large errors. The proportion of these “problem” stars, with proper-motion errors exceeding  $40 \text{ mas yr}^{-1}$  (circle in bottom panel), is significant (see Fig. 17). There is a mean offset in the proper-motion differences because LSPM lists absolute proper motion while USNO-B1.0 lists relative proper motions.

As discussed in Gould & Kollmeier (2004) these are not stars with measured proper motions of 0.0 but rather stars for which no significant proper motion was calculated (to within errors) in the construction of the USNO-B1.0 catalog. In any case, these zero proper motion stars were identified as low proper motion objects in the USNO-B1.0.

We emphasize that the high proper motion status of all LSPM stars has been systematically confirmed by visual inspection. Ambiguous matches with USNO-B1.0 counterpart have also all been resolved visually. Furthermore, the comparison between LSPM and NLTT proper motions shows a very good agreement.

Thus, the only explanation for the outliers in Figure 16 is that their USNO-B1.0 proper motion is in error.

The completeness of the USNO-B1.0 for high proper motion stars was investigated by Gould (2003b), from a comparison with the rNLTT. No USNO-B1.0 counterpart was found for  $\approx 10\%$  of the rNLTT stars (“missing” objects). About 1%–2% of the matched objects were also found to have discrepant (“bad”) USNO-B1.0 proper motions. The fraction of bad or missing stars (dubbed “problem fraction”) was found to be a function of both magnitude and Galactic latitude. The reason for this is that it is both more difficult to pair up detections of fast-moving stars from different epochs and to obtain accurate proper motions of bright stars, which are saturated on the POSS plates.

We calculate our own “problem fraction” for the USNO-B1.0, using all single stars in the LSPM catalog as a reference. We exclude close doubles from the analysis, as they are sometimes not resolved in the USNO-B1.0 and so might tend to overestimate “problem fraction.” We calculate the “problem fraction” by finding all LSPM stars with no USNO-B1.0 counterpart (“missing”) or with a USNO-B1.0 counterpart that has  $|\mu_{\text{LSPM}} - \mu_{\text{USNO-B1.0}}| > 40 \text{ mas yr}^{-1}$  (“bad”). We find that most of the problem stars are not “missing” objects, as in the Gould (2003b) analysis, but are mostly ( $> 95\%$ ) “bad” counterparts. Why this difference? Gould (2003b) matched rNLTT stars to USNO-B1.0 objects within a  $5''$  radius, while our own search radius was much larger (up to  $1'$ ). We have thus recovered most of those “missing” USNO-B1.0 counterparts. It appears that those stars have large position errors in the USNO-B1.0 because they also have large proper motion errors. The two values (position and proper motion) are linked, because the extrapolated 2000.0 positions are dependent on a good estimate of the proper motion. In other words, the counterparts were “missing” because of their very “bad” recorded proper motion. This is why our USNO-B1.0 “problem” stars are comprised of mostly “bad” counterparts.

In Figure 17, we plot our USNO-B1.0 problem fraction as a function of magnitude, proper motion, and Galactic latitude. A comparison with photographic  $V$  magnitude shows that large proper motions errors are more common for USNO-B1.0 counterparts with  $11 < V < 13$  and  $V > 19$ . The excellent agreement between the USNO-B1.0 and LSPM for the very brightest stars ( $V < 10$ ) reflects the fact that both the LSPM and USNO-B1.0 use Tycho-2 positions and proper motions in that range.

Following Gould (2003b), we interpret the larger problem fraction of the brighter stars from the fact that these objects are saturated on the POSS plates, making proper-motion determinations prone to large errors. The large problem fraction of faint ( $V > 19$ ) stars is simply explained by the fact that it is much more difficult to pair up faint objects detected in different epochs. This increase in the problem fraction near the faint star limit does not show up in the Gould (2003b) analysis, because the analysis was restricted to stars with counterparts in the USNO-A catalog, which has a brighter faint magnitude limit.

Large proper-motion errors on USNO-B1.0 counterparts are also more frequent for stars with larger proper motions ( $\mu_{\text{LSPM}} > 0.3 \text{ yr}^{-1}$ ), confirming again the analysis of Gould (2003b). It is simply more difficult to pair up stars that have moved very substantially between different photographic survey epochs. Finally, crowding is also a major source of confusion, leading to erroneous USNO-B1.0 proper motions. This is evidenced by the increase in the problem fraction at low Galactic latitude. This is much more significant than the low Galactic latitude problem fraction of Gould (2003b), which was high only because the low Galactic latitude rNLTT stars contain a larger proportion of

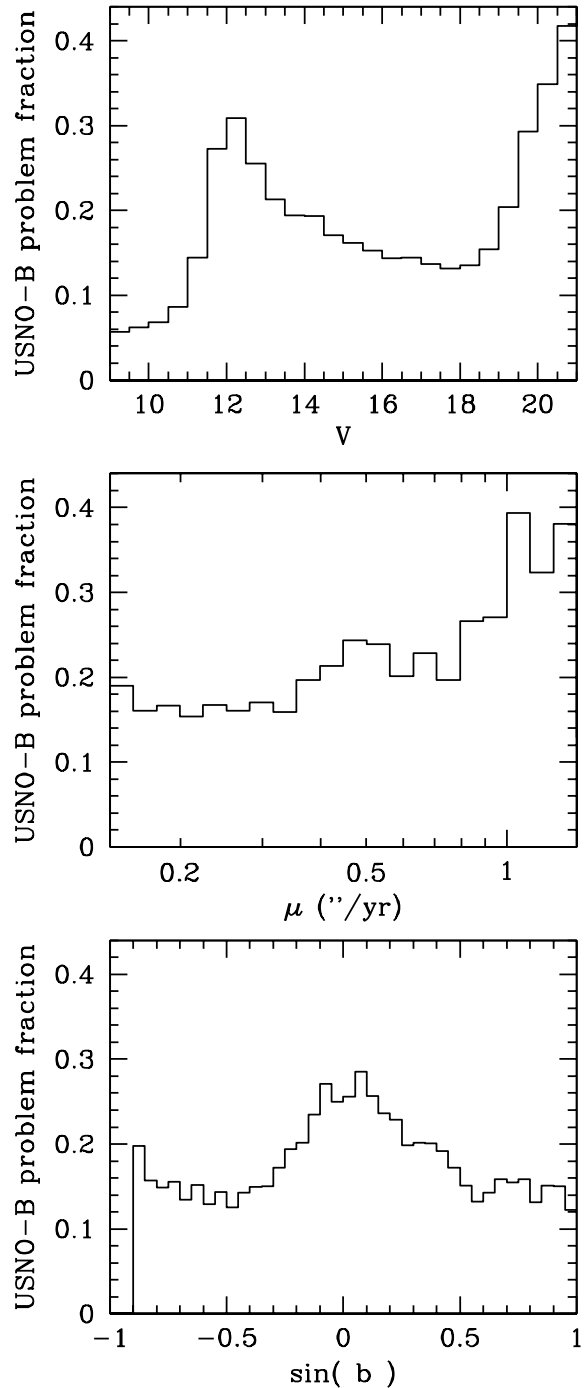


FIG. 17.—Fraction of stars in the LSPM catalog with no recorded USNO-B1.0 counterpart or with a large error in the USNO-B1.0 proper motion (as compared with the SUPERBLINK proper motion). Close binary stars are excluded from the analysis, as they may not be resolved in USNO-B1.0. The calculated USNO-B1.0 “problem fraction” is lowest for moderately faint stars ( $14 < V < 19$ ) with low proper motions ( $\mu < 0.3 \text{ yr}^{-1}$ ) at high Galactic latitudes ( $|b| > 20^\circ$ ), for which it is  $\approx 10\%$ .

bright, saturated objects. The high problem fraction at low Galactic latitude observed by Gould (2003b) was thus more the result of those stars being dominated by brighter, saturated objects. Our problem fraction is a more correct assessment of the completeness of the USNO-B1.0 at low Galactic latitude: the problem fraction reaches 25% near the Galactic plane.

The conclusion is that the USNO-B1.0 catalog is at best approximately 90% complete and accurate at high Galactic latitude,

for stars with  $\mu < 0''.5 \text{ yr}^{-1}$  and  $14 < V < 19$ . Otherwise the completeness falls to 70%. The LSPM is significantly more complete in high proper motion stars than the USNO-B1.0 (see § 7 below).

### 5.6. SUPERBLINK Proper-Motion Accuracy and the Astrometric Magnitude Equations

The SUPERBLINK proper motions are derived from measurements of photographic Schmidt plates (POSS-I, POSS-II). One important issue with these plates is that the measured positions of stars have a weak dependence on magnitude. The nonlinear response of photographic plates combined with asymmetric stellar images (from, e.g., imperfections in the optical system or inaccurate guiding) causes the photographic image centroids of the stars to be slightly offset compared with that on a linear detector. Because they arise from the nonlinear response of the substrate, these offsets are a function of the magnitude of the star, and they are generally largest for bright, saturated objects. These offsets, which are also generally dependent on the position on the plate, are referred to as the “astrometric magnitude equations.” Accurate astrometric measurements with photographic plates require the determination and application of a magnitude equation correction (Girard et al. 1998).

For the POSS plates, which we use in our SUPERBLINK survey, Monet et al. (2003) have shown the existence of fixed-pattern astrometric offsets that are on the order of  $0''.1$ – $0''.5$  and are strongly correlated with the  $XY$  position on the plate. Plotted for stars of different magnitudes, these patterns show striking differences, which indicate the existence of significant astrometric magnitude equations. The offsets tend to be larger at bright magnitudes and are also larger near the edges of the plates. However, the patterns are relatively regular, and much of the variability occurs on scales equivalent to at least several arcminutes.

As described in § 2.1, the SUPERBLINK software intrinsically corrects for large-scale plate distortions by measuring the relative proper motions of stars *in a frame defined by the local background of objects*, typically all stars within about  $7'$  of the high proper motion target. Because SUPERBLINK uses the local backdrop of stars to calculate relative proper motions and not the  $XY$  plate positions, distortions on the photographic plate on scales  $\geq 7'$  do not introduce any significant error on the SUPERBLINK proper motions. This, however, is generally true only if all the stars (target and background) are locally offset by the same amount. For example, if the local SUPERBLINK reference frame is defined by 16th magnitude stars, then the measured relative proper motions of 16th magnitude stars will not be affected by the astrometric magnitude equations (since the target and the reference stars are all offset by the same value). This, of course, is true even if the value of the offset is different on the first- and second-epoch images.

On the other hand, if a proper-motion target is significantly brighter or fainter than the background (reference) stars, the astrometric magnitude equations will generally introduce systematic errors in the SUPERBLINK proper motions. One exception to this case is if the *differences* in the offsets between the target and the reference stars *are the same in both the first- and second-epoch images*. This may happen, e.g., if the object was recorded at the same plate position ( $X, Y$ ) at both of the first and second epoch. Unfortunately, this is generally not the case for POSS-I and POSS-II, since their plate centers are on different grids.

Because the systematic proper-motion errors introduced by the astrometric magnitude equations depend on the difference between the magnitude of the target and the magnitude of the local background stars, their effect is very difficult to model.

One would need to estimate the local mean offset of the background stars, which have a variable range of magnitudes, and use estimates of the offsets expected for the target star given its magnitude. One would need to make these estimates separately for the first- and second-epoch images. Such a procedure would be extremely complex. We have thus made no attempt to correct the SUPERBLINK proper motions for the effects of the astrometric magnitude equations. It is very possible that the larger errors on the SUPERBLINK proper motions ( $\approx 8 \text{ mas yr}^{-1}$ ) compared with the proper-motion errors from the rNLTT ( $\approx 5.5 \text{ mas yr}^{-1}$ ) are due to the fact that astrometric magnitude equations have been neglected in SUPERBLINK proper-motion calculations.

## 6. THE CATALOG

### 6.1. Format

The complete catalog in ASCII format is available in the electronic edition of this paper. The catalog contains 61,977 lines, each 286 characters long. Each catalog entry consists of 29 fields; these are described in Table 1.

The first field gives the LSPM catalog name. The next nine fields provide identifications in the LHS, NLTT, *Hipparcos*, Tycho-2, ASCC-2.5, UCAC-2, 2MASS, and USNO-B1 catalogs, when these exist for the star. An additional field gives the original name of the star in the published literature (e.g., the LSR stars of Lépine et al. [2002b, 2003]). In the current version of the LSPM catalog, however, the original name is provided *only if the star does not have a counterpart in any of the LHS, NLTT, Tycho-2, ASCC-2.5, or UCAC-2 catalogs*. At this point, it is provided as a means to distinguish “rediscovered” LSPM stars from those that are genuine, “new” discoveries.

The astrometric information (position and proper motion) is detailed in the next nine fields and includes a flag that gives the origin of the astrometry. The next eight fields provide the photometric information, with optical, photographic, and infrared magnitudes. The last two fields give the estimated  $V$  magnitude and  $V - J$  color index.

A sample of the catalog is shown in Table 2, in which the first 12 lines are displayed as an example. The full catalog is available only in electronic format.

### 6.2. Names and Identifications

We assign a LSPM name to each star in our catalog, which is based on the star’s right ascension and declination at epoch 2000.0 in the ICRS (essentially equivalent to J2000). The first four characters (“LSPM”) are the catalog identifiers and stand for Lépine and Shara Proper Motion. A space then separates the catalog ID from the positional description. A “J” follows, which indicates the equinox of the position. The next four digits are the hours and minutes of the right ascension, then comes the sign of the declination (“+” for all our stars, since we do not have southern declinations—yet) followed by four more digits that represent the degrees and minutes of declination. Finally, there is one last character used to distinguish stars that would otherwise have the same name. Pairs of stars with the same hours/minutes in right ascension and degrees/minutes in declination have their names appended with an “N,” “S,” “E,” or “W” suffix. The choice of suffix depend on the orientation of the pair. Their separation in both right ascension and declination is determined. If the separation in declination is larger, then the stars are given a N/S suffix, with N (“North”) assigned to the star at higher declination and S (“South”) to the other star. If the separation in right ascension is the largest, then E/W suffixes

TABLE 1  
THE LSPM CATALOG—FIELD DESCRIPTION

Field	Datum	Units	Format
1.....	LSPM catalog name	...	a16
2.....	LHS catalog ID	...	a6
3.....	NLTT catalog ID	...	a6
4.....	<i>Hipparcos</i> catalog ID	...	a7
5.....	Tycho-2 catalog ID	...	a12
6.....	ASCC-2.5 catalog ID	...	a8
7.....	UCAC-2 catalog ID	...	a9
8.....	Other name	...	a31
9.....	2MASS catalog ID	...	a17
10.....	USNO-B1 catalog ID	...	a13
11.....	R.A.	degrees	f12.6
12.....	Decl.	degrees	f11.6
13.....	Total relative proper motion	arcsec yr <sup>-1</sup>	f8.3
14.....	Relative proper motion in R.A.	arcsec yr <sup>-1</sup>	f8.3
15.....	Relative proper motion in Decl.	arcsec yr <sup>-1</sup>	f8.3
16.....	Total absolute proper motion	arcsec yr <sup>-1</sup>	f8.3
17.....	Absolute proper motion in R.A.	arcsec yr <sup>-1</sup>	f8.3
18.....	Absolute proper motion in Decl.	arcsec yr <sup>-1</sup>	f8.3
19.....	Astrometric source flag	...	a2
20.....	Optical <i>B</i> magnitude	mag	f6.2
21.....	Optical <i>V</i> magnitude	mag	f6.2
22.....	Photographic blue ( <i>B<sub>p</sub></i> )	mag	f5.1
23.....	Photographic red ( <i>R<sub>p</sub></i> )	mag	f5.1
24.....	Photographic near-IR ( <i>I<sub>N</sub></i> )	mag	f5.1
25.....	Infrared <i>J</i>	mag	f6.2
26.....	Infrared <i>H</i>	mag	f6.2
27.....	Infrared <i>K<sub>s</sub></i>	mag	f6.2
28.....	Estimated <i>V</i> magnitude	mag	f7.2
29.....	Estimated <i>V–J</i> color	mag	f6.2

are used, with E (“East”) assigned to the star at larger right ascension and W (“West”) to the other one. By no means are stars with “NS” or “EW” suffixes necessarily common proper motion doubles. While this is often the case, there are a number of chance alignments for which two unrelated high proper motion stars happen to be in the same arcminute position bin. Conversely, not all common proper motion doubles have “NSEW” suffixes, since it is often the case that long-period doubles have angular separations large enough to put them in separate arcminute bins.

Identifications are given for the 2572 LSPM stars also listed in the LHS catalog and for the 31,361 stars listed the NLTT. The identification number for stars listed in the LHS catalog is their LHS number, which has been traditionally used in the literature. The identifications for stars listed in the NLTT catalog are the record number in the original NLTT table (“recno” in the electronic version of the NLTT catalog at the Vizier catalog service<sup>6</sup>).

We also provide identifiers for the 4839 stars listed in the *Hipparcos* catalog (HIP number), as well as for 7943 stars with a Tycho catalog number. A total of 4306 of the HIP stars also have data in the Tycho-2 catalog. We give ASCC-2.5 identification for a total of 11,430 stars; these include all the Tycho-2 stars as well as the HIP stars that are not in the Tycho-2. We give UCAC2 catalog numbers for the 9137 LSPM stars that are listed in the UCAC2 catalog. Note that since the bulk of the LSPM stars are fainter than the magnitude limits of these catalogs, the majority of LSPM stars do not have HIP, Tycho-2, ASCC-2.5, or UCAC2 identifiers.

A few hundred LSPM stars are not listed in any of the catalogs listed above but are not entirely “new” objects because they have been previously reported in the literature. An additional column provides the Simbad<sup>7</sup> designation for those objects. About a third of these are the “LSR” high proper motion stars found by our team (Lépine et al. 2002b, 2003). The other stars are a mix of objects, some from old proper-motion catalogs (but that had not been included in the NLTT or LHS) and some identified as M dwarfs or white dwarfs in field spectroscopic surveys. In particular, stars with 2MASS designations are objects identified recently in various searches of ultracool M and L dwarfs.

Finally, we give identifications for the counterparts of the LSPM stars in the 2MASS All-Sky Point Source Catalog and in the USNO-B1.0. Catalog identifiers provided in the LSPM make it easy to retrieve all relevant information from those catalogs.

### 6.3. Positions and Proper Motions

Positions in the LSPM catalog are given at the 2000.0 epoch in the ICRS system and for the great majority are obtained either by extrapolating from the Tycho-2 position using the Tycho-2 proper motion (for stars with Tycho-2 counterparts) or by extrapolating from the position of the 2MASS counterpart, using the SUPERBLINK-derived absolute proper motion or the ASCC-2.5 proper motion (see below for which proper motion is used).

For stars with no 2MASS counterpart (2345 objects) we used the coordinates calculated by SUPERBLINK from the DSS scans instead. The positions of those stars, extrapolated from the position of the star on the POSS-II scan, are much less accurate than the 2MASS-derived positions. Unfortunately, the accuracy of the SUPERBLINK-derived J2000 positions is only  $\approx 0''.5$  (as estimated from a comparison with the 2MASS catalog), and future efforts will be devoted to obtaining more accurate coordinates for those objects.

In the catalog, we list the relative and absolute proper motions in separate columns. The relative proper motions are always those determined by SUPERBLINK. This makes it easy to identify stars that have not been measured with SUPERBLINK: values for their relative proper motion are set to zero.

For the absolute proper motion, we use either the value derived from SUPERBLINK or quote the absolute proper motion from the Tycho-2 or ASCC-2.5 catalogs. The order of priority is as follows: (1) Tycho-2 proper motions, (2) SUPERBLINK proper motion, and (3) ASCC-2.5 proper motion. The quoted Tycho-2 proper-motion errors are  $< 8$  mas yr<sup>-1</sup> for all LSPM stars with a Tycho-2 counterpart. This is smaller than the estimated SUPERBLINK proper-motion errors and justifies that we always defer to the Tycho-2 proper motion. The quoted proper-motion errors for ASCC-2.5 stars that do not have Tycho-2 counterparts are generally  $> 12$  mas yr<sup>-1</sup> with a mean value  $\simeq 14.5$  mas yr<sup>-1</sup>, larger than the SUPERBLINK errors, so we use the ASCC-2.5 proper motions only for those stars that have no SUPERBLINK proper motions. The source of the proper motion is indicated by the astrometric flag: “T” if the Tycho-2 proper motion is used, “S” if it is the SUPERBLINK-derived proper motion, and “A” if the ASCC-2.5 proper motion is quoted.

A total of 508 stars in the LSPM catalog have no Tycho-2 counterparts nor ASCC-2.5 counterparts, and their proper motions have not been measured by SUPERBLINK either. For those objects, we obtain their proper motion from a variety of

<sup>6</sup> Available at <http://vizier.u-strasbg.fr/>.

<sup>7</sup> Available at <http://simbad.u-strasbg.fr/>.

TABLE 2  
THE LSPM CATALOG (NORTH)

Catalog name	LHS	NLTT	HIPP	Tycho-2	ASCC-2.5	UCAC2	Other name	2MASS	USNO-B1	R.A. (deg)	Decl. (deg)	$\mu_{\text{rel}}$ (arcsec yr <sup>-1</sup> )	$\mu\text{RA}_{\text{rel}}$ (arcsec yr <sup>-1</sup> )	$\mu\text{DE}_{\text{rel}}$ (arcsec yr <sup>-1</sup> )
LSPM J0000+0003 .....		58703						00001806+0003218	0900-0000025	0.075275	0.056054	0.246	0.239	-0.059
LSPM J0000+0041 .....		58724						00003113+0041085	0906-0000116	0.129708	0.685727	0.189	0.178	-0.065
LSPM J0000+0313 .....		58739						00004044+0313424	0932-0000102	0.168501	3.228500	0.342	0.170	-0.296
LSPM J0000+0356 .....		58690	6		1092876			00000449+0356472	0939-0000011	0.018675	3.946463	0.000	0.000	0.000
LSPM J0000+0409 .....				4 874 1	1092912	33159366		00005083+0409468	0941-0000118	0.211770	4.163031	0.167	0.157	-0.051
LSPM J0000+0812 .....								00005269+0812444	0982-0000215	0.219538	8.212363	0.181	0.176	-0.032
LSPM J0000+0852 .....		58753						00005069+0852540	0988-0000105	0.211180	8.881723	0.225	0.134	-0.177
LSPM J0000+1121 .....		58688						00000377+1121471	1013-0000009	0.015681	11.363118	0.174	0.147	-0.093
LSPM J0000+1348 .....		58687						00000538+1348007	1038-0000015	0.022462	13.800193	0.222	0.185	-0.124
LSPM J0000+1353 .....								00004529+1353230	1038-0000126	0.188751	13.889735	0.178	0.177	0.021
LSPM J0000+1434 .....		58752			912866			00005198+1434028	1045-0000228	0.216600	14.567470	0.343	0.339	-0.055
LSPM J0000+1628 .....								00004004+1628047	1064-0000112	0.166877	16.467981	0.441	0.439	-0.046

Catalog name	$\mu_{\text{abs}}$ (arcsec yr <sup>-1</sup> )	$\mu\text{RA}_{\text{abs}}$ (arcsec yr <sup>-1</sup> )	$\mu\text{DE}_{\text{abs}}$ (arcsec yr <sup>-1</sup> )	Flag	$B$ (mag)	$V$ (mag)	$B_J$ (mag)	$R_F$ (mag)	$I_N$ (mag)	$J$ (mag)	$H$ (mag)	$K_s$ (mag)	$V_e$ (mag)	$V-J_e$ (mag)
LSPM J0000+0003 .....	0.253	0.244	-0.068	S	99.99	99.99	15.8	14.1	13.0	11.75	11.15	10.90	15.02	3.27
LSPM J0000+0041 .....	0.198	0.183	-0.075	S	99.99	99.99	17.0	15.5	13.9	12.61	12.09	11.83	16.31	3.70
LSPM J0000+0313 .....	0.352	0.176	-0.305	S	99.99	99.99	18.3	16.4	14.6	13.71	13.21	12.96	17.43	3.72
LSPM J0000+0356 .....	0.227	0.226	-0.013	A	13.64	12.39	13.4	11.2	99.9	9.81	9.17	8.97	12.39	2.58
LSPM J0000+0409 .....	0.170	0.157	-0.065	T	12.70	11.71	12.2	11.1	10.6	9.93	9.35	9.26	11.71	1.78
LSPM J0000+0812 .....	0.185	0.181	-0.040	S	99.99	99.99	19.6	18.0	17.3	15.88	15.25	14.88	18.86	2.98
LSPM J0000+0852 .....	0.231	0.139	-0.185	S	99.99	99.99	17.4	15.6	13.9	12.78	12.28	12.05	16.57	3.79
LSPM J0000+1121 .....	0.183	0.153	-0.101	S	99.99	99.99	17.5	16.1	15.4	14.59	14.10	13.74	16.86	2.27
LSPM J0000+1348 .....	0.232	0.190	-0.132	S	99.99	99.99	17.8	14.7	13.3	12.33	11.76	11.55	16.37	4.04
LSPM J0000+1353 .....	0.183	0.182	0.013	S	99.99	99.99	17.7	15.7	14.0	12.51	11.92	11.62	16.78	4.27
LSPM J0000+1434 .....	0.350	0.345	-0.063	S	14.24	13.05	14.6	12.3	11.0	10.01	9.38	9.15	13.05	3.04
LSPM J0000+1628 .....	0.447	0.444	-0.054	S	99.99	99.99	20.6	19.0	15.9	14.06	13.52	13.16	19.86	5.80

NOTE.—Table 2 is presented in its entirety in the electronic edition of the *Astronomical Journal*. A portion is shown here for guidance regarding its form and content.

sources, mainly from the NLTT and rNLTT catalogs, and also from the catalog of revised proper motions of LHS stars of Bakos et al. (2002). These objects are denoted by the astrometric flag “O.”

Note that for LSPM stars with Tycho-2 counterparts that have also been measured with SUPERBLINK, values for the absolute proper motion are quoted from the Tycho-2 catalog but values for the relative proper motions are those from SUPERBLINK. Note also that zonal corrections are calculated individually for each star, using all Tycho-2 objects within  $7^\circ$  of that star. Our map of the zonal corrections can thus be recovered from the LSPM catalog, by differencing the relative and absolute proper motions for stars that have their absolute proper motions derived from the SUPERBLINK values.

#### 6.4. Magnitudes

The LSPM catalog lists optical  $B$  and  $V$  magnitudes from the Tycho-2 and ASCC-2.5 catalogs. It also gives the photographic blue ( $B_J$ ), red ( $R_F$ ), and near-infrared ( $I_N$ ) magnitudes extracted from the USNO-B1.0 catalog. Stars with no USNO-B1 counterparts are listed with  $B_J$  and  $I_N$  magnitudes of 99.9, indicating these to be unavailable. When a value for  $R_F$  could not be obtained from the USNO-B1.0 catalog, we used the value estimated by SUPERBLINK from the POSS-II red DSS scans. A value of 99.9 is also used whenever there is only partial magnitude information from the USNO-B1 counterpart (or counterparts, see § 4.2 above).

Infrared magnitudes for LSPM stars are obtained from their counterparts in the 2MASS All-Sky Point Source Catalog (Cutri et al. 2003). The accuracy is about 0.02 mag for  $5 < J < 14$ ,  $5 < H < 14$ , and  $4 < K_s < 13$ ; it is  $\approx 0.25$  mag for brighter stars (saturated on the 2MASS images). For fainter stars, the uncertainty increases with magnitude. The 2MASS catalog is complete to  $J \simeq 16.5$ ,  $H \simeq 16.0$ , and  $K_s \simeq 15.5$ .<sup>8</sup>

Finally, estimated  $V$  magnitudes and  $V - J$  colors are given in the last two columns. Values are provided for all but a few entries. These should be used for quick reference and for classification of the high proper motion stars. See § 4.4 for the caveats in using these estimated values.

### 7. COMPLETENESS OF THE LSPM CATALOG

#### 7.1. Comparison with the NLTT Catalog

The completeness of a proper-motion catalog can be a function of magnitude, proper motion, and position. The completeness is generally dependent on how easy it is to identify moving objects against the backdrop of the “fixed” stars. Detection will be more difficult if the star is fainter but also if it is moving faster or if the local density of background objects is larger. Traditionally, proper-motion surveys have been very incomplete for faint stars at low Galactic latitudes. As described above, our SUPERBLINK software, with its image subtraction algorithm, was specifically designed to address this problem and to detect moving stars in densely populated areas. We therefore expect the LSPM catalog to be significantly more complete than the NLTT at low Galactic latitudes. The main question is how much more complete the LSPM is. In particular, we would like to know whether the LSPM catalog still suffers from some incompleteness near the Galactic plane.

We first compare the distribution of NLTT and LSPM stars as a function of position, separating the stars into two groups: stars

brighter than  $V = 16$  and stars fainter than  $V = 16$ . Figure 18 shows the distribution of brighter stars. The distributions for both catalogs are relatively uniform (no sharp discontinuities, or “holes”). However, the density of objects is not strictly uniform because it appears to be larger in high Galactic latitudes. However, the decline is very gradual and this is in sharp contrast to the distributions of faint NLTT stars, shown in Figure 19. The density of faint NLTT objects falls very abruptly at low Galactic latitudes: a clear mark of true incompleteness in the NLTT catalog. On the other hand, the distribution of faint LSPM objects follows more or less the same trends as the distribution of bright high proper motion stars, with a gradual decline.

Two interpretations are possible. One is to say that the distribution of high proper motion stars should be uniform across the sky and that it is the completeness of the catalog that progressively diminishes as one goes to lower Galactic latitudes. With this interpretation, both the NLTT and LSPM are significantly incomplete, even at moderately high Galactic latitudes ( $20^\circ < |b| < 60^\circ$ ). The other interpretation, and the one we favor, is that the distribution of proper-motion–selected objects is naturally nonuniform over the sky, and that the progressive density variations observed in Figure 18 and in the top panel of Figure 19 have little to do with completeness. Under this second interpretation, the completeness of the LSPM catalog is uniformly high, both at high and low Galactic latitude. We demonstrate the truth of this statement as follows.

Figure 20 lets us estimate the completeness of the LSPM catalog from the rate at which NLTT stars are recovered by SUPERBLINK and Tycho-2. One can guess in advance that the rate is very high, since very few NLTT stars had to be separately incorporated into the catalog (see § 3.4). We exclude from this analysis the NLTT stars that were missed by SUPERBLINK because they are in areas that were not processed by the code, since their inclusion would underestimate the true efficiency of SUPERBLINK. We calculate the fraction of NLTT stars that have been recovered either by SUPERBLINK or from the Tycho-2/ASCC-2.5 catalogs. Results are shown in Figure 20. The recovery rate is  $\approx 99\%$  to a magnitude as faint as  $V = 19$ , falling to  $\approx 90\%$  at  $V = 20$ . Note also the small dip (to  $\approx 98\%$ ) at the boundary between Tycho-2 and SUPERBLINK stars ( $V = 12$ ), which we investigate further in § 7.2. The recovery does not vary significantly with the proper motion. There is, however, the expected trend that SUPERBLINK misses more stars at low Galactic latitudes, but the recovery rate still exceeds  $97\%$  at  $|b| < 10^\circ$ .

The recovery rate of NLTT stars by SUPERBLINK/Tycho-2 is a good estimate of the completeness of the LSPM catalog but is valid only in regions of the  $(\mu, V, b)$  parameter space that contain a sufficient number of NLTT stars. We know from Figure 19 that the NLTT catalog is significantly depleted at  $|b| < 15^\circ$  and  $V > 16$ , which means the completeness of the SUPERBLINK sample cannot be evaluated for faint stars at low Galactic latitudes using the above method. Outside of that specific range, however, we conclude that the completeness of the SUPERBLINK/Tycho-2 sample is indeed extremely high.

However, the completeness of the LSPM catalog itself is larger than the completeness of the SUPERBLINK/Tycho-2 sample, since the missing NLTT stars have been included in the LSPM. Assuming that the NLTT catalog is itself more than  $90\%$  complete for  $|b| > 15^\circ$  and  $V < 18$  stars suggests that  $90\%$  of the stars missed by Tycho-2 and SUPERBLINK might have been found by Luyten, in which case the LSPM catalog could be up to  $\approx 99.9\%$  complete down to  $V = 18$ . However, this assumes that both the SUPERBLINK/Tycho-2 and the NLTT

<sup>8</sup> Detailed documentation can be found at <http://www.ipac.caltech.edu/2mass/>.

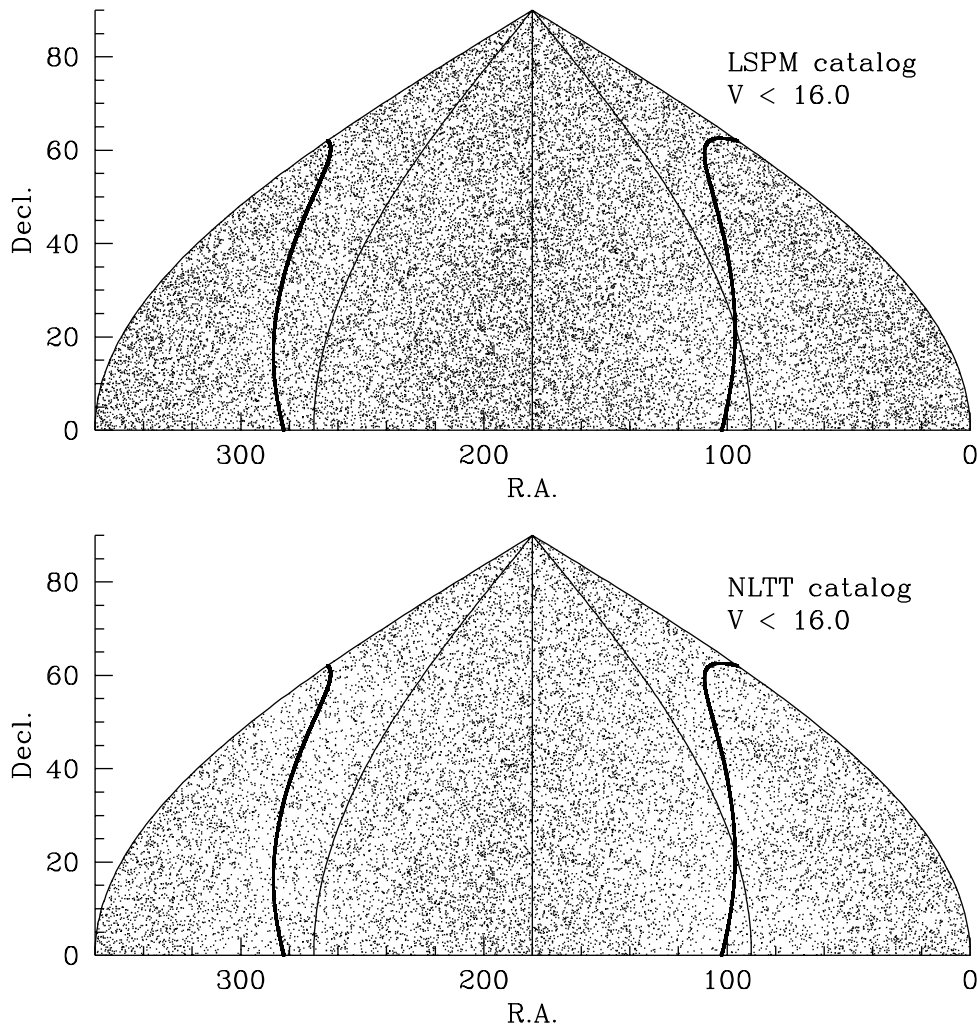


FIG. 18.—Distribution of high proper motion stars from our LSPM catalog (*top*) compared with the distribution of stars from the NLTT (*bottom*). Shown here are stars brighter than  $V = 16.0$  (see Fig. 19 for the distribution of fainter stars). The Galactic equator is shown (*thick line*). Note that even though both catalogs are expected to be relatively complete ( $>90\%$ ) in that range, it is obvious that the density of objects is larger at high Galactic latitudes. This suggests that proper-motion-selected samples are intrinsically nonuniform. Indeed, one does expect proper-motion surveys to be more sensitive to old disk and halo stars at high Galactic latitudes, because of the asymmetric drift.

samples are statistically independent, an assumption that may not be entirely valid. Indeed, it is very possible that stars that have been missed by SUPERBLINK have also been missed by Luyten for the exact same reason. From our experience, failed detections mostly occur when a faint star moves on pixels saturated by a bright nearby object at one of the two epochs (or worse, at both epochs). However, high proper motion stars eventually move out of the glare, so a star that is hidden at one epoch will be easy to spot at another. Indeed, this is what happens for several of the NLTT stars that SUPERBLINK failed to identify: the star is in the glare of a bright object on the POSS-II image. Because Luyten used his own 1960s plates as a second epoch, the object was then easy to identify. As was shown in Lépine et al. (2003), many of the new high proper motion stars found with SUPERBLINK follow the inverse pattern: easy to find on the POSS-II scans, their trajectory puts them in the glare of a brighter star in the 1960s. The real problem is for stars hiding on the POSS-I plates, since both we and Luyten are using it as the first epoch. Additionally, there might be a few faint stars lost in the extended, saturated patches from very bright stars at all epochs (if the total 45 yr motion of the star is shorter than the size of the saturated image), although these cases should be quite rare.

The bottom line is that for every star missed by SUPERBLINK but found by Luyten, there is probably at least another one that has been missed by both. Thus, despite the fact that the additional NLTT stars make the LSPM catalog more complete than the SUPERBLINK/Tycho-2 sample, we conclude that *the LSPM catalog is approximately 99.0% complete to as faint as  $V = 19$  and at high ( $|b| > 15^\circ$ ) Galactic latitudes.*

We now determine the completeness of the NLTT catalog by comparing it to the LSPM catalog, assumed to be 99% complete within the limits quoted above. We first plot the fraction of LSPM stars that are NLTT objects as a function of magnitude, proper motion, and Galactic latitude (Fig. 21). The general completeness of the NLTT over the whole northern sky for stars with  $\mu > 0''.15$  is a little above 60% down to  $V = 14$ , falls gradually to 40% at  $V = 19$ , and then drops more abruptly. This is, however, not a fair assessment of the completeness of Luyten's survey, because the LSPM catalog has a lower proper-motion limit and because the completeness of the NLTT is significantly lower at low Galactic latitudes.

First we want to determine the effective proper-motion limit of the NLTT, specifically the limit above which the NLTT is most complete. We find that the completeness of the NLTT

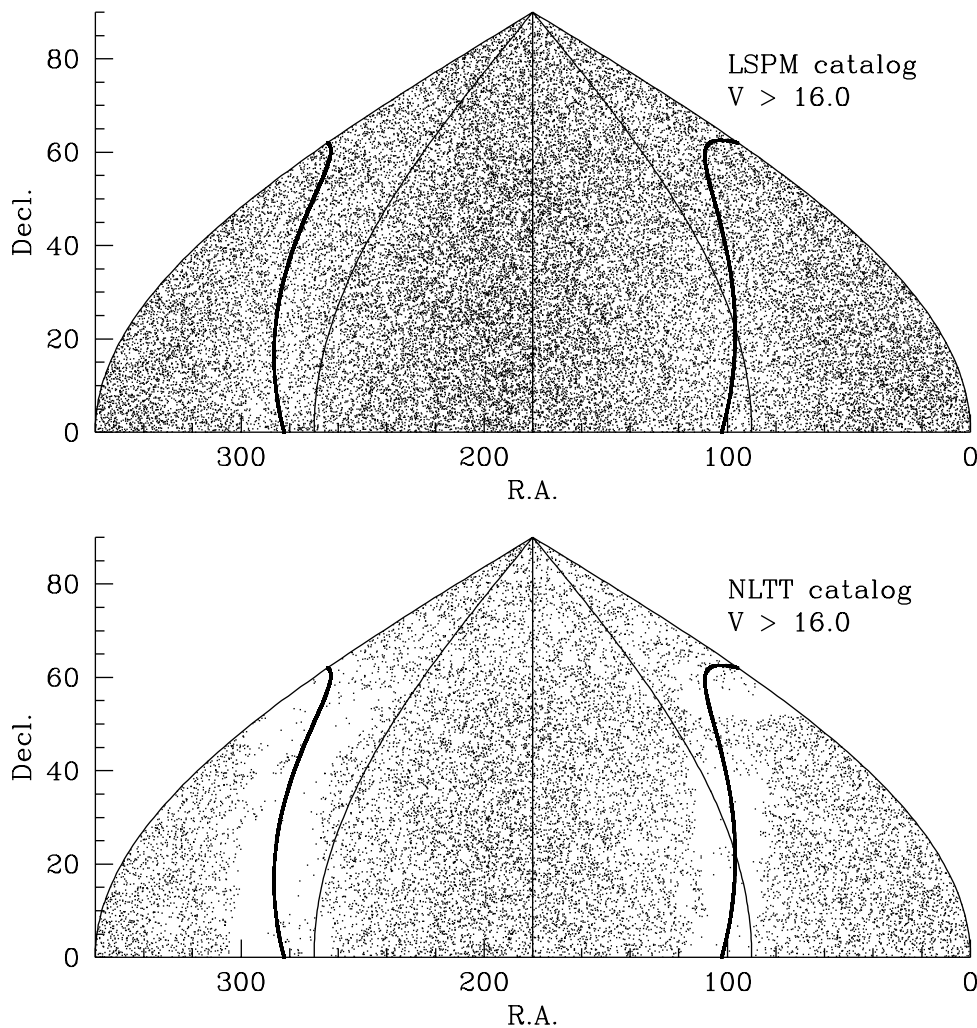


FIG. 19.—Same as Fig. 18, but for stars fainter than  $V = 16.0$ . The NLTT is dramatically incomplete in low Galactic latitudes. This situation is much improved with the LSPM catalog. One still observes a lower density of high proper motion stars at low Galactic latitudes.

catalog decreases sharply below  $\mu = 0''.20 \text{ yr}^{-1}$ . This is to be expected from the fiducial limit of  $0''.18 \text{ yr}^{-1}$  and the  $0''.02 \text{ yr}^{-1}$  measurement error. Because the drop in completeness starts a little above  $\mu = 0''.20 \text{ yr}^{-1}$ , we define the range of maximal completeness of the NLTT as  $\mu > 0''.25 \text{ yr}^{-1}$ .

The NLTT is supposed to be most complete within the CPR, as defined by Dawson (1986), which for the northern sky is simply  $|b| > 10^\circ$ , for stars with  $\mu > 0''.2 \text{ yr}^{-1}$ . However, we note that the completeness of the NLTT actually starts falling a few degrees above  $|b| = 10^\circ$ . We conclude that the NLTT is most complete for proper motions  $\mu > 0''.25 \text{ yr}^{-1}$  and Galactic latitudes  $|b| > 15^\circ$ .

We now proceed to check the completeness of the NLTT as a function of magnitude for three regions of parameter space (Fig. 22). First we check the completeness for the CPR. We find that the estimate of Dawson (1986) is accurate and that the NLTT catalog is indeed more than 80% complete down to  $V = 18$ . The second region is the one we identified as the most complete of the NLTT, with the  $\mu > 0''.25 \text{ yr}^{-1}$  stars at Galactic latitudes  $|b| > 15^\circ$ . For that restricted area, we find the NLTT to be 90% complete down to  $V = 18.5$ . Finally, we check the completeness of the NLTT at low Galactic latitudes  $|b| < 15^\circ$ , again for stars with  $\mu > 0''.25 \text{ yr}^{-1}$ . We now find that the completeness falls from about 90% at  $V = 15.0$  to only 30% below  $V = 17.0$ .

Our estimate of a fairly high completeness of the NLTT at high Galactic latitudes is very significant, because it indicates that the internal completeness test described by Flynn et al. (2001) underestimates the completeness of the proper-motion sample. The test of Flynn et al. (2001) suggested that the completeness of the NLTT in the CPR fell to 80% at  $V = 15$  and down to 60% at  $V = 18.5$ , which is significantly smaller than the results of our (external) test. It appears that the criticism offered by Monet et al. (2000) is legitimate and that changes in the space density of objects as a function of distance do lead to an underestimate of the completeness when applying the internal test of Flynn et al. (2001).

### 7.2. Completeness at the SUPERBLINK/Tycho-2 Boundary

Completeness problems in the LSPM catalog occur in the magnitude overlap region between Tycho-2 and SUPERBLINK stars ( $V \approx 12$ ). The problem arises because the completeness of the Tycho-2 catalog starts to decrease before SUPERBLINK reaches its full detection efficiency. As a result, it is very possible that relatively bright stars have been missed by SUPERBLINK because of plate saturation and at the same time are missing from the Tycho-2 (or ASCC-2.5) catalogs because they are fainter than these catalogs' completeness limits.

Fortunately, the Tycho-2 catalog has a small, but significant, overlap with the SUPERBLINK detections. A large fraction of the brighter SUPERBLINK stars are in the Tycho-2 catalog

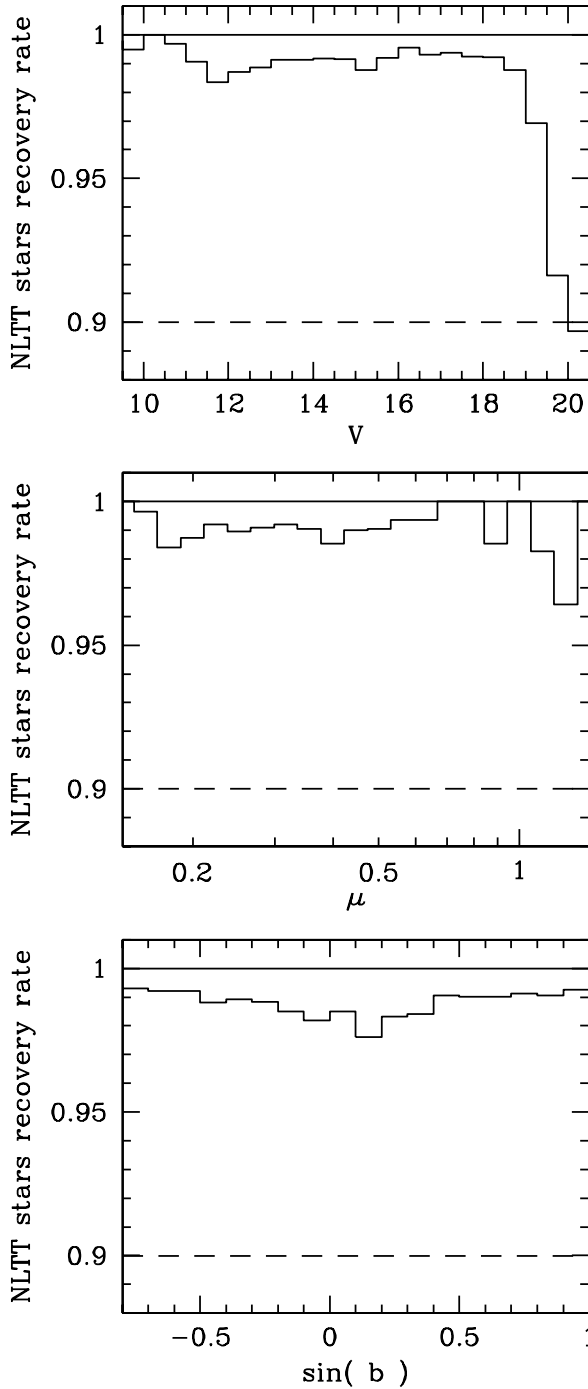


FIG. 20.—Estimated completeness of the LSPM catalog based on the recovery rate of NLTT stars. The recovery rate is  $>98\%$  for all values of the proper motion and for magnitudes  $V > 19.0$ . The recovery rate then drops to  $\sim 90\%$  at  $V = 20.0$ . The recovery rate is marginally smaller at low Galactic latitudes but still exceeds  $97\%$ .

and, likewise, a large fraction of the fainter Tycho-2 stars have been recovered by SUPERBLINK. There is no significant magnitude gap in the combined Tycho-2 + SUPERBLINK sample. This is clear from Figure 20 (*top*), which demonstrates that the combined Tycho-2/SUPERBLINK sample does recover more than  $98\%$  of the NLTT stars in that magnitude range. Since the completeness of the full LSPM (including the missed NLTT stars) is very high, we can use the assumption that it is in fact complete to estimate the completeness of both the Tycho-2 and SUPERBLINK samples as a function of magnitude. The

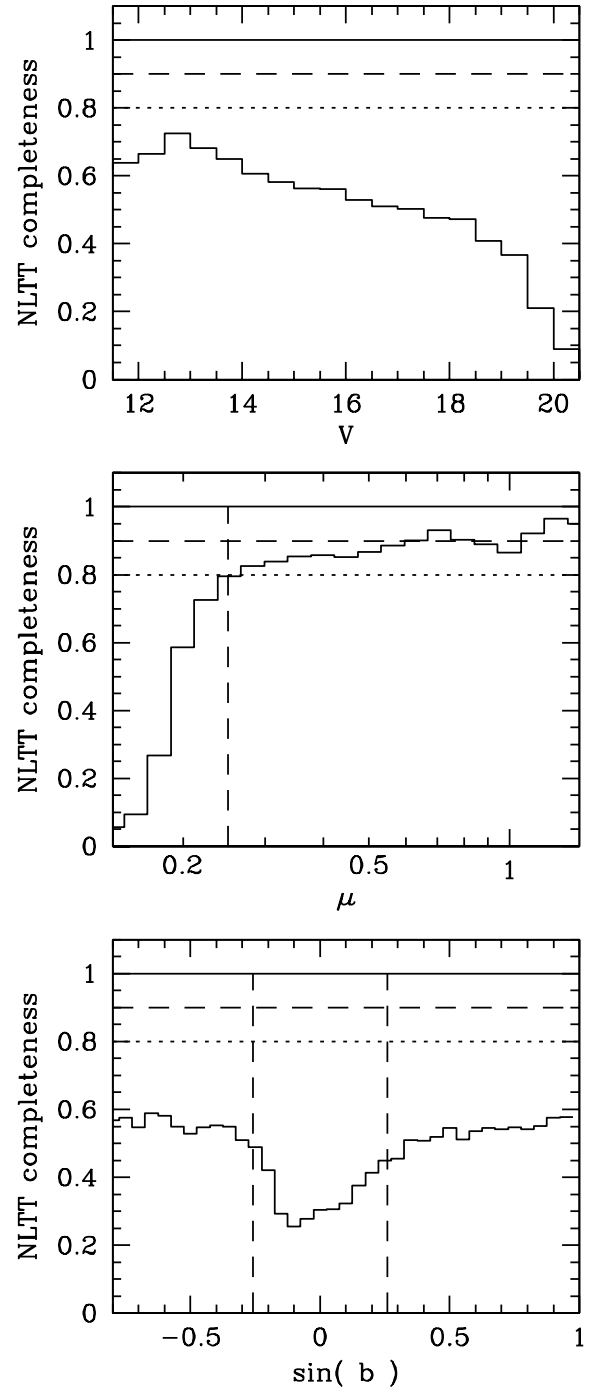


FIG. 21.—Completeness of the old NLTT catalog, estimated from the fraction of LSPM catalog objects that are NLTT stars. The NLTT completeness is a function of both magnitude and proper motion. Although the NLTT was relatively complete for stars with  $\mu > 0.3 \text{ yr}^{-1}$  and brighter than  $R_F = 14$ , its completeness dropped significantly at fainter magnitudes and was much more limited for proper motions near the cutoff at  $\mu = 0.18 \text{ yr}^{-1}$ .

estimated SUPERBLINK and Tycho-2 completeness is plotted in Figure 23 (*top two panels*).

We use a probabilistic approach to estimate the completeness of the combined sample. We can say that the completeness function  $f(V)$  is also the probability that a star of  $V$  magnitude will be in the sample. The probability that a star is in the Tycho-2 (or ASCC-2.5) catalog is  $f_{\text{TYCHO}}(V) \simeq N_{\text{TYCHO}}(V)/N_{\text{LSPM}}(V)$ , while the probability for a star to be detected by SUPERBLINK is  $f_{\text{SB}}(V) \simeq N_{\text{SB}}(V)/N_{\text{LSPM}}(V)$ , where  $N_{\text{LSPM}}(V)$  is the total

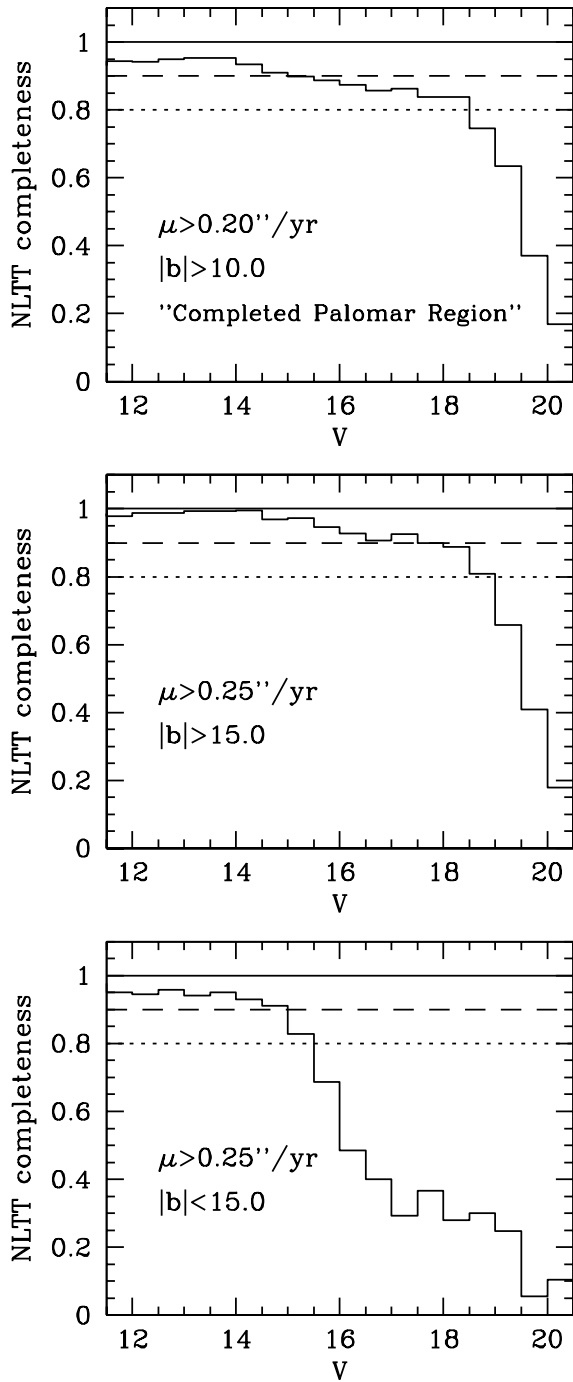


FIG. 22.—Completeness as a function of magnitude for the NLTT catalog, based on a comparison with the LSPM, for various ranges of proper motion and Galactic latitudes. The CPR is traditionally assumed to be the most complete (*top*), although the NLTT is significantly more complete if we exclude the bands  $10^\circ < |b| < 15^\circ$  (*middle*). At low Galactic latitudes (*bottom*), the completeness of the NLTT drops significantly beyond  $V = 15$ .

number of LSPM stars as a function of  $V$  magnitude,  $N_{\text{SB}(V)}$  is the total number of LSPM stars detected with SUPERBLINK, and  $N_{\text{TYCHO}(V)}$  is the total number of LSPM stars detected that are also in the Tycho-2 catalog. The probability that a star is missing from the Tycho-2 is thus  $1 - f_{\text{TYCHO}}$ , while the probability that a star will be missed by SUPERBLINK is  $1 - f_{\text{SB}}$ . Assuming the two samples to be independent, we can say that the probability that a star is missing from *both* the Tycho-2 and SUPERBLINK samples is  $(1 - f_{\text{TYCHO}})(1 - f_{\text{SB}})$ . Thus, the completeness of

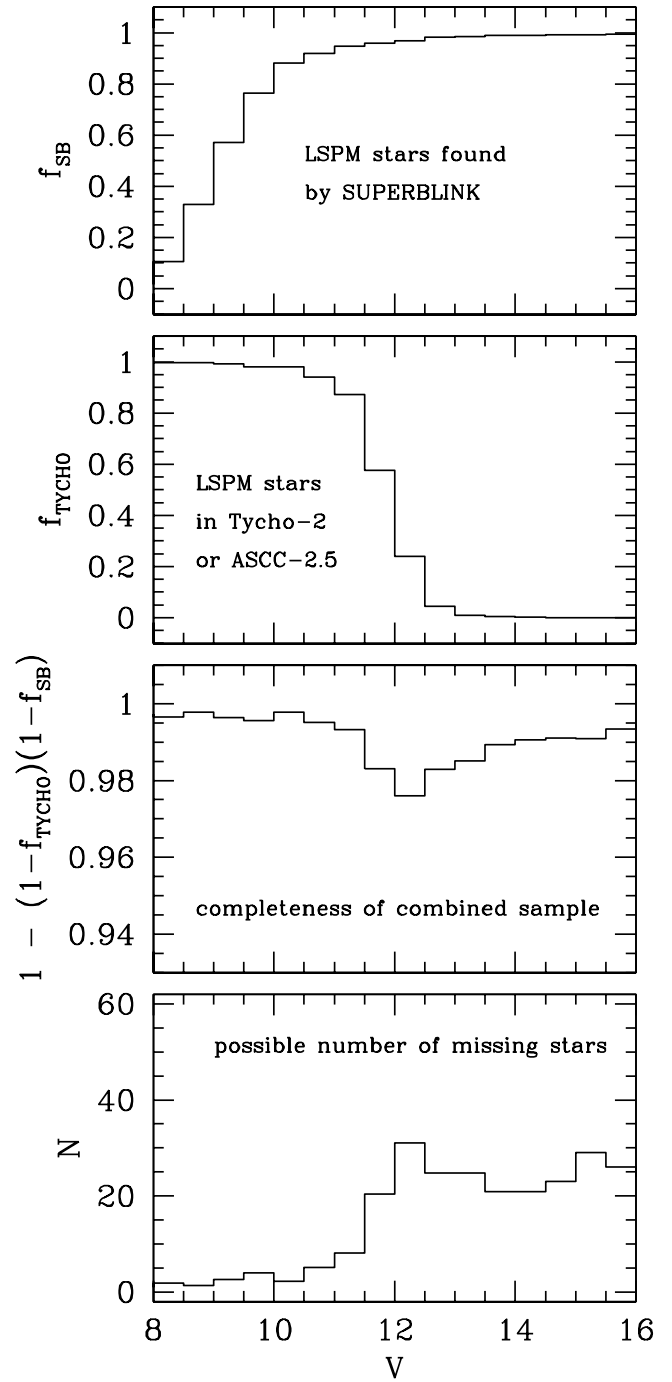


FIG. 23.—Estimated completeness of the LSPM catalog at the magnitude boundary between the Tycho-2/ASCC-2.5 catalog and the SUPERBLINK stars. The LSPM is built from the combination of the two samples, which overlap over a relatively small magnitude range. The coverage appear to be tight enough that few stars should have been missed at the boundary; the estimated completeness of the combined sample only drops to  $\approx 98\%$  around  $V = 12.0$ , compared with  $\approx 99.5\%$  at brighter magnitudes and  $\approx 99\%$  at fainter magnitudes. The estimated number of stars missing from the LSPM because of the boundary effect should be  $\leq 100$ . Note that several of these were recovered as additional NLTT objects (see Fig. 7).

the combined sample will be  $1 - (1 - f_{\text{TYCHO}})(1 - f_{\text{SB}})$ , which is a function of  $V$  magnitude. From this, we calculate the completeness of the combined SUPERBLINK+Tycho-2 list and the total number of stars that would presumably be missing from the LSPM because of this incompleteness (Fig. 23, *bottom two panels*). The effect is very small, and the completeness only drops to

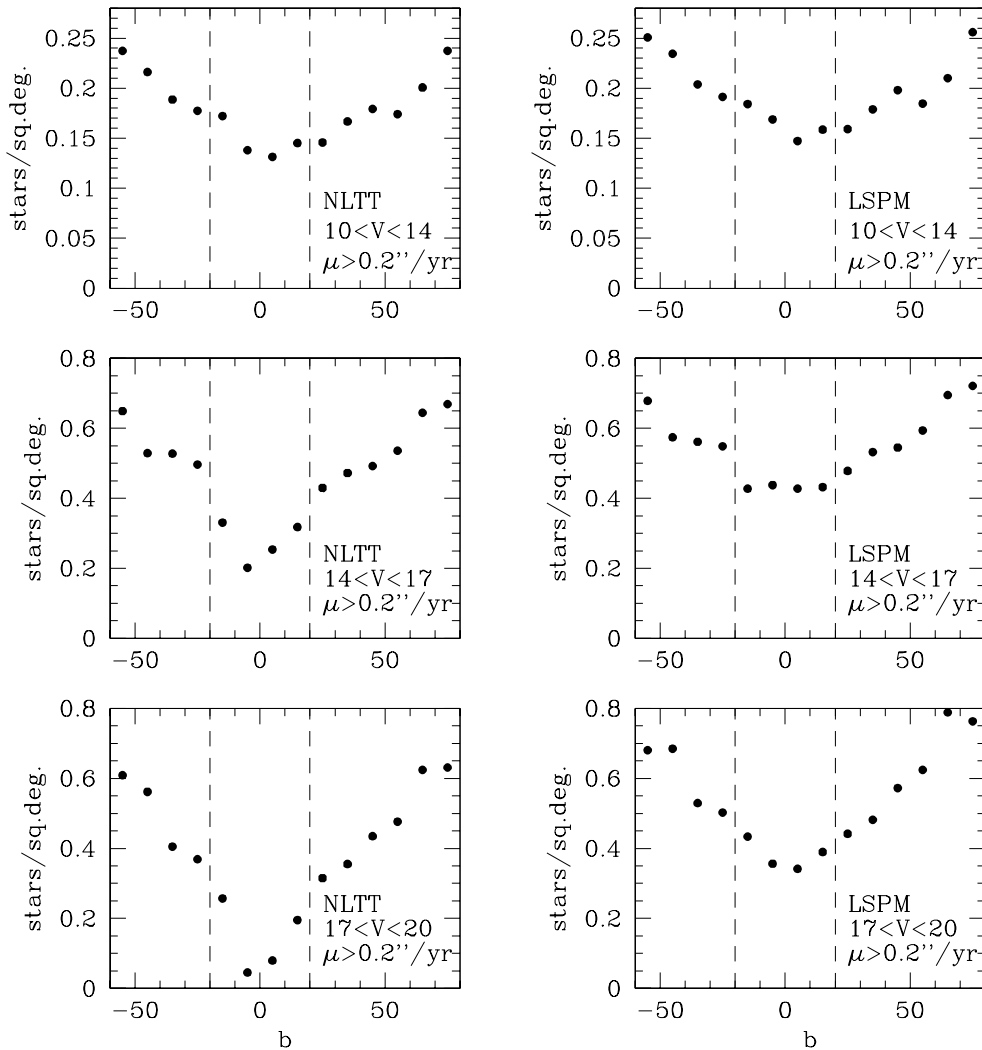


FIG. 24.—Surface density of (in stars per square degree) of the NLTT and LSPM catalogs as a function of Galactic latitude for three groups of  $\mu > 0''.2 \text{ yr}^{-1}$  stars: bright (*top*), moderately faint (*middle*), and faint (*bottom*). At high Galactic latitudes, outside of the area delimited by the dashed line ( $|b| > 20^\circ$ ), the NLTT is more than >90% complete, and the LSPM is >99% complete, for  $V < 18$ . Both catalogs are >90% complete for bright stars ( $V < 14$ ) in low Galactic latitudes ( $|b| < 20^\circ$ ). The drop in the density of  $V < 14$  NLTT stars at low Galactic latitudes is largely due to catalog incompleteness. Not so for the LSPM catalog, which appears to be largely complete at  $|b| < 20^\circ$ , given the intrinsic trend in number density with the Galactic latitude  $b$ .

$\approx 98\%$  around  $V = 12$ . Overall, we expect to be missing  $\approx 50$ – $100$  stars because of the boundary effect.

We note that  $\approx 60$  additional NLTT stars have been found in the  $10 < V < 14$  magnitude range that were neither in the SUPERBLINK nor Tycho-2/ASCC-2.5 lists (Fig. 7). The NLTT thus recovers some of the missing stars. But because the NLTT has a higher proper motion limit than the LSPM, additional stars in the  $0''.15 \text{ yr}^{-1} < \mu < 0''.18 \text{ yr}^{-1}$  range are probably still missing. Since about a third of the LSPM stars are in the  $0''.15 \text{ yr}^{-1} < \mu < 0''.18 \text{ yr}^{-1}$  range, the LSPM catalog is probably still missing  $\approx 30$  stars in the  $10 < V < 14$  magnitude range.

### 7.3. Completeness of the LSPM at Low Galactic Latitudes

A close examination of Figures 18 and 19 makes it very apparent that the number density of LSPM stars is not uniform over the sky. Clearly, there are more LSPM stars at higher Galactic latitude than near the Galactic plane. The lower counts at low Galactic latitude are actually a natural consequence of the low proper-motion cutoff of the catalog and not a result of decreased completeness in low Galactic latitude fields.

The first line of evidence that this is true is that the lower density of LSPM stars at low Galactic latitude is observed both

for bright and fainter stars. Figure 24 shows that there are  $\approx 40\%$  fewer LSPM stars at low Galactic latitudes than there are at high Galactic latitudes and that this is independent of the magnitude of the stars. If there were completeness problems in the LSPM because of crowding, or other low Galactic latitude effects, the proportion of low Galactic latitude stars would drop with fainter magnitudes, as is observed in the NLTT catalog (see Fig. 24).

If the distribution of LSPM stars is not uniform over the northern sky, it must be because of proper-motion selection effects. The velocity components of the stars in the vicinity of the Sun are not isotropic, because of Galactic rotation and because of the Sun's motion relative to the LSR. The distribution of stellar proper-motion vectors is very much dependent on the position on the sky, as illustrated in Figure 25. One naturally expects to find more high proper motion stars at high Galactic latitude because of the large apparent drift of the halo and old disk stars in that direction, as seen from the Sun.

If the distribution of high proper motion stars were uniform over the sky, estimating the completeness at low Galactic latitudes would be straightforward. Since the LSPM is nearly complete at high Galactic latitudes (for  $V < 19$ ), the completeness at low Galactic latitudes could then be estimated from the ratio

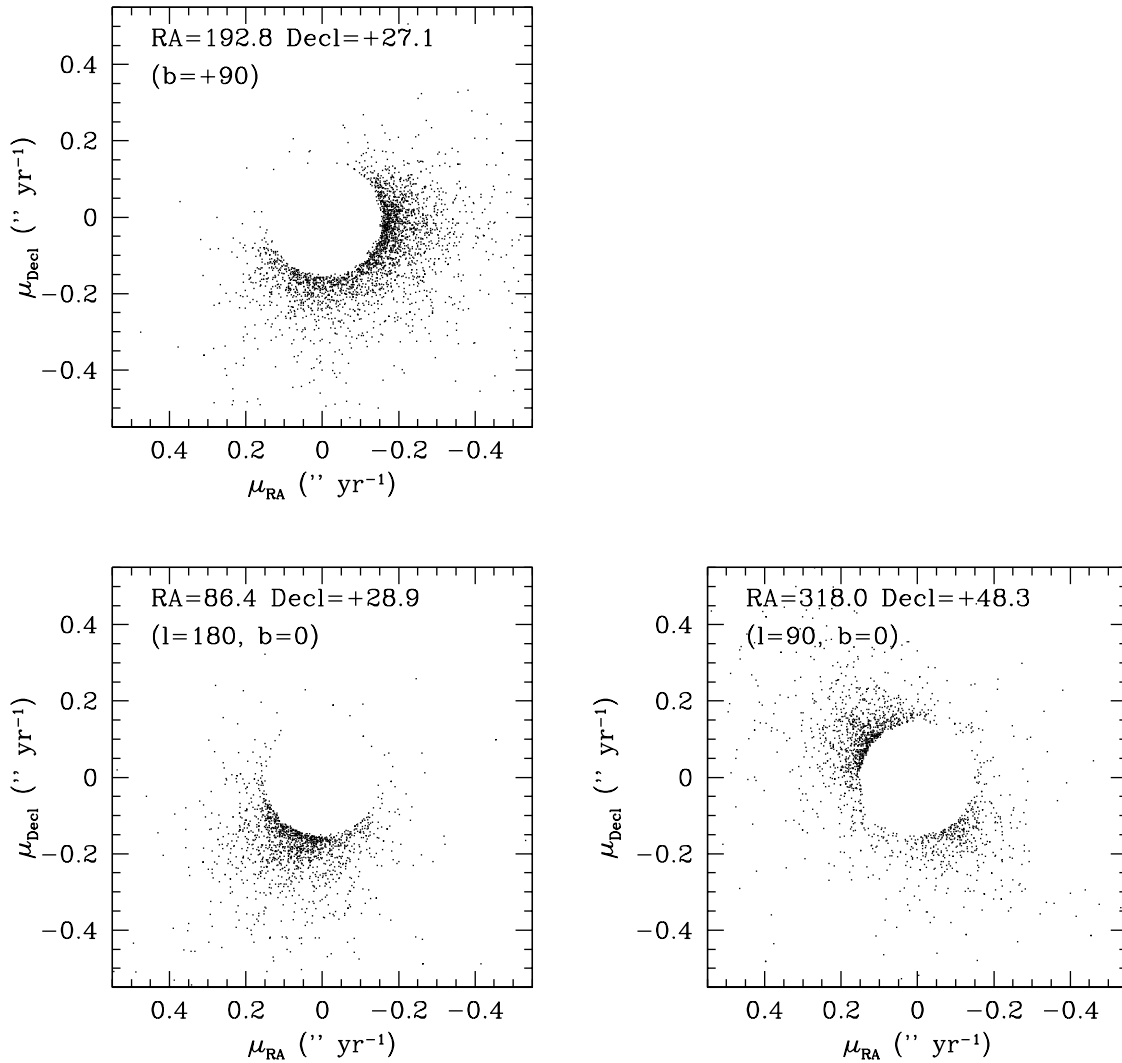


FIG. 25.—Distribution of absolute (zonal-corrected) proper motions for LSPM stars within  $15^\circ$  of the north Galactic pole (*top*), the direction of Galactic rotation (*bottom right*), and the Galactic anticenter (*bottom left*). The distribution of proper-motion vectors is not uniform, and shows a distinct pattern that is clearly dependent on the position on the sky. The fixed, low- $\mu$  cutoff of the catalog (*empty disks centered on the origin*) determines how many stars are locally included in the LSPM catalog. The larger scatter and larger offset in the proper-motion vectors near the Galactic pole implies that more stars in that direction will make it into the LSPM. This explains the higher density of LSPM objects at high Galactic latitudes, near the north Galactic pole.

between the number density of low Galactic latitude stars to the number density of high Galactic latitude stars. This could be calculated for each magnitude bin to obtain the completeness as a function of magnitude. However, because the distribution of high proper motion stars is intrinsically nonuniform over the sky, one has to predict what the density of stars at low Galactic latitudes should be. Estimates of the completeness will be dependent on the predicted number density of high proper motion stars in the low Galactic latitude regions.

To estimate the completeness of the LSPM in low Galactic latitude fields, we use the following test. For stars in some magnitude bin  $[V, V + \Delta V]$ , we first calculate the number density of LSPM objects (in stars per square degrees) in the area located within  $15^\circ$  of the Galactic plane ( $|b| < 15^\circ$ ). We then calculate the number density of  $[V, V + \Delta V]$  stars in  $10^\circ$  bands located above and below this region ( $15^\circ < |b| < 25^\circ$ ). We assume that the survey is complete in the  $15^\circ < |b| < 25^\circ$  region and that the distribution of high proper motion stars should be uniform over the whole  $|b| < 25^\circ$  area. The completeness in the  $|b| < 15^\circ$  region is thus simply the ratio between the measured density in  $|b| < 15^\circ$  to the measured density in  $15^\circ < |b| <$

$25^\circ$ . We repeat the calculation for a range of magnitude bins to obtain the completeness as a function of  $V$ . Note that this method essentially provides an *internal* test of completeness. The main caveat is that the density of high proper motion stars is not uniform over the sky, as demonstrated above. However, the use of relatively low Galactic latitude bands ( $15^\circ < |b| < 25^\circ$ ) as a reference should minimize the effects of the intrinsic nonuniformity. Nevertheless, since the density of high proper motion stars decreases with Galactic latitudes, our internal completeness test is expected to slightly *underestimate* the actual completeness level at low Galactic latitude, possibly by as much as  $\approx 5\%$ – $10\%$ , although a detailed modeling of the distribution of high proper motion stars would be required to determine the exact value.

Results of the completeness test are shown in Figure 26, where we have applied it separately to the complete LSPM catalog (*top*) and to the subsample of LSPM stars that are in the NLTT catalog (*bottom*). Results for the NLTT stars are consistent with the external completeness test shown in Figure 22 (which is based on a comparison between NLTT and LSPM), with a sharp drop in completeness at  $V = 16$ . Note that at moderately bright magnitudes ( $13 < V < 15$ ) the internal test

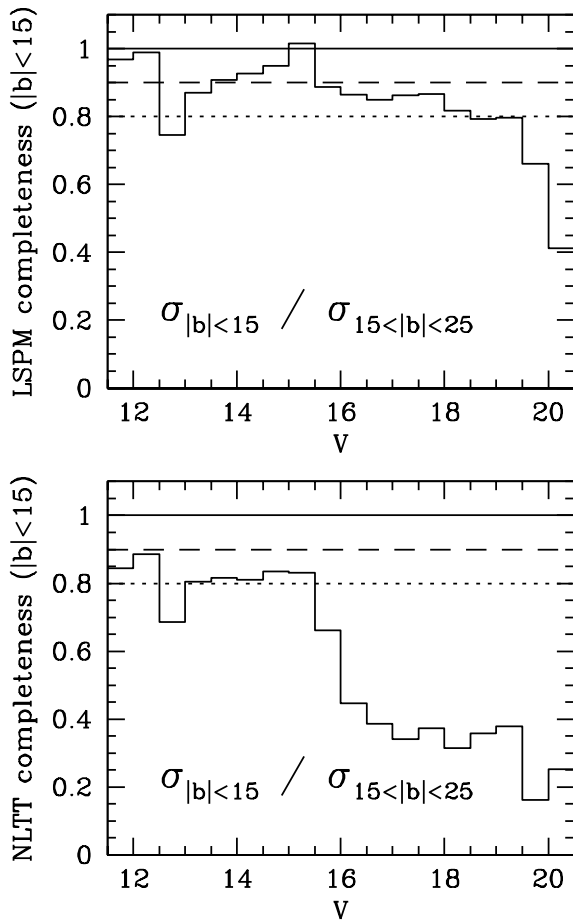


Fig. 26.—Completeness at low Galactic latitude, estimated from the ratio between the number density of high proper motion stars at  $|b| < 15^\circ$  and the number density of high proper motion stars at  $15^\circ < |b| < 25^\circ$ . This internal test suggests that the LSPM is  $>80\%$  complete at low Galactic latitudes for  $V < 19$  (top). Applied to NLTT stars (bottom) this completeness test yields results that are very similar with the completeness estimate shown in Fig. 22, with a sharp drop at  $V = 16$ . This internal test probably underestimates the completeness by 5%–10%, since there are intrinsically fewer high proper motion stars at lower Galactic latitudes (see Fig. 24).

suggests that the NLTT is only  $\approx 80\%$ – $85\%$  complete, which is lower than estimated from the external test ( $\approx 95\%$ , see Fig. 22). There are two different interpretations for the differences in the two NLTT completeness estimates. First, if the LSPM is only 90%–95% complete at  $|b| < 15^\circ$ ,  $13 < V < 15$  (as suggested by the internal test), then the external test overestimates the NLTT completeness, because it assumes the LSPM to be 100% complete. If indeed the LSPM is only 90%–95% complete, then the external test possibly overestimates the completeness by 5%–10%, which would bring both values in closer agreement. The second interpretation is that the external test is right and the LSPM is 100% at  $|b| < 15^\circ$ ,  $13 < V < 15$ , but the internal test underestimates the completeness level because there are intrinsically fewer stars at  $|b| < 15^\circ$  than at  $15^\circ < |b| < 25^\circ$ . If the second interpretation is valid, then our internal test indeed underestimates the completeness by as much as 10%.

The internal test suggests that the LSPM catalog is at least 80% complete at low Galactic latitudes for stars brighter than  $V = 19$ . This should be taken as the lowest possible value; as discussed above, the internal test may be underestimating the completeness by up to 10%. Thus, it is likely that the LSPM is actually  $\approx 90\%$  in low Galactic latitude regions. For stars fainter

than  $V = 19$ , the internal completeness test shows a drop to  $\approx 40\%$  just below  $V = 20$ . The LSPM catalog is thus definitely shallower at low Galactic latitudes, by 1 to 2 mag. While the LSPM should be regarded as largely complete to at least  $V = 20.0$  at high Galactic latitudes, it should be regarded as relatively complete only down to  $V = 19.0$  in low Galactic latitude regions.

Our completeness estimates at low Galactic latitudes are relatively crude at this point, and we are sorry we cannot provide more accurate values. More accurate completeness estimates could only be obtained if we had better estimates of the expected density of high proper motion stars in the low Galactic latitude regions. Alternatively, a proper modeling of all the effects that result in SUPERBLINK missing high proper motion stars might also provide more accurate completeness estimates. We believe the first option to be beyond the scope of this paper. The second option, in our opinion, would be extremely difficult to carry out, because of the complexity of the SUPERBLINK algorithm, but also because one would need to characterize the combined effects of all the pairs of POSS-I/POSS-II plates used, with their variety of saturation levels, PSFs, and a complete assessment of plate defects. Ultimately, the most accurate estimates of the LSPM completeness levels will come from better, more accurate proper-motion surveys at low Galactic latitudes (even of limited areas), which will provide true external tests to the completeness of the LSPM catalog.

## 8. STELLAR CONTENTS OF THE LSPM CATALOG

### 8.1. Color-Magnitude Classification

The apparent  $V$  magnitude of LSPM stars is plotted in Figure 27 as a function of the  $V - J$  color index. The LSPM stars are nicely clumped in four main groups. The interpretation is straightforward when one considers the selection effects implied in a sample of stars selected for high proper motions. Catalogs of high proper motion stars essentially contains subsamples of *nearby* stars. However, the spatial extent of the detection range depends on the transverse velocity of the star. Hence, high-velocity (halo, old disk) stars tend to be selected from a larger distance. It is thus fair to say that, on first approximation, high proper motion catalogs combine nearby disk stars with more distant halo/old disk stars. Because of the limiting distance, a diagram of apparent magnitude as a function of color will have the same general features as a color-magnitude diagram: a main sequence extending from upper left to lower right and a white dwarf sequence at the bottom left. This is indeed what we see in Figure 27. Because the stars are not exactly at the same distance, all sequences are thicker and fuzzier, but they are recognizable. Because high-velocity stars are detected to a larger distance, they will form their own sequence but *shifted down* because of their larger distance and hence larger mean apparent magnitude. Again this feature is quite apparent in Figure 27.

Note in Figure 27 the concentration of stars on the lower left of the plot, where the nearby white dwarfs are expected to be found. All stars with a 2MASS counterpart are plotted in red, while stars with no 2MASS counterparts are plotted in blue. It is clear that the majority of the high proper motion stars with no 2MASS counterparts are white dwarfs, which confirms the conjecture posed by Salim & Gould (2003).

In the  $H, J - K$  color-magnitude diagram, the brighter stars are separated into two main groups: a dense clump of stars around  $J - K_s = 0.8$  and a more diffuse one extending from the blue edge of the first one to around  $J - K_s = 0.3$  (Fig. 28). While the

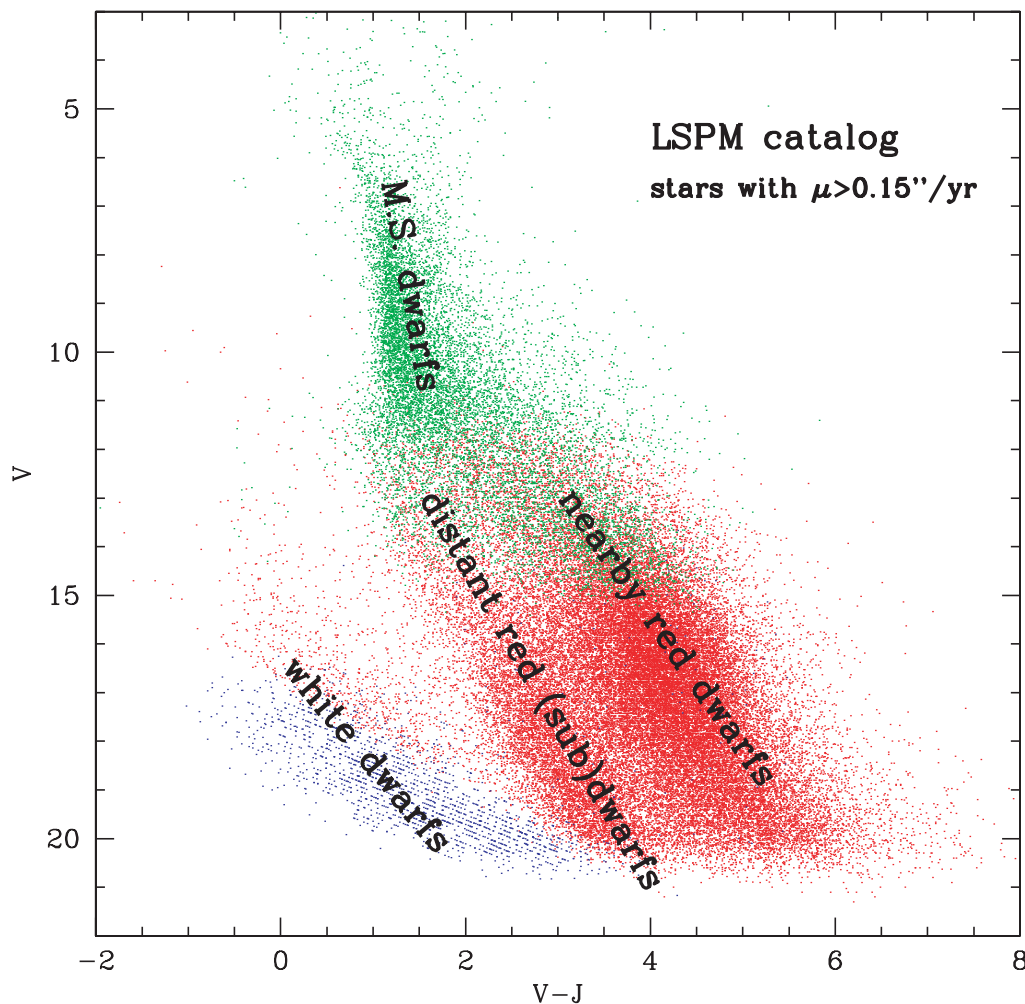


FIG. 27.—Optical/infrared color-magnitude diagram of all stars in the LSPM catalog. Stars with Tycho-2 or ASCC-2.5 counterparts are plotted in green; these have the most accurate values of  $V$  and  $V - J$ . Stars with no 2MASS counterparts are plotted in blue; most of them are consistent with being white dwarfs.

blue clump extends only down to about  $H = 13$ , the red clump extends all the way down to the magnitude limit, where the larger magnitude errors scatter the stars about in  $J - K_s$ . The big red clump is populated by M dwarfs and subdwarfs, which are degenerate in  $J - K$  color from M2 to M7 (Bessell & Brett 1988). The blue, diffuse clump consists of F–K dwarfs and subdwarfs. The fact that the distribution of main-sequence stars other than M dwarfs ends (at  $H = 13$ ) well before the 2MASS magnitude limit indicates that the LSPM is complete for those stellar subtypes. Note also the diffuse wisp that extends from  $(J - K_s, H) = (0.9, 7.5)$  to  $(1.5, 4.5)$ ; these are the very few giant stars that have proper motions large enough to be included in the LSPM.

Dwarfs and subdwarfs are expected to occupy distinct loci on the color-magnitude diagram because these populations have different mean distances in proper-motion catalogs. The proper-motion limit ( $\mu > 0''.15 \text{ yr}^{-1}$ ) restricts the detection range of disk objects, whose transverse velocities are typically  $< 50 \text{ km s}^{-1}$ , while halo objects (subdwarfs) with typical transverse velocities 2–5 times as large can find their way into the proper-motion catalog from distances 2–5 times larger. This is again apparent in Figure 28, where we note the probable positions of subdwarfs, 3–4 mag below the dwarfs.

We also note in Figure 28 the locations expected to be populated by white dwarfs, late-type M dwarfs (M7–M9), and L dwarfs. Of course, one has to look for those objects above the limit ( $H = 15$ ) below which 2MASS colors become less reli-

able. We nevertheless find a significant number of objects with 2MASS counterparts that are convincing white dwarf candidates. Late-type M dwarfs (M7–M9) are found in the range  $1.0 < J - K_s < 1.3$ , while L dwarfs normally occur beyond  $J - K_s > 1.3$  (Kirkpatrick et al. 1999). Several candidates are detected, and they warrant further investigation. While many might be known objects, chances are high that at least a few will be new ones, in particular if they occur at low Galactic latitudes, which have largely been avoided by previous L dwarf surveys (Kirkpatrick et al. 1999; Cruz et al. 2003).

The  $J - H, H - K$  color-color diagram is largely consistent with the vast majority of LSPM objects being main-sequence stars with no significant reddening (Fig. 29). The distribution is very similar to the general color-color diagram of 2MASS sources in high Galactic latitude fields and follows the standard sequence determined by Bessell & Brett (1988). The loci of different types of objects are indicated, as in Figure 28.

Overall, the accuracy of the 2MASS  $J, H,$  and  $K_s$  magnitudes allows one to separate different object subtypes and populations (much better than the photographic magnitudes). They should be very useful in planning follow-up observations of the LSPM stars.

## 8.2. Reduced Proper Motions

Reduced proper-motion diagrams are a major tool in the classification of local stars into different stellar populations

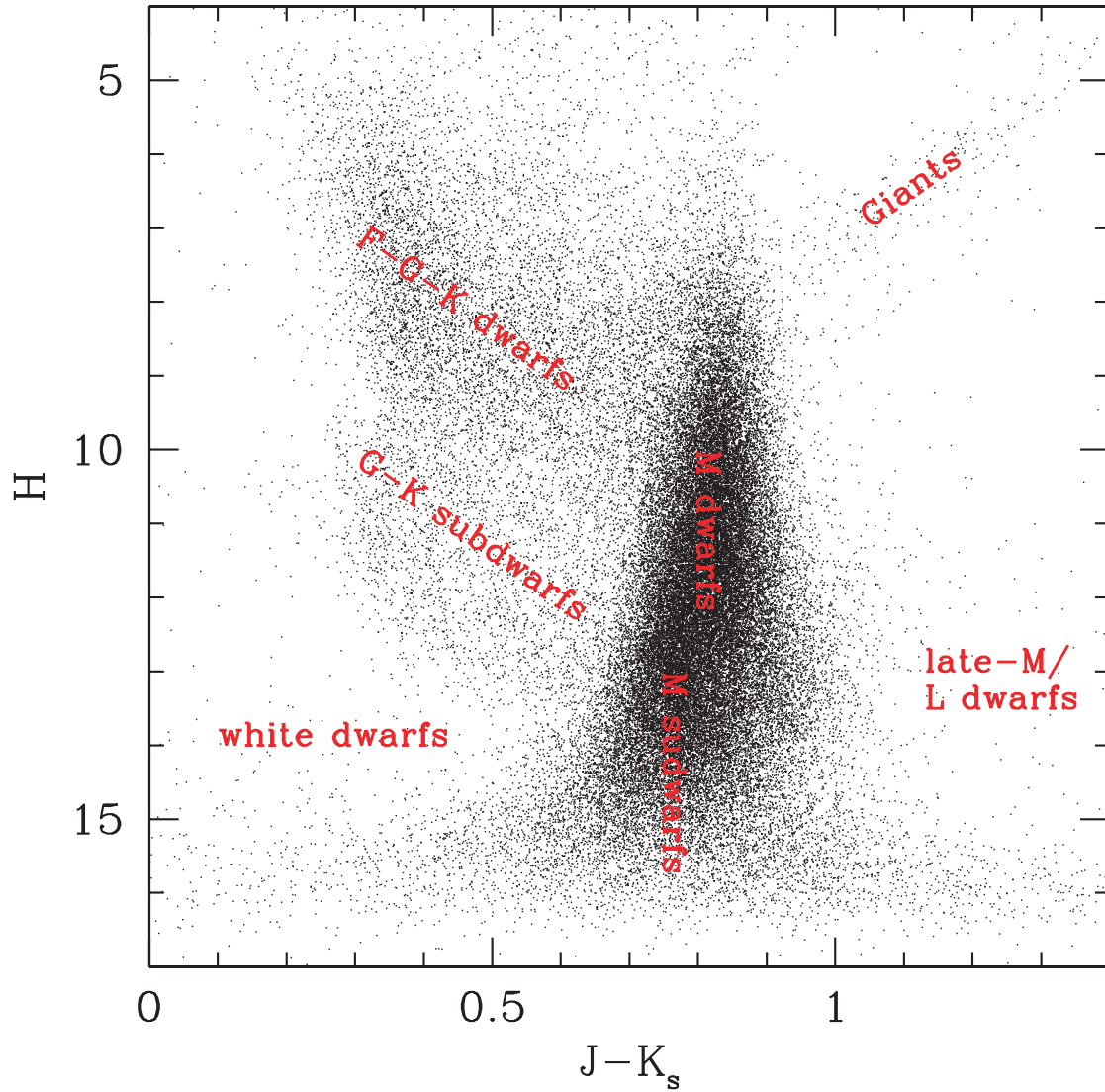


FIG. 28.—Infrared color-magnitude diagram of stars in our proper-motion catalog, based on  $JHK_s$  magnitudes extracted from the 2MASS All-Sky Point Source Catalog. Main-sequence F–K stars populate the upper left of the distribution, while M dwarfs are clumped around  $J - K_s = 0.8$ . A diffuse wisp of giant stars can be seen at the upper right. Below  $H = 15$ , errors in 2MASS magnitudes increase, which blurs out the color distribution.

(Jones 1972; Evans 1992; Salim & Gould 2000). It was recently demonstrated by Salim & Gould (2002) that *optical-infrared* reduced proper-motion diagrams are very efficient in separating samples of high proper motion stars into three distinct classes: main-sequence disk dwarfs, halo subdwarfs, and white dwarfs.

Using the proper motions and magnitudes in the LSPM catalog, we build a reduced proper-motion diagram for all but 27 LSPM stars using a reduced proper motion calculated from the  $V$  band ( $H_V$ ) and the  $V - J$  color. The reduced proper motion is analogous to an absolute magnitude in which the proper motion is used in place of the parallax. While the absolute magnitude is defined as

$$M_V = V + 5 \log \pi + 5,$$

where  $\pi$  is the parallax in arcseconds, the reduced proper motion is defined as

$$H_V = V + 5 \log \mu + 5,$$

where  $\mu$  is the proper motion in arcseconds per year. The reduced proper motion is directly related to the absolute magnitude:

$$H_V = M_V + 5 \log v_T - 3.38,$$

where  $v_T$  is the projected velocity of the star in the plane of the sky, in kilometers per second.

The reduced proper-motion diagram is thus analogous to a color-magnitude diagram, except for the fact that the usual stellar sequences are “blurred” by the  $\log v_T$  term. However, different populations have different ranges of possible  $v_T$ . Disk stars, on the one hand, have a mean transverse velocity  $\langle v_T \rangle \simeq 50 \text{ km s}^{-1}$ , which yields

$$\langle H_V \rangle_{\text{disk}} = M_V + 5.1.$$

Halo stars, on the other hand, have significantly larger mean transverse velocities,  $\langle v_T \rangle \simeq 300 \text{ km s}^{-1}$ , so their  $H_V$  are generally larger:

$$\langle H_V \rangle_{\text{halo}} = M_V + 9.0.$$

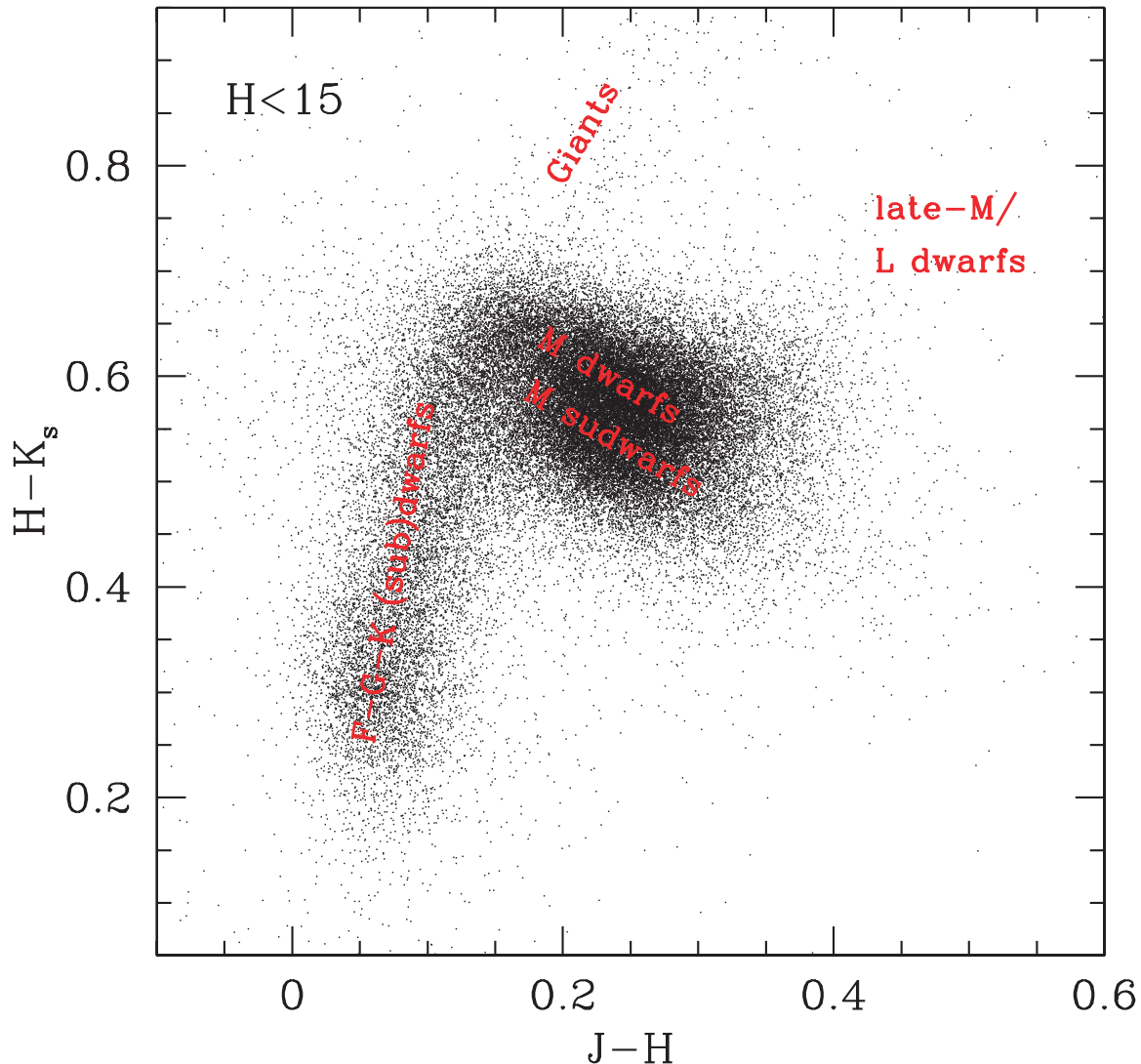


FIG. 29.—Infrared  $J - H$ ,  $H - K_s$  color-color diagram of stars in the proper-motion catalog. The distribution is consistent with stars on the main sequence with no reddening.

The (disk) dwarfs and (halo) subdwarfs thus form distinct sequences in the reduced proper-motion diagram, with halo subdwarfs located well below the disk dwarfs. White dwarfs occupy a distinct locus on the lower left of the diagram, a position familiar to users of color-magnitude diagrams.

We show in Figure 30 the reduced proper-motion diagram for LSPM stars. The corrected, absolute proper motions were used. The loci of the different stellar classes and populations are labeled. Note the similarity with Figure 27, which plotted the apparent magnitude as a function of color. The two plots are fundamentally very different, however. The reduced proper motion is a function of *luminosity and velocity*, while the apparent magnitude is a function of *luminosity and distance*. The two plots look similar only because stars are piled up against the LSPM proper-motion limit of  $0''.15 \text{ yr}^{-1}$ , which introduces a correlation between the velocity and distance. High-velocity stars can make it into the catalog even at large distances, while only the nearest of the low-velocity stars have proper motions large enough to be in the LSPM. Figure 27 thus separates the halo stars based on their larger average distances, while Figure 30 separates halo stars based on their larger transverse velocities. For classification purposes, the reduced proper-motion diagram should be preferred.

The reduced proper-motion diagram contains a wealth of information, and the separation between the different populations

warrants a more detailed analysis of the individual populations represented here. Such a detailed analysis is beyond the scope of this paper. Nevertheless, we wish to emphasize the significant potential of the LSPM catalog in the study of the local stellar populations.

## 9. CONCLUSIONS

We have generated a new catalog of stars with proper motions larger than  $0''.15 \text{ yr}^{-1}$  that currently is the most complete of its kind. We have achieved our initial goals of locating new high proper motion stars and redetermining to higher accuracy the positions and proper-motion estimates of previously known objects, especially the high proper motion stars from the LHS and NLTT catalogs.

The catalog is limited to northern declinations and lists 61,977 stars down to a magnitude  $V = 21$ . This essentially doubles the number of previously cataloged high proper motion stars in this hemisphere. The catalog is estimated to be  $>99\%$  complete for  $V < 19$  stars at high Galactic latitude ( $|b| > 15^\circ$ ) and  $\approx 90\%$  complete for  $V < 19$  stars at low Galactic latitude ( $|b| < 15^\circ$ ). This is a very significant improvement over previous catalogs.

We provide photometric estimates in the three optical bands of the POSS-II survey:  $B_J$  (IIIaJ emulsion with GG385 filter),  $R_F$  (IIIaF emulsion with RG610 filter), and  $I_N$  (IVN emulsion with RG9 filter). We also provide  $B$  and  $V$  magnitudes for the

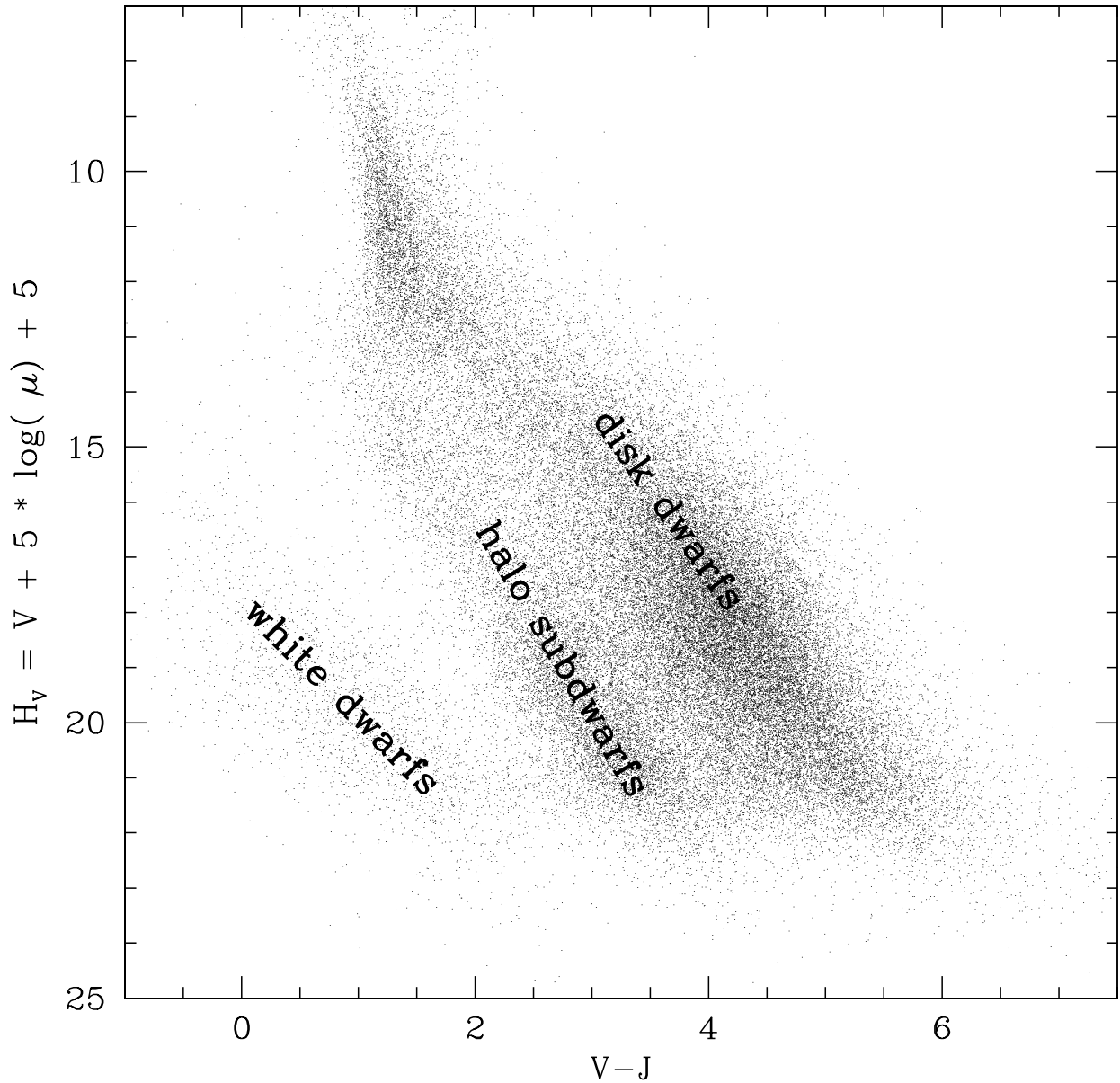


FIG. 30.—Reduced proper-motion diagram of the LSPM stars. Stars are distributed in four major groups: brighter stars, cool disk dwarfs, cool halo subdwarfs, and white dwarfs.

brighter stars, from their Tycho-2/ASCC-2.5 catalog counterparts. While the  $B$  and  $V$  magnitudes are very accurate, much room for improvement remains with the optical photometry of fainter stars. The infrared photometry, on the other hand, was extracted from the 2MASS All-Sky Point Source catalog and is accurate down to about 15th magnitude in each band ( $J$ ,  $H$ , and  $K_s$ ). The probability of our stars having been mismatched in the 2MASS catalog is almost zero.

To compare all stars in the same color/magnitude system, we provide an estimate of the apparent  $V$  magnitude and the  $V - J$  color index for all but 814 LSPM stars. These estimates are most reliable for the brighter ( $V < 12$ ) stars but should be used with caution for fainter stars, for which  $V$  is estimated from the USNO-B1.0 photographic magnitudes.

The LSPM catalog is a work in progress. An extension to the southern sky is currently underway. We are also working on an expansion to lower proper motions, down to  $0''.10 \text{ yr}^{-1}$ . Future plans include an improvement of the magnitudes, especially in the optical bands, by using magnitude estimates from a variety

of other sources (SDSS, USNO-A2 catalog, GSC-2.2 catalogs, and future versions of the UCAC catalog).

At this point, the LSPM catalog is ideally suited for follow-up observations of selected targets of interest. Indeed, we are currently working on a massive spectroscopic survey of selected LSPM objects, including all stars with proper motions  $\mu > 0''.45 \text{ yr}^{-1}$ , for which spectroscopic observations are now in hand (Lépine et al. 2005, in preparation).

The LSPM catalog will be updated as new discoveries are made. We invite investigators who discover new high proper motion objects in the northern sky to contact the authors so that their discovery can be included in the catalog. Likewise, investigators who notice that a known high proper motion star is missing from the LSPM or who find errors in our data are invited to communicate with us.

We would like to thank the referee, A. Gould, for invaluable comments and suggestions.

We are very grateful to Brian McLean, head of the Catalogs and Surveys Branch of the STScI, for allowing us to massively access the DSSs. We also thank Michael Benedetto, of the AMNH IT department, for network connectivity from AMNH to STScI. M. S. acknowledges the leadership, support, and friendship of the late Barry Lasker, who guided the DSSs project until his untimely death. Riccardo Giacconi's vision led to the DSS, and M. S. acknowledges that seminal idea with gratitude.

R. Michael Rich has been an early and enthusiastic user of this catalog, and we thank him for his support and ongoing collaboration.

This work has been made possible through the use of the DSSs. The DSSs were produced at the STScI under U.S. Government grant NAG W-2166. The images of these surveys are based on photographic data obtained using the Oschin Schmidt Telescope on Palomar Mountain and the UK Schmidt Telescope. The plates were processed into the present compressed digital form with the permission of these institutions. The National Geographic Society-Palomar Observatory Sky Atlas (POSS-I) was made by the California Institute of Technology with grants from the National Geographic Society. The Second Palomar Observatory Sky Survey (POSS-II) was made by the California Institute of Technology with funds from the National Science Foundation (NSF), the National Geographic Society, the Sloan Foundation, the Samuel Oschin Foundation, and the Eastman Kodak Corporation. The Oschin Schmidt Telescope is operated by the California Institute of Technology and Palomar Observatory. The UK Schmidt Telescope was operated by the Royal Observatory Edinburgh, with funding from the UK Science and Engineering Research Council (later the UK Particle Physics and Astronomy Research Council), until 1988 June, and thereafter by the Anglo-Australian Observatory. The blue plates of the southern Sky Atlas and its Equatorial Extension (together known as the SERC-J), as well as the Equatorial Red (ER), and the Second Epoch (red) Survey (SES) were all taken with the UK Schmidt.

This publication makes use of data products from 2MASS, which is a joint project of the University of Massachusetts and the Infrared Processing and Analysis Center/California Institute of Technology, funded by the National Aeronautics and Space Administration and the NSF.

The data mining required for this work has been made possible with the use of the SIMBAD astronomical database and VizieR astronomical catalogs service, both maintained and operated by the Centre de Données Astronomiques de Strasbourg (<http://cdsweb.u-strasbg.fr/>).

This research program has been supported by NSF grant AST-0087313 at the AMNH, as part of the NASA/NSF NSTARS program. M. S. and S. L. gratefully acknowledge support from the Cordelia Corporation, from Hilary Lipsitz, and from the AMNH.

## APPENDIX

NLTT STARS NOT INCLUDED  
IN THE LSPM-NORTH CATALOG

A total of 1859 objects listed in the NLTT catalog and claimed to be located north of the celestial equator did not make it into the LSPM catalog. The reasons why these stars were not included in the LSPM catalog fall into four categories: (1) the object is moving slower than the  $0''.15 \text{ yr}^{-1}$  limit of the LSPM catalog, (2) the object does not show up on the POSS plates, (3) the object is a duplicate NLTT entry, and (4) the object is a high proper motion nebula.

Most of the slow-moving objects are stars that are incorrectly listed in the NLTT as having large proper motions. A total of 208 such objects are stars that are listed in the Tycho-2 catalog; their Tycho-2 proper motions unambiguously place them under the LSPM inclusion limit. An additional 1104 stars had their proper motions remeasured with SUPERBLINK, and the updated value makes them low proper motion ( $\mu < 0''.15 \text{ yr}^{-1}$ ) stars.

There are also 76 objects that have a quoted NLTT proper motion under the  $0''.15 \text{ yr}^{-1}$  limit of the LSPM. While some of these are possibly bogus (see below), four of them have their low proper motion status confirmed in the Tycho-2 catalog. Another 63 have their low proper motion confirmed by SUPERBLINK. Three more stars did not have their proper motion remeasured by SUPERBLINK, but direct examination of DSS scans confirms they are low proper motion stars.

We have identified 39 objects to be duplicate entries of other NLTT stars. In all cases, the duplicate entry was listed with a

TABLE 3  
NLTT STARS NOT LISTED IN THE LSPM CATALOG

NLTT	R.A. <sub>NLTT</sub> (deg)	Decl. <sub>NLTT</sub> (deg)	R <sub>NLTT</sub> (mag)	B <sub>NLTT</sub> (mag)	$\mu$ <sub>NLTT</sub> (arcsec yr <sup>-1</sup> )	pma <sub>NLTT</sub> (deg)	f <sub>flag</sub>	R.A.	Decl.	$\mu$	$\mu$ R.A.	$\mu$ decl.
								(deg)	(deg)	(arcsec yr <sup>-1</sup> )	(arcsec yr <sup>-1</sup> )	(arcsec yr <sup>-1</sup> )
48.....	0.850	39.887	16.1	17.4	0.189	87	S	0.849922	39.887436	0.127	0.119	0.045
137.....	1.270	13.255	18.4	18.6	0.235	68	B	0.000000	0.000000	0.000	0.000	0.000
156.....	1.345	11.969	18.4	20.6	0.206	109	B	0.000000	0.000000	0.000	0.000	0.000
247.....	1.691	8.657	11.4	12.9	0.202	203	T	1.682560	8.657199	0.063	-0.031	-0.055
249.....	1.698	33.628	16.9	18.4	0.183	206	S	1.699144	33.628593	0.139	-0.058	-0.126
331.....	2.009	32.244	17.5	19.2	0.227	253	S	2.009742	32.243969	0.122	-0.114	-0.043
367.....	2.201	49.597	17.8	20.8	0.180	70	S	2.197109	49.596958	0.130	0.123	0.042
376.....	2.230	14.264	18.0	19.7	0.205	351	B	0.000000	0.000000	0.000	0.000	0.000
377.....	2.236	9.834	18.6	21.0	0.188	112	S	2.234560	9.832853	0.131	0.118	-0.057
396.....	2.329	65.070	7.0	8.1	0.280	80	T	2.319856	65.070892	0.136	0.131	0.037
402.....	2.316	30.380	17.4	19.5	0.196	123	S	2.314764	30.380768	0.065	0.063	-0.017
417.....	2.345	3.840	11.9	12.8	0.299	111	T	2.344284	3.837747	0.147	0.083	-0.121
430.....	2.407	49.555	18.9	18.6	0.188	249	S	2.407427	49.555573	0.132	-0.121	-0.051
478.....	2.606	21.850	11.9	13.0	0.180	82	S	2.605807	21.851067	0.142	0.142	-0.008
479.....	2.606	21.847	17.4	18.7	0.180	82	S	2.606189	21.848387	0.149	0.149	0.008

NOTE.—Table 3 is presented in its entirety in the electronic edition of the Astronomical Journal. A portion is shown here for guidance regarding its form and content.

slightly different position, generally within a few arcminutes of the primary entry.

The remaining 395 objects could not be recovered on the POSS plates and are listed as “bogus.” An NLTT star can be missing if it initially was a spurious detection. This is highly probable for stars initially reported to have a magnitude near the plate limit ( $V > 18$ ). Another possibility is that the quoted NLTT catalog position was very far off from the actual location of the star. In this case, it is very likely that the object has been picked up by SUPERBLINK and is now listed in the LSPM catalog as a “new” high proper motion star. Thus the object is not really missing but was rather lost and has now been rediscovered.

Two high proper motion “stars” in the NLTT are found to be small, compact nebulae with large proper motions. The two objects are NLTT 13414 and NLTT 13424. Moving nebula are not included in the LSPM catalog at this point. These and other candidate high proper motion nebulae found with SUPERBLINK will be discussed in an upcoming paper.

All NLTT objects north of the celestial equator that are not in the LSPM catalog are listed in the accompanying table (see Table 3 for a sample of the first 15 lines). The table lists the

NLTT catalog number, followed by the position, red and blue magnitudes, and proper motion as quoted in the NLTT catalog. The NLTT positions are transformed into J2000 coordinates from their original values. A flag value of “B” indicates that the star could not be found by direct examination of the DSS scans of the POSS photographic plates. A flag value of “D” means that the object is a duplicate NLTT catalog entry. A flag value of “L” means that the star has an NLTT proper motion under the nominal lower limit ( $0''.15 \text{ yr}^{-1}$ ) of the LSPM catalog. A flag value of “N” means that, although the object was found to be real, it is not a star but rather a proper-motion nebula. A flag value of “S” means that the proper motion of the star was remeasured by SUPERBLINK and found to be under the nominal lower limit ( $0''.15 \text{ yr}^{-1}$ ) of the LSPM catalog. A flag value of “T” means that the star is in the Tycho-2 catalog and that its Tycho-2 proper motion is under the nominal lower limit ( $0''.15 \text{ yr}^{-1}$ ) of the LSPM catalog. The corrected position and proper motion is given for all stars that could be recovered.

We note that this list does not contain a single star from the LHS catalog. Every one of the northern LHS stars has been accounted for and is now included in the LSPM catalog.

#### REFERENCES

- Bakos, G. A., Sahu, K. C., & Nemeth, P. 2002, *ApJS*, 141, 187  
 Barnard, E. E. 1916, *AJ*, 29, 181  
 Bergeron, P., Ruiz, M.-T., & Leggett, S. K. 1992, *ApJ*, 400, 315  
 Bessell, M. S. 1991, *AJ*, 101, 662  
 Bessell, M. S., & Brett, J. M. 1988, *PASP*, 100, 1134  
 Cruz, K. L., & Reid, I. N. 2002, *AJ*, 123, 2828  
 Cruz, K. L., Reid, I. N., Liebert, J., Kirkpatrick, J. D., & Lowrance, P. J. 2003, *AJ*, 126, 2421  
 Cutri, R. M., et al. 2003, *The 2MASS All-Sky Catalog of Point Sources* (Pasadena: IPAC)  
 Dahn, C. C., et al. 2002, *AJ*, 124, 1170  
 Dawson, P. C. 1986, *ApJ*, 311, 984  
 ESA. 1997, *The Hipparcos and Tycho Catalogues* (ESA Publ. SP-1200) (Noordwijk: ESA)  
 Evans, D. W. 1992, *MNRAS*, 255, 521  
 Fehrenbach, C., Dufhot, M., & Burnage, R. 2001, *A&A*, 369, 65  
 Flynn, C., Sommer-Larsen, J., Fuchs, B., Graff, D. S., & Salim, S. 2001, *MNRAS*, 322, 553  
 Giclas, H. L., Burnham, R., & Thomas, N. G. 1971, *Lowell Proper Motion Survey Northern Hemisphere*. (Flagstaff: Lowell Obs.)  
 Giclas, H. L., Burnham, R., Jr., & Thomas, N. G. 1978, *Lowell Obs. Bull.*, 8, 89  
 Girard, T. M., Platais, I., Kozhurina-Platais, V., & van Altena, W. F. 1998, *AJ*, 115, 855  
 Gizis, J. E., & Reid, I. N. 1997, *PASP*, 109, 849  
 Gould, A. 2003a, *ApJ*, 583, 765  
 ———. 2003b, *AJ*, 126, 472  
 Gould, A., & Kollmeier, J. A. 2004, *ApJS*, 152, 103  
 Gould, A., & Salim, S. 2003, *ApJ*, 582, 1001  
 Hambly, N., Henry, T. J., Subasavage, J. P., Brown, M. A., & Jao, W.-C. 2004, *AJ*, 128, 437  
 Hawley, S. L., et al. 2002, *AJ*, 123, 3409  
 Hintzen, P. 1986, *AJ*, 92, 431  
 Høg, E., et al. 2000, *A&A*, 355, L27  
 Innes, R. T. A. 1915, *Union Obs. Circ.* 30  
 Jones, E. M. 1972, *ApJ*, 173, 671  
 Kharchenko, N. V., 2001, *Kinematika Fiz. Nebesn. Tel.*, 17, 409  
 Kirkpatrick, J. D., et al. 1999, *ApJ*, 519, 802  
 ———. 2000, *AJ*, 120, 447  
 Klemola, A. R., Jones, B. F., & Hanson, R. B. 1987, *AJ*, 94, 501  
 Lee, S.-G. 1991, *J. Korean Astron. Soc.*, 24, 161  
 Leggett, S. K., Ruiz, M. T., & Bergeron, P. 1998, *ApJ*, 497, 294  
 Lépine, S., Rich, R. M., Neill, J. D., Caulet, A., & Shara, M. M. 2002a, *ApJ*, 581, L47  
 Lépine, S., Shara, M. M., & Rich, R. M. 2002b, *AJ*, 124, 1190  
 ———. 2003, *AJ*, 126, 921  
 Liebert, J., Dahn, C. C., & Monet, D. G. 1988, *ApJ*, 332, 891  
 Luyten, W. J. 1968, *MNRAS*, 139, 221  
 ———. 1979a, *LHS Catalogue* (2nd ed.; Minneapolis: Univ. Minnesota Press)  
 ———. 1979b, *New Luyten Catalogue of Stars with Proper Motions Larger than Two Tenths of an Arcsecond* (Minneapolis: Univ. Minnesota Press)  
 Monet, D. G., Fisher, M. D., Liebert, J., Canzian, B., Harris, H. C., & Reid, I. N. 2000, *AJ*, 120, 1541  
 Monet, D. G., et al. 1998, *USNO-A V2.0* (Flagstaff: USNO and USRA)  
 ———. 2003, *AJ*, 125, 984  
 Munn, J. A., et al. 2004, *AJ*, 127, 3034  
 Pokorny, R. S., Jones, H. R. A., & Hambly, N. C. 2003, *A&A*, 397, 575  
 Reid, I. N., & Cruz, K. L. 2002, *AJ*, 123, 2806  
 Reid, I. N., Kilkenny, D., & Cruz, K. L. 2002, *AJ*, 123, 2822  
 Reid, I. N., et al. 1991, *PASP*, 103, 661  
 ———. 2003, *AJ*, 126, 3007  
 Ross, F. E. 1939, *AJ*, 48, 163  
 Ruiz, M. T., & Anguita, C. 1993, *AJ*, 105, 614  
 Ruiz, M. T., Leggett, S. K., & Allard, F. 1997, *ApJ*, 491, L107  
 Ruiz, M. T., Wischnjewsky, M., Rojo, P. M., & Gonzalez, L. 2001, *ApJS*, 133, 119  
 Ryan, S. G. 1989, *AJ*, 98, 1693  
 Salim, S., & Gould, A. 2000, *ApJ*, 539, 241  
 ———. 2002, *ApJ*, 575, L83  
 ———. 2003, *ApJ*, 582, 1011  
 Scholz, R.-D., Irwin, M., Ibata, R., Jahreiss, H., & Malkov, O. Y. 2000, *A&A*, 353, 958  
 Sesar, B., et al. 2005, *AJ*, in press  
 Stoughton, C., et al. 2002, *AJ*, 123, 485  
 Teegarden, B. J., et al. 2003, *ApJ*, 589, L51  
 van Altena, W. F., & Lopez, C. E. 1991, *Ap&SS*, 177, 59  
 van Biesbroeck, G. 1915, *AJ*, 66, 528  
 van Maanen, A. 1915, *ApJ*, 41, 187  
 Vennes, S., & Kawka, A. 2003, *ApJ*, 586, L95  
 Weis, E. W. 1984, *ApJS*, 55, 289  
 ———. 1996, *AJ*, 112, 2300  
 Wolf, M. 1919, *Veroeff. des Badischen Sternw. Heidelberg*, 7, 195  
 Wroblewski, H., & Costa, E. 1999, *A&AS*, 139, 25  
 ———. 2001, *A&A*, 367, 725  
 Wroblewski, H., & Torres, A. 1989, *A&AS*, 78, 231  
 ———. 1991, *A&AS*, 91, 129  
 ———. 1994, *A&AS*, 105, 179  
 ———. 1996, *A&AS*, 115, 481  
 ———. 1997, *A&AS*, 122, 447  
 Zacharias, N., et al. 2000, *AJ*, 120, 2131  
 ———. 2004, *AJ*, 127, 3043